FINAL REPORT

ARCTIC ABSORPTION AT OBLIQUE INCIDENCE OBSERVED AT 32 MC ON RIOMETERS AND SCATTER SIGNALS

PAGE COMMUNICATIONS ENGINEERS, INC.
A Subsidiary of Northrop Corporation
2001 Wisconsin Avenue, N. W.
Washington 7, D. C.

PCE-R-9063A
Contract AF19(604)-7354
December 1961

Prepared for
ELECTRONICS RESEARCH DIRECTORATE
AIR FORCE CAMBRIDGE RESEARCH LABORATORIES
OFFICE OF AEROSPACE RESEARCH
UNITED STATES AIR FORCE
Bedford, Massachusetts

AFCRL-62-26

ARCTIC ABSORPTION AT OBLIQUE INCIDENCE OBSERVED AT 32 MC ON RIOMETERS AND SCATTER SIGNALS

FINAL REPORT

PAGE COMMUNICATIONS ENGINEERS, INC.
A Subsidiary of Northrop Corporation
2001 Wisconsin Avenue, N. W.
Washington 7, D. C.

PCE-R-9063A

Contract AF19(604)-7354

December 1961

Prepared for

ELECTRONICS RESEARCH DIRECTORATE
AIR FORCE CAMBRIDGE RESEARCH LABORATORIES
OFFICE OF AEROSPACE RESEARCH
UNITED STATES AIR FORCE
Bedford, Massachusetts

Requests for additional copies by Agencies of the Department of Defense, their contractors, and other Government agencies should be directed to the:

ARMED SERVICES TECHNICAL INFORMATION AGENCY
ARLINGTON HALL STATION
ARLINGTON 12, VIRGINIA

Department of Defense contractors must be established for ASTIA services or have their need-to-know certified by the cognizant military agency of their project or contract.

All other persons and organizations should apply to the:

U. S. DEPARTMENT OF COMMERCE
OFFICE OF TECHNICAL SERVICES
WASHINGTON 25, D. C.

CONTENTS

CONTENTS (Continued)

LIST OF ILLUSTRATIONS

ABSTRACT

Ionospheric absorption in the arctic has been studied using riometers and ionospheric scatter signals at 32 mc. Oblique measurements were made in all cases on three antennas at Sondrestrom, Greenland, pointing NW, SE, and SW respectively. Several events in the period September 1960 through October 1961 are analyzed. Total ionospheric absorption is inferred from riometer measurements, while low-level absorption is inferred from the scatter signal-intensity variations. Auroral absorption observations indicated that the size of absorbing areas usually does not exceed 10,000 sq km. Evidence of noise generated in the aurora is discussed. Polar-cap absorption events showed severe absorption, often exceeding 30 db at oblique incidence. Polar-cap absorption effects were found to be more intense in the auroral zone, probably because of a strong dependence on solar zenith angle, although the effects persisted longer at the higher latitudes. Good correlation between the onset of the events on the various antennas showed the effects to be widespread. The signal and noise absorption variations during these events, when compared with a simple model, indicate considerable variation of scattering and/or absorption heights during the events.

PROJECT PERSONNEL

William Collins	Assistant Director, Research and Development
Joseph Mitchell	Research Engineer
Phillip Rockmaker	Technician
James Farrell	Technician
William Albright	Research Engineer
Winifred de los Santos	Supervisor, Data Analysis and Computing
Roberta Schreiber	Data Analyst
John Hepner	Data Analyst
D. N. Steel	Technical Editor

This work was performed under the administrative and technical guidance of:

Gail E. Boggs	Vice President and Director of Research and Development
Ross Bateman	Senior Vice President and Executive Director of Engineering and Research & Development

SECTION I

INTRODUCTION

1.1 BACKGROUND

The variation of intensity of high-latitude signals propagated by ionospheric scatter has been found to be a sensitive indicator of the occurrence of polar cap absorption (PCA) events. A technique for recognizing PCA events from these data has been developed by D.K. Bailey. Signal intensity data from the USAF North Atlantic Ionospheric-Scatter Communication System, at 32 mc, have been analyzed by Bailey,[1] and he has reported on PCA occurrences appearing in these data since 1952.* This system utilizes 40-kw transmitters, large corner-reflector antennas, and sensitive receivers and provides unusually high communications reliability for arctic circuits. Signal-absorption data are therefore available during all but the most severe events.

1.2 PURPOSE

The purpose of the program carried out under this contract was to provide additional absorption data by the use of relative ionospheric opacity meters (riometers) which measure total ionospheric absorption in terms of variations in cosmic noise intensity. The contract embraced three objectives:

a. Measurement of the increase in absorption in the total ionosphere during absorption events.

b. Determination of the absorption in the upper ionosphere by comparing the increase in total ionospheric absorption during an event with the absorption in the lower ionosphere as observed by variations in the scatter-signal intensities.

c. Determination of the extent and movement of the ionospheric absorption phenomena by utilizing the spatial coverage afforded by the three antenna.

---

* See Section IX, Bibliography.

SECTION II

PROGRAM DESCRIPTION

This program made extensive use of United States Air Force facilities previously installed by Page at Sondrestrom, Greenland, under National Bureau of Standards Contracts CST-1057 and CST-4035. Riometer receivers were furnished the Contractor by the Government. Each receiver was thoroughly tested, repaired, and aligned at the Page Laboratory before shipping. Certain modification were also made, as discussed later in this section. Permission to install the riometer equipment as an integral part of the communications system at Sondrestrom was granted by The Norlant Air Force Communications Region and the installation was completed on 28 August 1960.

The riometer receivers were connected to three of the large corner-reflector antennas used by the scatter communication circuits, thus permitting comparison of signal and noise absorption at oblique incidence to the ionosphere in the same direction. Since each of the three antennas is oriented in a different direction, absorption in the ionosphere was observed in three widely different areas forming roughly the corners of an equilateral triangle 1000 km on a side. Signal and absorption measurements were all made at 32 $\pm$0.5 mc, near the operating frequencies of the existing system.

2.1 SITES AND ANTENNAS

Sondrestrom Air Base is on Sondrestrom Fjord, a few miles north of the arctic circle in western Greenland. The geographic coordinates of the receiving terminal at Sondrestrom are shown in Figure 2-1. Two sites are used for the ionospheric-scatter terminals. One, at Lake Ferguson, approximately three miles south of the Air Base, is used for the facilities communicating with Thule, Greenland, and Keflavik, Iceland. Suitable fresnel regions are provided by Lake Ferguson. A second site, for receiving Goose Bay, is at Michigan Bay, approximately 9 miles down the fjord. A salt-water fresnel region is provided by the fjord.

Antennas at each site are placed the proper distance above the fresnel region to direct the main lobe upward at an angle calculated to illuminate the ionosphere at a height of 85 km at the path midpoint. The antennas at each site are 60° corner reflectors employing four full-wave collinear dipoles, in phase, and having a 3-db beamwidth of approximately 10° in the horizontal plane. The computed vertical free-space 3-db beamwidth is approximately 18°. The pointing data for these antennas are shown in Figure 2-2.

2.2 PATHS

The facilities described above utilize ionospheric-scatter propagation to communicate with stations using antennas of similar characteristics at Thule, Keflavik, and Goose Bay. The path parameters are shown in Figure 2-1.

2.3 EQUIPMENT

At both Lake Ferguson and Michigan Bay stations, the receiving antennas are several thousand feet from the equipment building. To overcome the high line-loss on transmission line running for such distances, a remote preamplifier system is used at the antennas to amplify the signal and noise. The signal and noise arrive at the receiver building at a suitable level to insure that the overall receiving-system noise figure is largely determined by the remote-preamplifier noise figure.

The riometers were installed in the equipment building and were connected to the distribution panel where the amplified noise was available. See Figure 2-3. A gain-stable preamplifier and adjustable attenuator were added to the riometer between the noise diode and the switching network to amplify the noise from the diode and to prevent burn-out of the diode which might be caused by the high noise levels required to match the level of the incoming (amplified) cosmic noise.

These variations from the usual method of operating riometers were necessary to permit their integration with the communication system in a way that would not interfere with its operation. This method, however, presented problems that would not have existed had more conventional methods been used. For example, as would be expected, the system experienced some drift. This drift is thought to be largely caused by temperature variations in the long coaxial line from the antenna to the equipment building. The line is above ground, rather than buried as is usually done, and is much longer than would normally be used. The preamplifiers used at the antenna and in the riometer were quite reliable and free from excessive drift, although some of the drift may be attributed to them. The total drift attributable to these causes is not known but is thought to not exceed 2 db for seasonal and diurnal temperature variations. The Thule antenna transmission line, however, is over a mile long and required a special amplifier following the preamp. This system was very unstable, thus invalidating much of the data obtained on the antenna.

The riometer receivers were tuned within the bandwidth of the preamplifiers but sufficiently far removed from the scatter signals to avoid interference under normal circumstances. They were operated on a fixed frequency without sweeping. Interfering signals were not a problem in that area.

2.4 DATA ACCUMULATION

Data recording began on 28 August 1960 on each riometer receiver. Accumulation of data on the Keflavik and Goose Bay circuits continued until 31 October 1961. The Thule riometer recordings were terminated early in 1961 because of the problems described above.

The operational need for communications on the Thule and Goose Bay circuits ceased in early 1961 (January for Thule and April for Goose Bay). The signal-intensity data were consequently not available on these circuits subsequent to that time. The riometer operation, however, continued on the Goose Bay and Keflavik circuits through the entire program.

2.4.1 Outage

For the riometers on the Goose Bay and Keflavik antennas, outage of all types resulting in unreliable data or absence of a record of noise intensity totaled about 10% of the time. Of this, about 4 percent was caused by power or other equipment failures not under the direct control of this program. The remaining 6 percent outage was riometer or associated-equipment failure. This factor would have been substantially less if the technician responsible for maintenance of the riometers had had ready transportation to the stations rather then depending on the relatively infrequent military shift-change transportation.

The Thule remote preamplifying system and transmission line proved to be extremely unstable as mentioned previously. The only realistic solution to this problem would have been placement of the noise diode and switching unit of the riometer at the remote preamplifier, thus making the entire recording system insensitive to gain variations. This approach was not possible when the system was being used for communications but was feasible following that time. Page Laboratory personnel in Washington had built a portion of a riometer for this purpose and it was ready to install when the program was terminated. The labor and materials for this work were not charged to the contract.

2.4.2 Calibration and Recording Techniques

To provide data calibrated in terms of absolute power levels and to compensate for any possible long-term drift in the preamplifiers and long transmission lines, it was necessary to calibrate the recording system with a noise generator at the antenna. A Kay Lab 240-B noise generator was used as a standard.

To make noise powers available which were equivalent to +26 db above

$290^{\circ}K$, the 600-ohm balanced output was converted to unbalanced by means of an external balun and then transformed to 50 ohms. The losses associated with this procedure were a few tenths of a decibel. In addition to the standard noise diode, heads were constructed having 800-ohm unbalanced outputs with transformers for conversion to 50.0 ohms. These heads were installed at the antenna and switched to the preamplifier input by relays actuated from the building. The test-diode circuitry in the riometer was then used to supply B+ and filament power to this remote noise-diode generator head. This procedure alleviated the need for exposure of personnel and equipment to severe winter weather when calibrating. The output of these sources agreed with that of the standard generator within a few tenths of a decibel.

Transmission lines from the antenna to the preamp were 500-ohm open-wire, about 50 feet in length, having less than 1-db loss. These lines were equipped with baluns and impedance matching devices which were adjusted to 50.0 ohms at the preamplifier input.

The signal-intensity measurement system was also calibrated at the remote preamplifier by inserting a test signal from a calibrated transmission line. A generator in the equipment building provided this signal. The signal recording equipment was part of the original communication system and was not supplied under this contract. Signal data were made available, however, through the courtesy of the U.S. Air Force and National Bureau of Standards.

The signal-intensity recording system had a dynamic range of about 80 db, while the riometer receiver used to measure noise has a usable range of about 15 db. Sample charts with calibrations are shown in Figure 2-4.

2.4.3 Interference

As mentioned previously, little interference was experienced from unwanted signals. Some problems did exist, however, from self-interference in the system. Since the riometer was utilizing the same remote preamplifier as the communication system, excessively strong signals in the passband due to sporadic-E, strong meteors, or other causes tended to overload the preamp and cause limiting. This limiting sharply reduced the gain of the preamplifier, thus producing an erroneously low noise reading in the riometer.

On the Goose Bay circuit, voice and FSK signals were frequency-division multiplexed in the passband. Preamplifier overloading caused by occasional high signal intensities on this circuit resulted, then, in an increase in noise level at the riometer due to intermodulation products, generated in the overloaded, and therefore nonlinear, preamplifier. Fortunately, both of

these erroneous effects were easily detectable, at they had a one-to-one correlation with excessively strong signals on the signal-intensity chart.

It should be noted that some reduction in noise or increase in absorption might be expected when a sporadic-E cloud was in the beam. It is certain, however, that this effect was not the controlling one and that the previously mentioned overloading problem did exist.

Although these erroneous readings were easily detectable, they did affect the problem in one important way. To the extent that absorption coincided with enhanced signals, these absorption data were lost. Although it is not well established, there appears to be a connection between the occurrence of visible aurora near the path midpoint and the occurrence of enhanced signals on ionospheric-scatter paths.[2] Little and Leinbach report a good correlation between absorption observed on a riometer and certain types of visible aurora. On this program, auroral absorption was observed only rarely, although enhanced signals were quite frequent. It is likely that strong signals occurred frequently during periods of auroral absorption, thus obscuring its effect. Some antenna considerations discussed later may also partially account for the fact that auroral observations on this system were rare.

Path	Terminal Geographic Coordinates	Path Length	Path Midpoint Geographic Coordinates	Path Midpoint Geomagnetic Latitude	Sondrestrom Receiving Frequency, MC
Thule Sondrestrom	76°33'N 68 36 W 66 58 N 50 40 W	1, 223. 9 km 760. 6 mi	71°57'N 57 20 W	82°50'N	31. 5
Goose Bay Sondrestrom	53 30 N 60 04 W 66 58 N 50 57 W	1, 593. 3 km 990. 3 mi	60 44 N 56 40 W	71 49 N	32. 0
Keflavik Sondrestrom	63 55 N 22 38 W 66 59 N 50 42 W	1, 327. 9 km 825. 1 mi	66 06 N 35 50 W	74 29 N	32. 4

Figure 2-1. Path Data

Directed Toward	Antenna Azimuth (E of N)	Main-Lobe Vertical Elevation	GHA	Declination
Thule	338°02'	5°18'	206°	26. 5°
Goose Bay	202 33	2 55	75	-18. 3
Keflavik	91 27	4 24	324	3. 1

Figure 2-2. Pointing Data for Sondrestrom Antennas

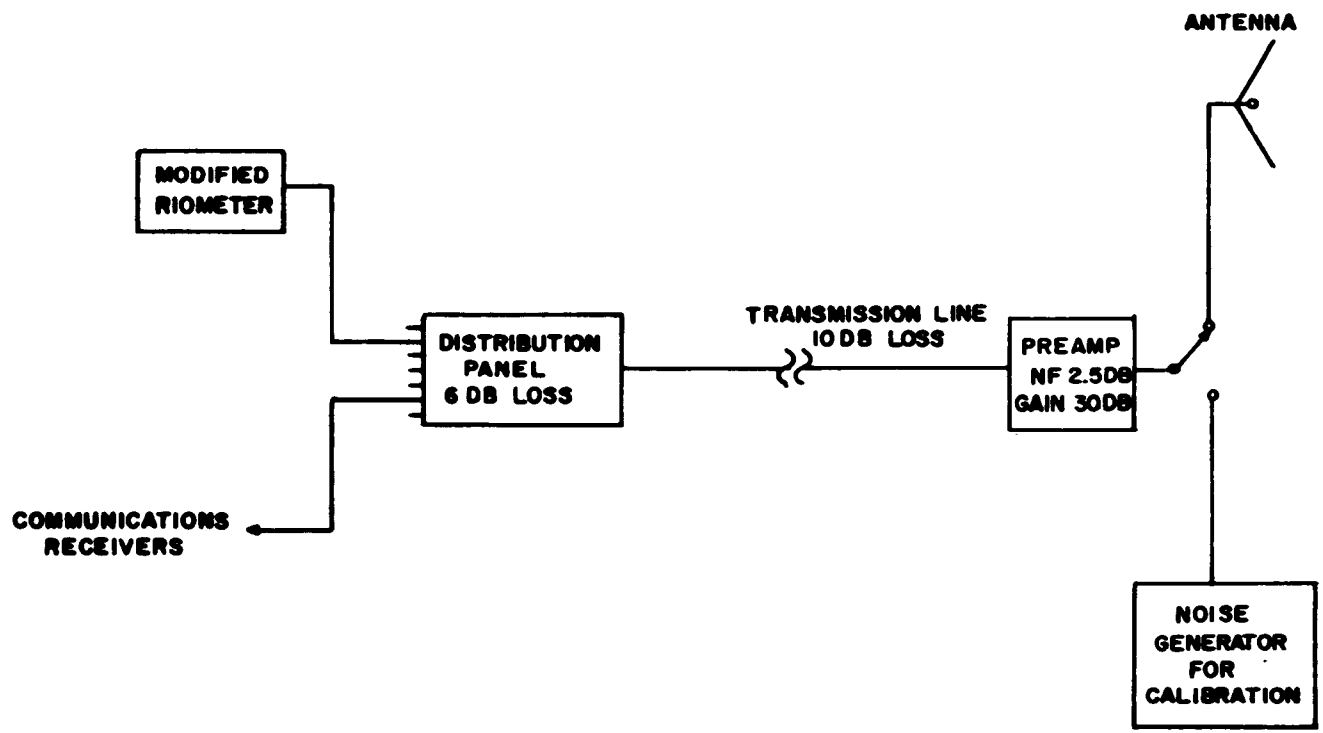

Figure 2-3. System Block Diagram

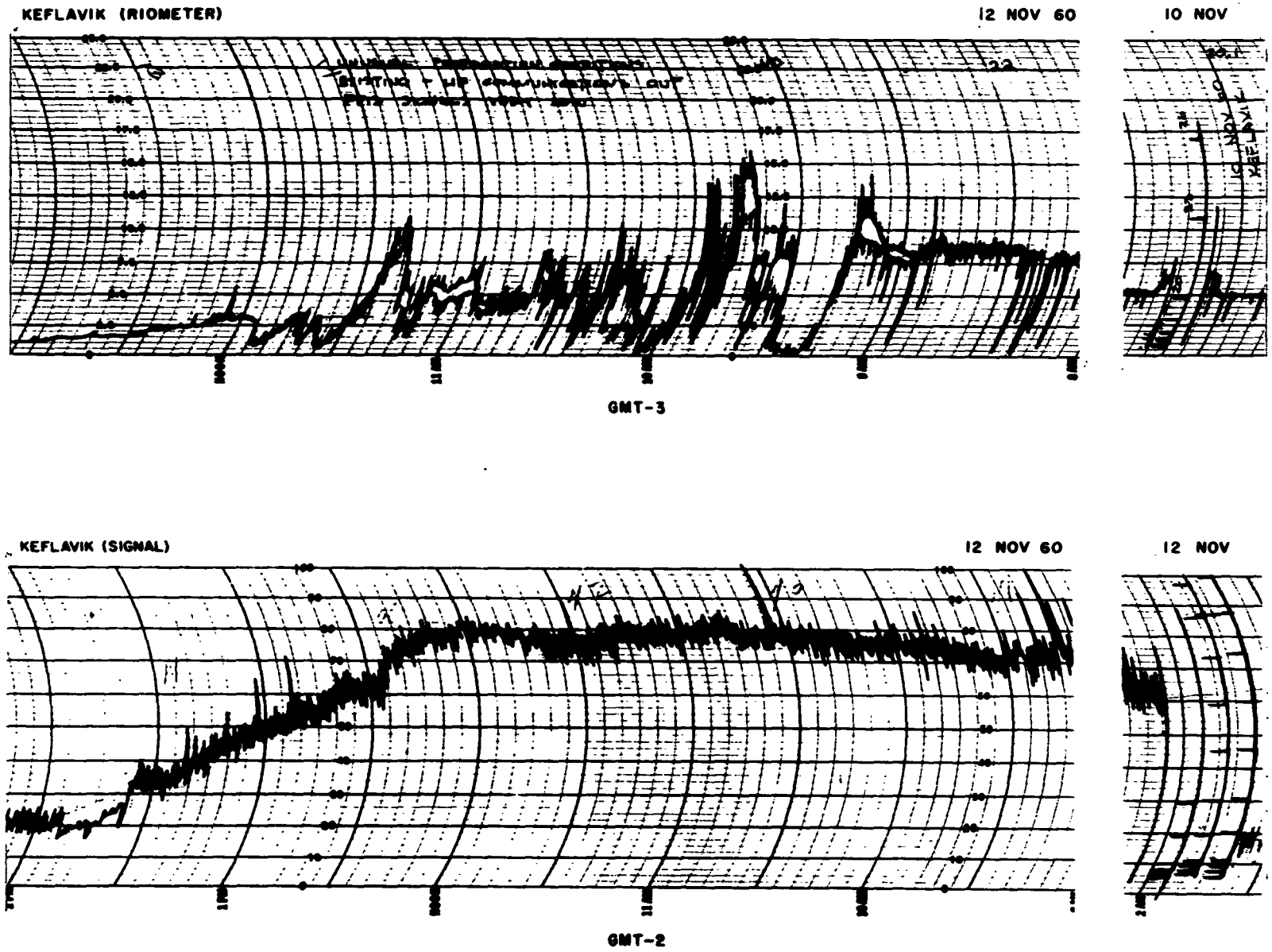

Figure 2-4. Sample Riometer and Signal Recordings, Showing Onset of PCA

SECTION III

BASIC DATA ANALYSIS

The data were taken on graphic recorders at a rate of 3 inches per hour. The noise values at 30 minutes after the hour were scaled and tabulated for each antenna. Notes regarding reasons for outage were attached to the tabulations and, together with the recorder charts, were sent to the Page Washington Office for further analysis.

3.1 TEMPORARY NORMS

Noise values were plotted for each hour for the undisturbed days in three months, April through June 1961. The noise intensity, of course, varies diurnally according to the direction of the antenna beam relative to the cosmic sources. The cosmic noise reaching the antenna is normally absorbed to some extent by the ionosphere. This absorption is small on undisturbed days, especially during the early morning hours when D and F-layer ionization is minimum. The median noise values for each hour for these three months were taken as a temporary norm. Absorption values could then be determined at any time by comparing the received noise with the norm. These temporary norms are shown in Figure 3-1. The ionospheric absorption values obtained relative to these norms are actually measurements of relative absorption, as some residual absorption may be present even on quiet days. This is especially true since the temporary norm is taken from only three months of data. A correction, however, has been derived and is discussed. in Section V.

The data taken on this program have been plotted relative to the temporary norm. The data are shown in Appendix A for the entire period. The ordinate is noise intensity in decibels relative to the norm, which was corrected for sidereal-solar time differences. The abscissa is in 45°W meridian time. The noise-intensity data in Appendix A show frequent excursions above the norm during certain months. This is usually indicative of errors in the norm, although it may, of course, be noise received from other than cosmic sources. The value plotted is noise power (or minus absorption) relative to the norm. Absorption appears as a drop in the trace in the same manner as it appears on the riometer.

Antenna pattern corrections need to be applied before these data can be used in the study of specific absorption events.

3.2 ANTENNA PATTERN CORRECTIONS

For comparison with absorption observed on the scatter signal, it is desirable to interpret the noise absorption observed on the same antennas in

terms of the absorption of a pencil beam at the angle of maximum response of the antenna. The absorption experienced by noise passing through the ionosphere is dependent upon the total path length through the absorbing layers; therefore, for horizontal layers of finite thickness, the absorption is greater for oblique rays than for vertical rays. Allowances must therefore be made for noise received on the antenna at other vertical angles, since this noise passes through the ionosphere either more or less obliquely than the pencil beam, thus experiencing different amounts of absorption. During severe absorption events, the only measurable noise received in the antenna may be that penetrating the ionosphere vertically and being received on the vertical minor lobes of the antenna. Therefore for severe events, the correction for this effect is sizable.

The correction has been computed for the case of a uniform absorbing layer for each of the three antennas. Figure 3-2 shows the intersection of the antenna pattern with the D-layer, taken at a height of 60 km. The computed 3-db and 15-db pattern contours are shown for the main lobe and the important vertical and horizontal minor lobes. The noise received on the horizontal lobes does not introduce error, since the noise power received on those lobes experiences ionospheric absorption equal to that arriving at the same vertical angles in the main lobe. The vertical antenna patterns were integrated and corrections computed using a Bendix G-15D computer. Allowances were made for ionospheric curvature in the computations.

Since noise penetrating normal to the ionosphere is subject to a relatively small amount of absorption even during PCA's, the response of the antenna in that direction is of considerable importance. The theoretical pattern of 60° corner-reflector antennas, based on the usual assumptions, does not have any response beyond $\pm 30^{\circ}$ from the beam. It is, of course, true that a practical antenna will have some minor lobes beyond the theoretical pattern. As a control factor in the calculation a minor lobe 22 db down from the main beam and sinusoidal in shape was assumed between 80 and 90°. The total vertical pattern was then multiplied by a function describing the noise penetrating a curved absorbing ionosphere, and integrated. The relationship between the absorption observed on the antenna, A_r, and the absorption that would have been observed on a pencil beam, $A\theta$, was then calculated. These curves are shown in Figure 3-3 for the three antennas. The confidence limits shown were determined by considering the power received in the added control vertical lobe in each integration. In each case when the power in that lobe was 1/4 or more of the total power received, the results were considered unreliable because of the uncertainty of the response of the antenna toward the zenith.

The parameter $A\theta$ is used extensively in this report as a measure of total ionospheric absorption in the direction of maximum response of the antenna on which the measurements were made. $A\theta$ is the value of noise absorption measured on the riometer corrected for side-lobe effects.

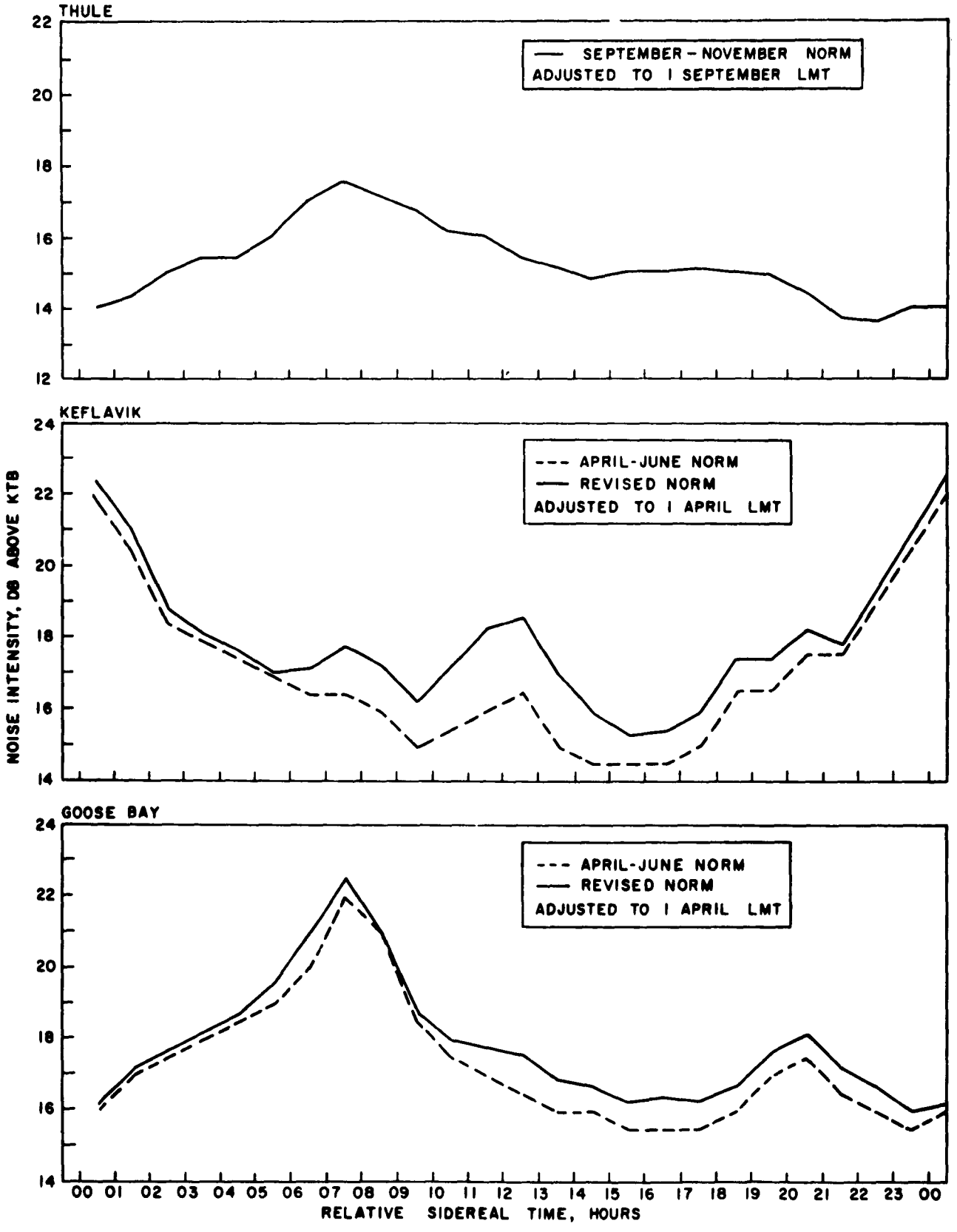

Figuer 3-1. Normal Cosmic-Noise Intensities

PCE-R-9063A

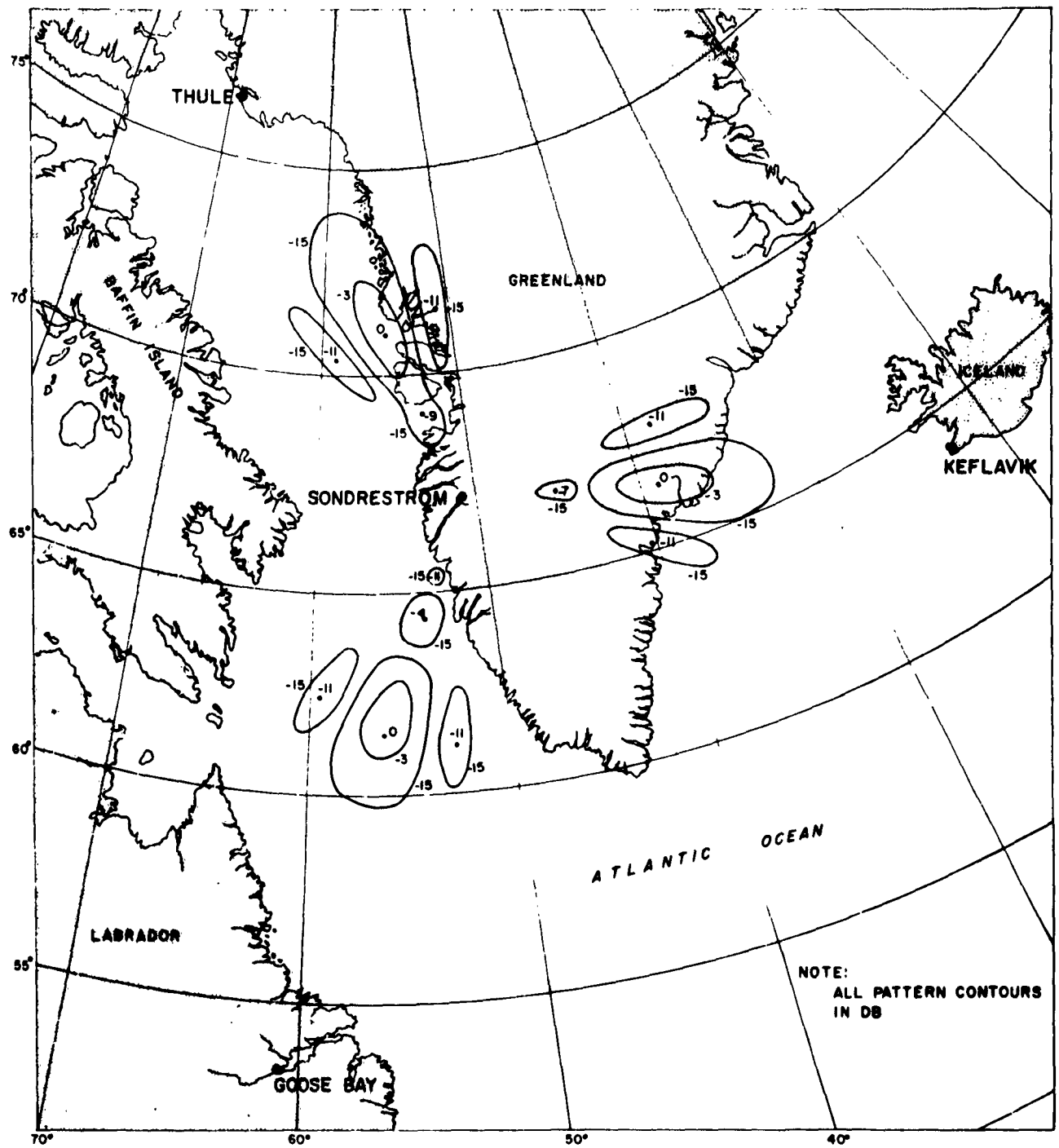

Figure 3-2. Map showing Intersection of Antenna Patterns with D-Layer

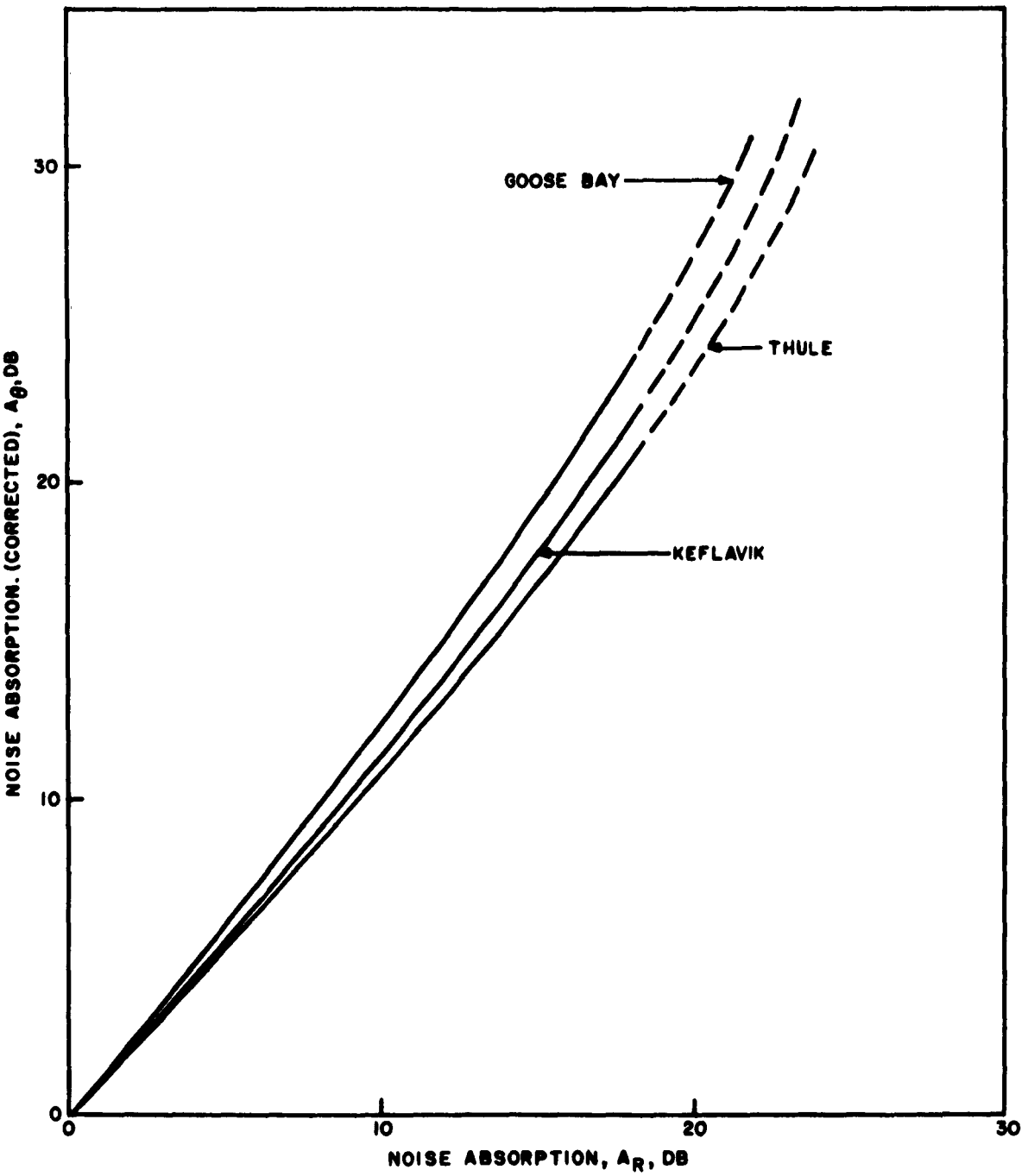

Figure 3-3. Antenna Pattern Correction, A_r vs A_θ

SECTION IV

GENERAL CONSIDERATIONS

4.1 ABSORPTION

The following general considerations of absorption are after similar considerations expressed by Little and Leinbach.[3] Application of the magnetoionic theory of Appleton-Hartree[4] gives ionospheric absorption per unit length for a uniform layer as

$$A_{db} \propto \left(\frac{1}{\mu}\right)\left(\frac{N\nu}{\nu^2 + (\omega \pm \omega_l)^2}\right) , \qquad (1)$$

where A_{db} = the absorption in db per unit length in the layer,
μ = the refractive index,
N = the electron density,
ν = the electron collision frequency,
ω = the angular frequency of the incident radio wave,
ω_l = the angular-gyromagnetic frequency corresponding to the longitudinal component of the magnetic field.

For the case of extraterrestrial radio noise observations at 32 mc, well above the critical frequency, μ may be taken as unity. For many purposes in vhf ionospheric studies, the electron collision frequency ν is considered much less than ω. However, this assumption is not necessarily valid for PCA studies because of the low height of the absorption region, as concluded by Little and Silberstein[5] from frequency-dependence measurements. The electron collision frequency ν, of course, increases rapidly with decreasing height because of the increasingly dense atmosphere.

From equation (1) it can be seen that at low heights, 50-70 km, where the electron collision frequency is the same order of magnitude as, or perhaps higher than, 30 mc, the absorption will tend to become independent of frequency; while at greater heights, where the collision frequency is much less, the absorption will be inversely proportional to the square of the frequency. At a given frequency and height, the absorption in decibels per unit distance is $A_{db} = KN$.

4.2 SCATTERING INTENSITY

Total absorption has been measured in terms of attenuation of cosmic noise. In addition, data are available regarding the signal intensities for

transmissions received by means of ionospheric scattering. The reduction of scattered signals relative to their normal values could be interpreted as a measure of the absorption of the lower ionosphere below the scattering level. Some assumptions must be made, however, regarding the effects of the event on the scattering mechanism itself.

According to the various theories discussed by Bailey, Bateman, and Kirby,[2] the scattered power is directly proportional to f_n^4, where f_n is the critical plasma frequency corresponding to the electron density N.

Therefore,

$$\frac{P_r}{P_t} \propto f_n^4 \propto N^2. \tag{2}$$

It is likely, therefore, that the increased electron density occurring during absorption events will also result in enhanced scattering. The net result of simultaneously increased absorption and enhanced scattering may be either enhanced or lower-than-normal signals, depending upon the severity of the event and the extent to which the signals pass through the absorbing layers.

The combined effect on the normal transmission loss (P_{tn}/P_{rn}) of these two effects can be expressed as

$$\left(\frac{P_{tn}}{P_{rn}}\right)_{db} \propto -20 \log K_1 N_1 + 2 \left(\frac{A}{B}\right) K_2 N_2, \tag{3}$$

where N_1 and N_2 are the electron densities at the scattering and absorbing heights respectively, considering both as uniform layers; K_1 and K_2 are constants involving many factors including layer thickness, and A/B is the fraction of the absorbing layer the signal passes through on its upward or downward passage to the scattering point. For scattering above the absorbing layer, $A/B = 1$, and for scattering totally below the absorption, $A/B = 0$.

It can be seen that the $K_1 N_1$ term causes the transmission loss to decrease as N_1 increases. Conversely, the $K_2 N_2$ term causes the loss to increase. The value of the constants is such that on a normal day the second term is small. For slight increases in electron density above normal, the first term, due to its logarithmic nature, causes a reduction in transmission loss which more than offsets the increased loss due to the second term. As the electron density increases further to much greater values, the first term saturates or levels off, while the second term continues to rise.

These effects, as pointed out by Bailey*, are perhaps an explanation for the enhanced signals at night during absorption events, when the electron density is enhanced, but reduced signals during the day when the electron density is even greater due to photodetachment of many additional electrons by sunlight.

*Private Communication, D. K. Bailey.

SECTION V

DATA ON THE NORMAL IONOSPHERE

As a basis for understanding ionospheric structure during PCA events, it is necessary to refine the temporary norm previously established and to determine the absorption of the normal ionosphere at these latitudes insofar as possible.

The following technique is due to Mitra and Shain, [6] who have shown that the normal ionospheric absorption could be divided into D and F-layer components. Absorption in the D layer is caused principally by very high electron-collision frequencies, and in the F layer by high electron content. Except in the case of aurora, absorption at heights between the D and F layers is usually much less since both the electron content and collision frequency are relatively low.

5.1 F-LAYER ABSORPTION

Many of the current workers in this field elaborate on the method introduced in the Mitra paper to isolate F-layer absorption This technique attributes the component of the absorption which is correlated with the vertical-incidence critical frequency of the F layer, f_oF2, to F-layer absorption It is recognized, however, that there may be F-layer absorption components not correlated with f_oF2, since the f_oF2 values are not dependent upon the state of the F layer above the reflection point. Extra absorption possibly attributable to the ionization in the upper F regions has been reported by Lusignan [7] and Ramanathan et al. [8,9]

The method, however, does isolate absorption present in the F region and has been used here. Absorption values were taken four times daily--0000, 0600, 1200, and 1800--on each circuit for each day of valid data and plotted against f_oF2 from Narsarssuak, Greenland. A sample plot for noon values in December 1960 for the Goose Bay and Keflavik antennas is shown in Figure 5-1. The curve fit to the data is from Lusignan [7] for f_oF2 vs. absorption at 27.5 mc, corrected to 32 mc. The absorption values in decibels have also been multiplied by three, so they may be applied to these oblique (rather than vertical) F-layer measurements. The curve (Fig. 5-1) was adjusted vertically so that half of the points fell each side of the curve, a median of sorts. The $A\theta$ intercept of the curve has been taken as the median absorption value for that month and time of day excluding absorption due to the F layer. It should be noted that this excludes consideration of possible "extra" F-layer absorption present in the upper F layer. Since the f_oF2 data show a very small amount of absorption at these latitudes correlated with f_oF2, as discussed below, it has been assumed that possible extra absorption will also be small.

In the above analysis, points have been plotted only when f_oF2 values were available. This automatically excludes periods of blackout and therefore utilizes data from days not seriously disturbed. Auroral effects may account for some of the scatter in the data.

Although F-layer absorption has been included in this analysis, the results show it is a very small factor. The vertical-incidence sounder data show f_oF2 exceeding 10 mc only 9 percent of the noon observations for November and December 1960 and January 1961. In terms of F-layer attentuation, this means oblique-incidence attentuation of 0.5 db or vertical-incidence attentuation of 0.15 db exceeded only 9% of the winter noon values.

5.2 D-LAYER ABSORPTION

The monthly median absorption values taken at the previously specified times were plotted versus sidereal time after the F-layer absorption was removed by the above procedure. Data for all hours when the antennas were pointing at the same point in space are plotted at the same point on the abscissa even though the local solar time varies according to the time of year. It may be used to correct the norm by means of extracting the component correlated with sidereal time variations and applying these values as norm corrections.

It was noted in this sidereal time plot that the noon values of absorption for June and July for both Keflavik and Goose Bay antennas were noticeably higher than the median absorption values. The average of these two values relative to the median was taken as normal D-region absorption, dependent upon solar zenith angle. This value of June and July noon D-region absorption was then used to compute D-region absorption for all other months and times according to the variation in solar zenith angle and season from data in NBS Circular 462.[10] Based on the June and July values, the computed D-region absorption for each month and hour was subtracted from the total absorption measured at those times. A plot of these corrected values is shown in Figure 5-2. The line connects the median value for each hour. The position of the symbols Je and Jy denote the values of absorption at noon during June and July respectively before D-region absorption was removed.

The D-region absorption determined by this technique is shown in the table below. The measured oblique values, their vertical-incidence equivalent, and the absorption computed separately for these latitudes from NBS Circular 462 are shown.

Normal D-Layer Absorption

Noon, June-July

Path	Measured Absorption		Computed Absorption
	Oblique Incidence	Vertical Incidence Equivalent	Vertical Incidence
Goose Bay	1.5 db	0.25 db	0.24 db
Keflavik	1.0	0.17	0.23

The line connecting the median values shown in Figure 5-2 was applied as a correction to the norm since it represents a component of the daily median noise intensity values which is correlated with sidereal time variations.

5.3 AURORAL EFFECTS

The oblique riometer measurements reported here did not prove to be very sensitive to auroral absorption effects. Auroral absorption was occasionally observed on the charts as shown at the top of Figure 5-3. The magnitude of the absorption effects at oblique-incidence ranges from less than a decibel to usually not more than 3 db. They were most obvious on the charts when the noise was running high because of the typical nonlinearity of the calibration.

Several reasons can be postulated for the infrequent observation of auroral absorption:

a. As previously discussed (par. 2.4.3, "Interference"), the recording system was desensitized when excessively strong signals were received. This usually caused the noise recording to drop to near zero on the chart. To the extent that strongly enhanced signals were received during periods of auroral absorption, the absorption effects were obscured. As shown in Figure 5-3, for example, short periods of strong signals did occur during the absorption period. A good correlation can be seen between the periods of high signal and the downward spikes on the noise recordings caused by preamplifier overload. Some thinning of the signal trace, known as sputter, is also identified with auroral effects.[2]

Periods of strong signals occurred frequently on these paths. It is felt that auroral absorption would have been observed more frequently during these high-signal periods if the equipment had not been desensitized by the strong signals.

b. Although narrow antenna beams were used for these oblique-incidence measurements, the actual area of the E region included in the main beam was much greater than usually observed with vertical riometers due to the great distances involved. In terms of E-region area observed, this experiment covered about 10 times the total area covered by the antennas usually used with vertical riometers. The fact that few identifiable auroral events were observed may also be partially the result of the basic insensitivity of this system to small absorption areas. These negative results may indicate that auroral absorption effects are generally limited to sizes substantially smaller than the size of our beam at the E region. Since these effects are readily observable on vertical riometers,[3] the size of typical auroral absorption areas is therefore thought to not usually exceed approximately 10,000 km.[2]

c. The question of the nature of the auroral absorption areas should be considered. If the auroral absorption clouds lie in horizontally stratified layers, the secant factor for absorption should apply, and oblique measurements should show greater absorption than vertical measurements. Since auroral absorption was observed infrequently and at magnitudes not exceeding those of vertical measurements generally observed by others, it is possible that the absorbing regions are not horizontally stratified layers.

d. In studying auroral absorption by riometer techiques, the question of auroral noise should be considered. Of course, if there were noise generated in or near auroral absorption areas but still in the beam of the antenna, the absorption effects would be obscured, Egan and Peterson [11] have reported auroral noise at hf observed at Stanford on a backscatter sounder and at Pullman and Meanook on riometers as well.

The possibility of aurorally generated noise is supported by reference to Figures 5-2 (a) and (b). The noise values for September, October, and November--months of high auroral activity--have been labeled. It can be seen that for Goose Bay the September and October absorption values for both 1960 and 1961 were substantially lower than the median. Values for both years agree rather well. It is possible that this "low absorption" was really a measurement of auroral noise, the mean for the month being 1 to 1.5 db greater than the cosmic-noise norm.

For the Keflavik antenna, the same is true except that the "maximum noise" months are October and November. It is not clear why this should be different. However, the area of the ionosphere under study is slightly north of the maximum auroral belt, while the Goose Bay antenna looks at the center of the auroral belt.

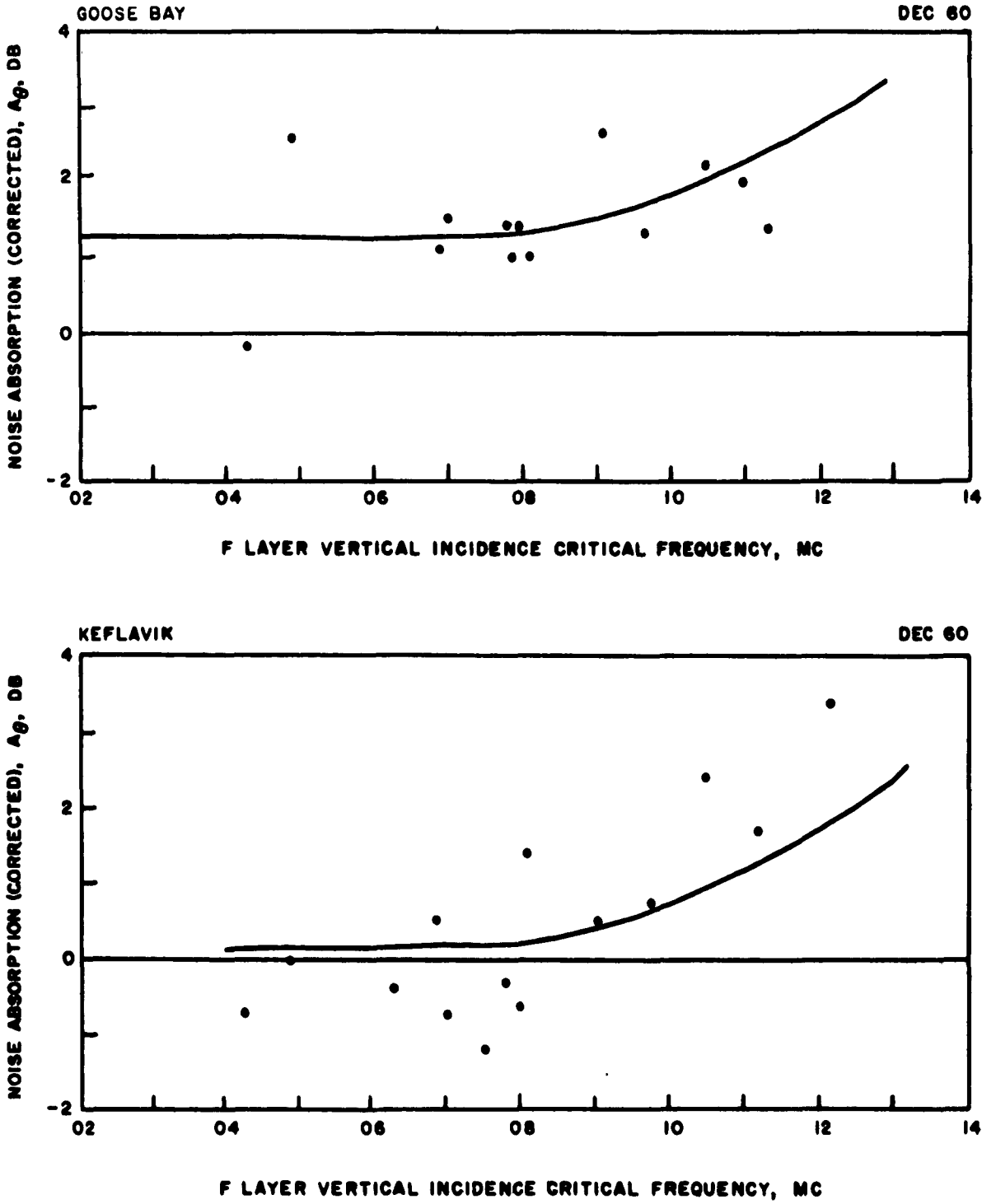

Figure 5-1. F-Layer Vertical-Incidence Critical Frequency vs A_θ

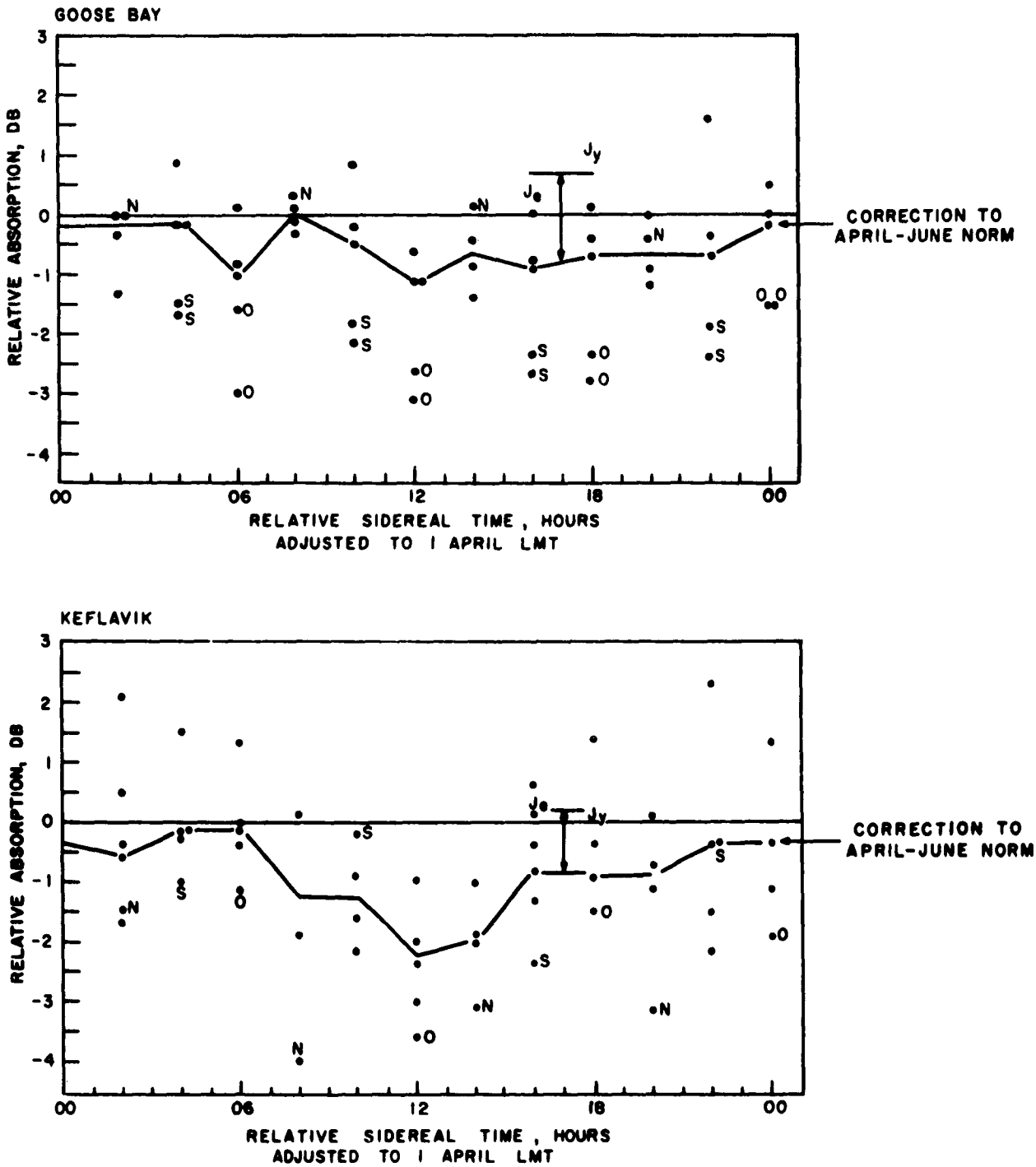

Figure 5-2. Monthly Median Absorption for Specified Hours (LMT) Relative to April-June Norm

PCE-R-9063A

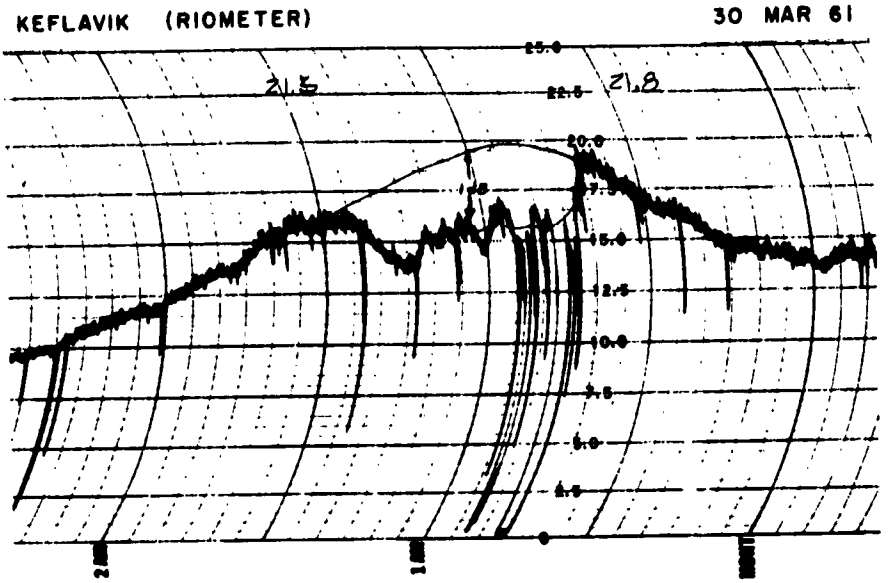

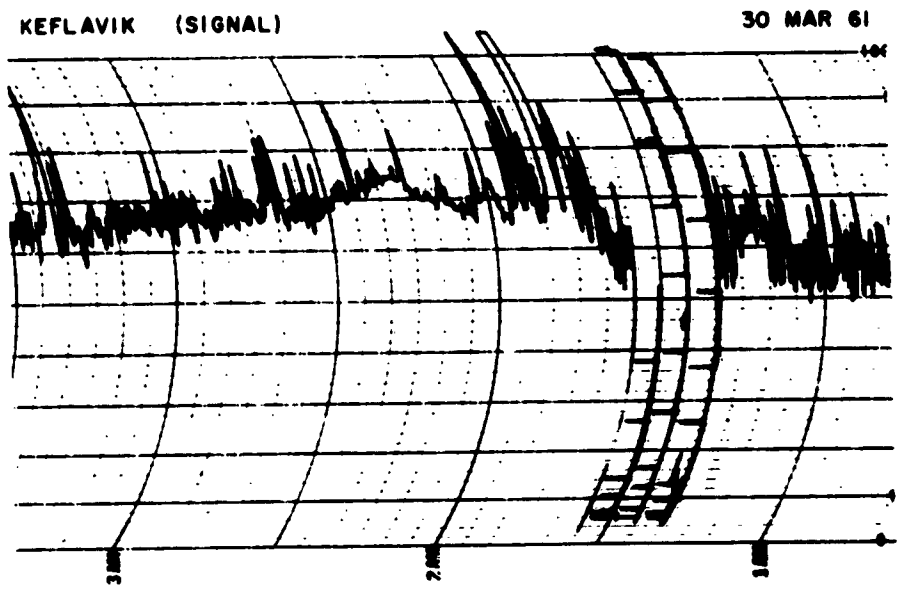

Figure 5-3. Auroral Effects on Riometer and Signal Recordings

SECTION VI

ANALYSIS OF POLAR CAP ABSORPTION EVENTS

As mentioned previously, this experiment is particularly interesting with respect to the study of polar-cap absorption events. The riometer data can be interpreted in terms of total ionospheric absorption at the angle of maximum response of the antenna. The signal intensity data provide information relative to the attenuation through the D region below the height of the scattering. Certain assumptions must be made regarding the scattering height and intensity, and these are discussed later.

6.1 PCA EVENTS

The following polar-cap absorption events were identified during the test period:

1	1960	Sep 2, 3, 4, 5
2		Nov 12, 13, 14, 15
3		Nov 21, 22, 23
4	1961	Jul 12, 13, 14, 15
5		July 18, 19, 20
6		Sep 7, 8
7		Sep 11, 12
8		Sep 28, 29, 30

Of these events, the first five were examined in detail, the signal-intensity data being unavailable for the others at this writing.

6.1.1 September 1960 Event

On 2 September, the Keflavik riometer showed an absorption event commencing about 1700 GMT, perhaps due to a 2+ flare at 0620. A sudden commencement in magnetic activity occurred about 1700 GMT also. The following three days were disturbed magnetically.

The behavior of the signals, together with riometer absorption for the period of the event, is plotted in Figure 6-1. The dashed lines are normal signal intensities taken from a period of several days immediately before and after the event. A_θ is plotted relative to the revised norm except for Thule, which had insufficient valid data to permit refinements. Small negative values of A_θ are probably not significant. Large negative values occurring occasionally during September, October, and November may be due to auroral noise. See par. 5.3.

The Keflavik circuit showed signal and noise absorption starting at 1700 and continuing through the daylight hours each day through the 5th.

The Goose Bay circuit showed a signal enhancement the night of 2 September, followed by severe absorption during the daylight hours of the 3rd. Lesser amounts of absorption occurred during the daylight hours of the 4th and 5th. The riometer showed no significant absorption on this antenna, although recordings did not commence until 1700 GMT on the 5th. The Thule circuit showed little signal absorption during the entire period. The noise data show wide fluctuations even on normal days and are probably not significant.

6.1.2 November 1960 Events

On 12 November at 1130 GMT, the Keflavik riometer trace began to show erratic abnormal absorption (see Figure 2-4). Two hours later a sudden commencement occurred, as shown in Figure 6-2 (perhaps due to an importance 3 flare at 1014 GMT on 10 November). Shortly thereafter, at 1323 GMT, another importance 3+ flare occurred. At 1430 GMT, a PCA event commenced. Its effects were evident through the 17th. A plot of signal behavior and riometer noise absorption for this period is shown in Figure 6-3.

The Goose Bay circuit showed enhanced nighttime signals and attenuated daytime signals through 16 November. The riometer showed high absorption for several days following the 12th, even at night, gradually reducing in intensity and showing the usual increase in absorption during the daylight.

The Keflavik circuit showed signal enhancements at night and attenuated signals in the daytime. The daytime signal absorption was less than on the Goose Bay circuit.

The Thule circuit showed enhanced signals during the entire event except for a short period in the early afternoon each day when some signal absorption was evident.

This event may have been acually two PCA's, one commencing on 12 November and the other on the 15th.

On the 21st, after a sudden commencement, absorption was observed on the Keflavik and Goose Bay riometers, as shown in Figure 6-3, Sheet 2. Some signal absorption was evident on the Goose Bay signal. None was evident on the Keflavik signal. The Thule signal was enhanced. The absorption observed may be largely auroral, although the slight signal enhancements and attenuations indicate the presence of some enhanced (D-layer) ionization.

6.1.3 July 1961 Events

On 12 July 1961 at 1200 GMT, the Goose Bay and Keflavik riometers showed absorption commencing. The start was much more abrupt on the Keflavik recording. The absorption continued for four days, showing the

usual diurnal variation. This event may be attributed to the effects of an importance 3 flare at 1000 GMT on the 12th. A sudden commencement in magnetic activity followed at 1115 GMT on the 13th, during the PCA, and continued for several days. See Figure 6-4.

The only signal data available were those for Keflavik, since the other circuits had been shut down. The Keflavik signal showed some absorption on the 12th, lasting until about midnight GMT. A slight nighttime enhancement then occurred, followed by severe absorption during most of the 13th. As the event subsided, less signal absorption was evident on the 14th, followed by some signal enhancement on the 15th.

Conditions were quiet until 18 July, when the riometer again showed signal absorption beginning during midday. This may be associated with the effects of an importance 3+ flare at 0930 GMT on the 18th.

The Keflavik signal recordings showed signal absorption commencing about 1200 GMT. It continued during the day until late evening when some signal enhancement occurred. The absorption returned early on the 19th and gradually diminished in intensity. Conditions on the 20th were almost normal. Some absorption appeared on the Goose Bay riometer through 22 July.

6.1.4 Discussion of PCA Events

Although in many respects the events observed seem to be quite different, there are some features that can be cited as general characteristics:

a. Diurnal Variations. The absorption has a strong diurnal characteristic, increasing markedly during the daylight and diminishing at night. Although there does appear to be some delay in the build-up and decay, it appears to be strongly dependent upon solar zenith angle.

As discussed in Section 4, the signal intensity received is dependent upon not only the absorption in the D layer but the scattering intensity as well. Weak absorption, evidenced on the riometer, may accompany enhanced signals. This is often true at night.

b. Absorption Intensity. The five events studied here show greater daytime absorption at latitudes corresponding to the auroral belt than occurs farther north in the polar cap region. This may be due either to latitude concentration of the incoming particles, causing the enhanced ionization, or to the greater solar radiation at the lower latitudes. The latter appears more likely, as there is also a tendency for the effects of the event to persist longer at the higher latitudes.

c. Timing. The PCA has been generally thought to follow the occurrence of a solar flare by a few hours but to precede by a day or so the occurrence of a sudden commencement in magnetic activity resulting from

the flare effects, if one occurs. This general pattern is evident in most of the events studied here, although the abundance of flares and generally high level of magnetic activity during the period studied tend to obscure positive evidence of such an interdependent relationship.

6.2 SIGNAL AND NOISE ABSORPTION COMPARISONS

Certain days during the PCA events are of particular interest relative to the relationship between signal and noise absorption. First, the anticipated relationships between signal and noise absorption are considered.

6.2.1 Computed Relationships

If the path loss for normal conditions can be represented as in equation 3, and the path loss at a particular time during disturbed conditions as

$$\left(\frac{P_{td}}{P_{rd}}\right)_{db} = -20 \log K_1 N_1' + 2 \left(\frac{A}{B}\right)' K_2 N_2', \tag{4}$$

where N_1' and N_2' are disturbed values of electron density and $\left(\frac{A}{B}\right)'$ is another height factor applicable at the time, then the signal absorption relative to normal conditions may be represented as

$$A_s = -20 \log \frac{N_1'}{N_1} + 2 \left(\frac{A}{B}\right)' K_2 N_2' - 2 \frac{A}{B} K_2 N_2. \tag{5}$$

If, for the sake of simplification, we assume the scattering height and the shape of the electron profile with height are the same as during normal conditions (i.e., the electron density at all heights is proportionally enhanced), then

$$\left(\frac{A}{B}\right)' = \left(\frac{A}{B}\right),$$

and

$$A_s = -20 \log \frac{N_1'}{N_1} + 2 \left(\frac{A}{B}\right) K_2 (N_2' - N_2). \tag{6}$$

If all of the abnormal absorption occurs in a uniform layer having an electron density of N_2', then the absorption measured on the riometer A_θ, is

$$A_\theta = K_2 (N_2' - N_2), \tag{7}$$

and

$$A_s = -20 \log \frac{N_1'}{N_1} + 2\left(\frac{A}{B}\right) A_\theta. \tag{8}$$

In the above expression, it was assumed that the scattering height and the shape of the electron density vs. height profile was constant.

If it is assumed instead that the scattering takes place above the absorbing layer--i.e., $\left(\frac{A}{B}\right) = 1$--the above assumptions are not required and the expression simplifies to

$$A_s = -20 \log \left(\frac{N_1'}{N_1}\right) + 2A_\theta, \tag{9}$$

where

$$A_\theta = K_2 (N_2' - N_2). \tag{10}$$

The assumption of scattering above the absorbing region is reasonably good, at least relative to normal conditions. Bailey, Bateman, and Kirby[2] consider scattering heights in the arctic at 75-90 km. Little and Silberstein[5] measure polar cap absorption at about 60 km. Enhanced scattering at lower levels during PCA events is possible and is discussed later.

To evaluate the above equation, values of N_1 and N_2 for normal conditions must be assumed. The results of rocket sounding measurements by J. C. Seddon and J. E. Jackson reproduced by Ratcliffe[12] show noon values of electron density over Fort Churchill, Canada, during July of about 10^4 electrons/cc at 85 km and 10^3 electrons/cc at 60 km, extrapolating the data presented. In spite of the low electron density in this range, the absorption is maximum in the 60-70 km range, probably due to the high collision frequency at these low altitudes. Nighttime values during the winter were very low at 85 km and unmeasurable at 60 km.

From the above, an approximately two-to-one normal daytime difference in electron density exists between the usual scattering and absorbing regions. Therefore, N_2 will be taken as equal to $N_1/2$, and $N_2' = N_1'/2$, in the following computations.

From equation 10 above,

$$A_\theta = \frac{N_1 K_2}{2}\left(\frac{N_1'}{N_1} - 1\right) \tag{11}$$

As discussed earlier, when the electron density increases from normal values, the signal scattering is enhanced as well as the absorption. The net effect for small increases in electron density is signal enhancement and, for large increases in electron density, signal attenuation, due to much increased absorption. Typical values of crossover where no signal enhancement or absorption is noted occur at about 3-db absorption as observed on the riometer, as is shown later.

If this occurs at an electron density N_3, equation 12 follows:

$$3 = \frac{N_1 K_2}{2} \left(\frac{N_3}{N_1} - 1 \right) . \tag{12}$$

Also, from equation 9,

$$0 = -20 \log \left(\frac{N_3}{N_1} \right) + 2(3); \tag{13}$$

therefore,

$$\frac{N_3}{N_1} = 2 \tag{14}$$

and

$$N_1 K_2 = 6. \tag{15}$$

Therefore, for the example,

$$A_\theta = 3 \left(\frac{N_1'}{N_1} - 1 \right) \tag{16}$$

and

$$A_s = -20 \log \left(\frac{N_1'}{N_1} \right) + 2A_\theta . \tag{17}$$

These equations have been used to plot A_s vs. A_θ for various ratios of $\frac{N_1'}{N_1}$ and are shown in Figure 6-5.

It can be seen that the maximum signal enhancement predicted is only about 1 db and that the slope of the curve in the $0 < A_s < 15$ range is

about 1. For much higher values of $\frac{N_1'}{N_1}$, the slope approaches 1/2 because the signal was assumed to pass completely through the absorbing regions twice. It never reaches 1/2, however, due to the continued enhancement of scattering as N_1' increases.

According to the simple model described here, no conditions can exist which would allow the slope of the curve to be less than 1/2. Any value greater than 1/2 can, however, result if the scattering takes place inside or below the absorbing region i.e., $\frac{A}{B} < 1$. Likewise, no enhancements in signal greater than 1 db would be expected for $\frac{A}{B} = 1$, although greater enhancements would result if a portion of the scattering occurred in or below the absorbing region ($\frac{A}{B} < 1$).

6.2.2 Absorption Measurements

The computed relationships discussed above were compared with $A\theta$ vs. A_s data selected from several days of the previously discussed PCA events. The days selected were those of moderate absorption where both signal and noise absorption values were available. Noise intensities on days having greater absorption fell below resolvable levels and thus could not be used.

Figure 6-6 shows $A\theta$ vs. A_s for 3, 4, and 5 September 1960 on the Keflavik antenna. A line has been fit to the points for values $0 < A_s < 15$ by the method of least squares for orthogonal deviations from the line. The equation of the line and the correlation of the data with the line are shown in the illustrations. Data for $A_s < 0$ were excluded since it can be seen from Figure 6-5 that a straight line would not approximate the curve including those values. Value of $A_s > 15$ were excluded since the riometer equipment could not accurately resolve the corresponding noise levels in determining $A\theta$. Data for 22 and 23 November are shown in Figure 6-7, and for 18, 19, and 20 July in Figure 6-8. The values of the slope and $A\theta$ intercept for these days from the straight line fit to the data are:

Date	Correlation	Slope	$A\theta$ Intercept
3 Sep	0.61	0.373	1.1
4 Sep	0.84	0.25	3.5
5 Sep	0.53	0.12	3.5
22 Nov	0.79	0.34	1.8
23 Nov	0.27	0.13	0.9
19 Jul	0.71	0.63	2.0

It is interesting to note that although the line fitting the data in most cases is reasonably good, as indicated by the correlation coefficients, only one of the lines has a slope exceeding 0.5, the previously determined minimum expected value. Furthermore, it is interesting to note from the curves that the signal enhancements much exceed the values predicted by the simple model.

The following conclusions are drawn from these results:

a. At night, the signal intensities are enhanced much more than would be predicted from the model. This suggests that the dominant scattering region at these times is largely below the absorbing layer. Bailey* has suggested the existence of a low turbulent layer which does not normally contribute to the scattering, owing to insufficient numbers of electrons. During the early part of the event, the influx of high-energy protons may penetrate to this low level, causing sufficient numbers of electrons in the turbulent layer to form the dominant scattering strata. Thus the signal is not attenuated as would be expected.

b. When the ionization increases during the day, the signal is also attenuated, indicating this component of absorption is below the scattering region.

c. For periods of high absorption during the day, the slope of the line indicates that the signal absorption is greater than twice the "total ionospheric absorption," an impossible situation. This is especially true for the days near the end of the event, as can be seen in the above table. This indicates again the likelihood of auroral noise, commencing late in the event and received by the riometer, thus obscuring the cosmic noise and resulting in erroneous attenuation measurements.

---

*Private communication, D. K. Bailey.

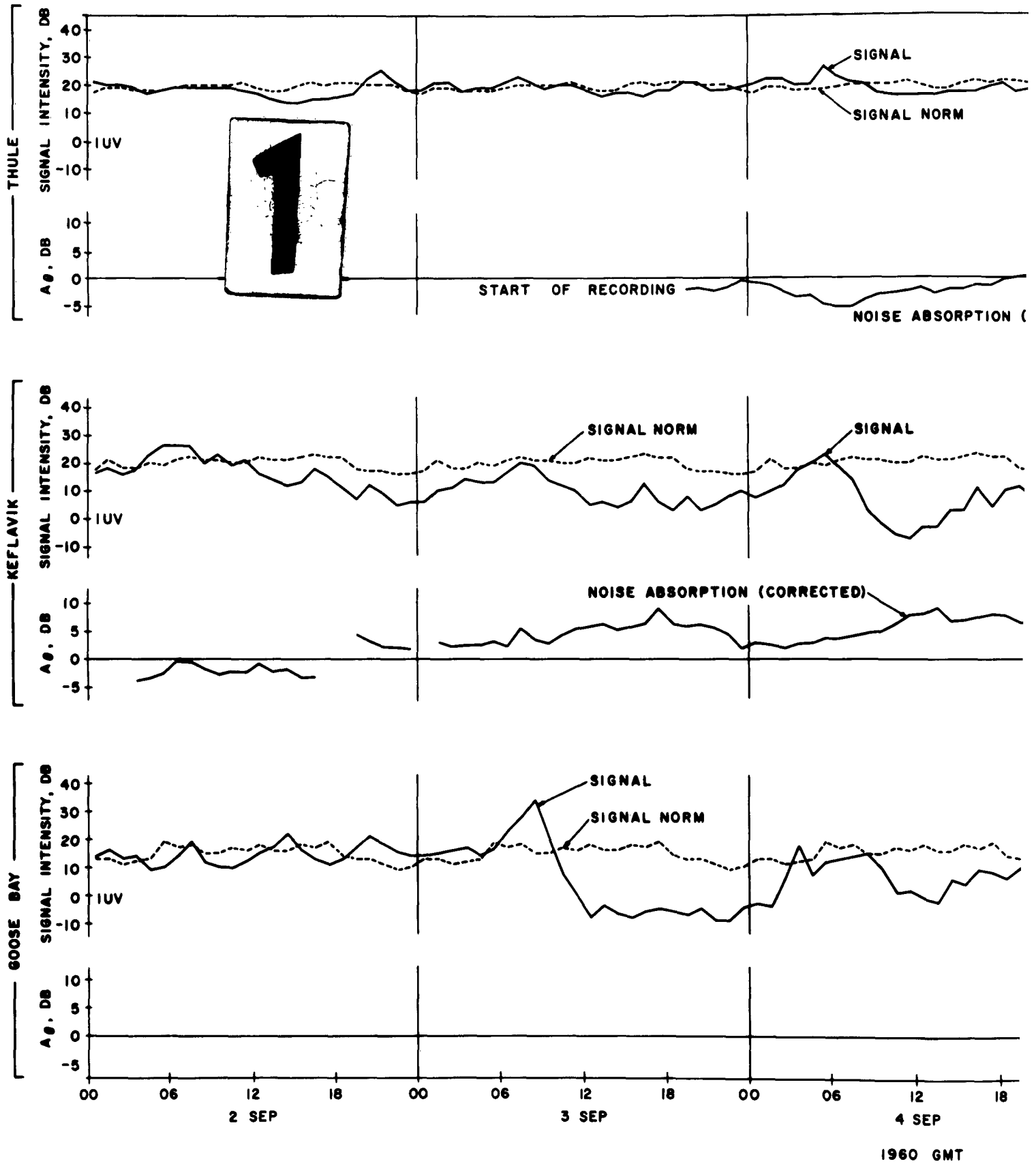
THULE
SIGNAL INTENSITY, DB
40
30
20
10
0
-10
1UV
SIGNAL
SIGNAL NORM
Aϕ, DB
10
5
0
-5
START OF RECORDING
NOISE ABSORPTION (
KEFLAVIK
SIGNAL INTENSITY, DB
SIGNAL NORM
SIGNAL
1UV
Aϕ, DB
NOISE ABSORPTION (CORRECTED)
GOOSE BAY
SIGNAL INTENSITY, DB
SIGNAL
SIGNAL NORM
1UV
Aϕ, DB
00
06
12
18
2 SEP
3 SEP
4 SEP
1960 GMT

PCE-R-9063A

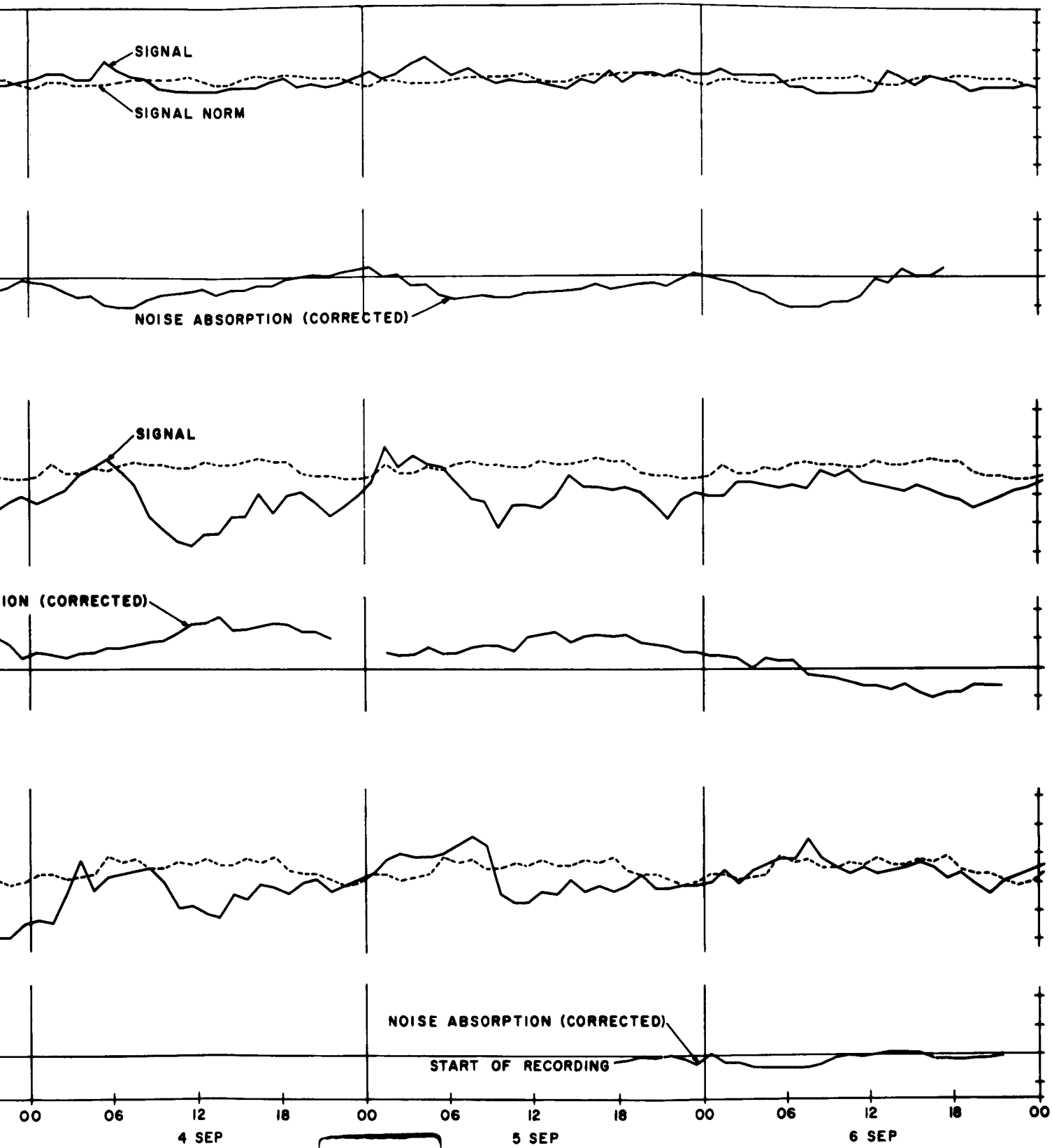

Figure 6-1. Signal and Noise Absorption Variations for the September 1960 Event

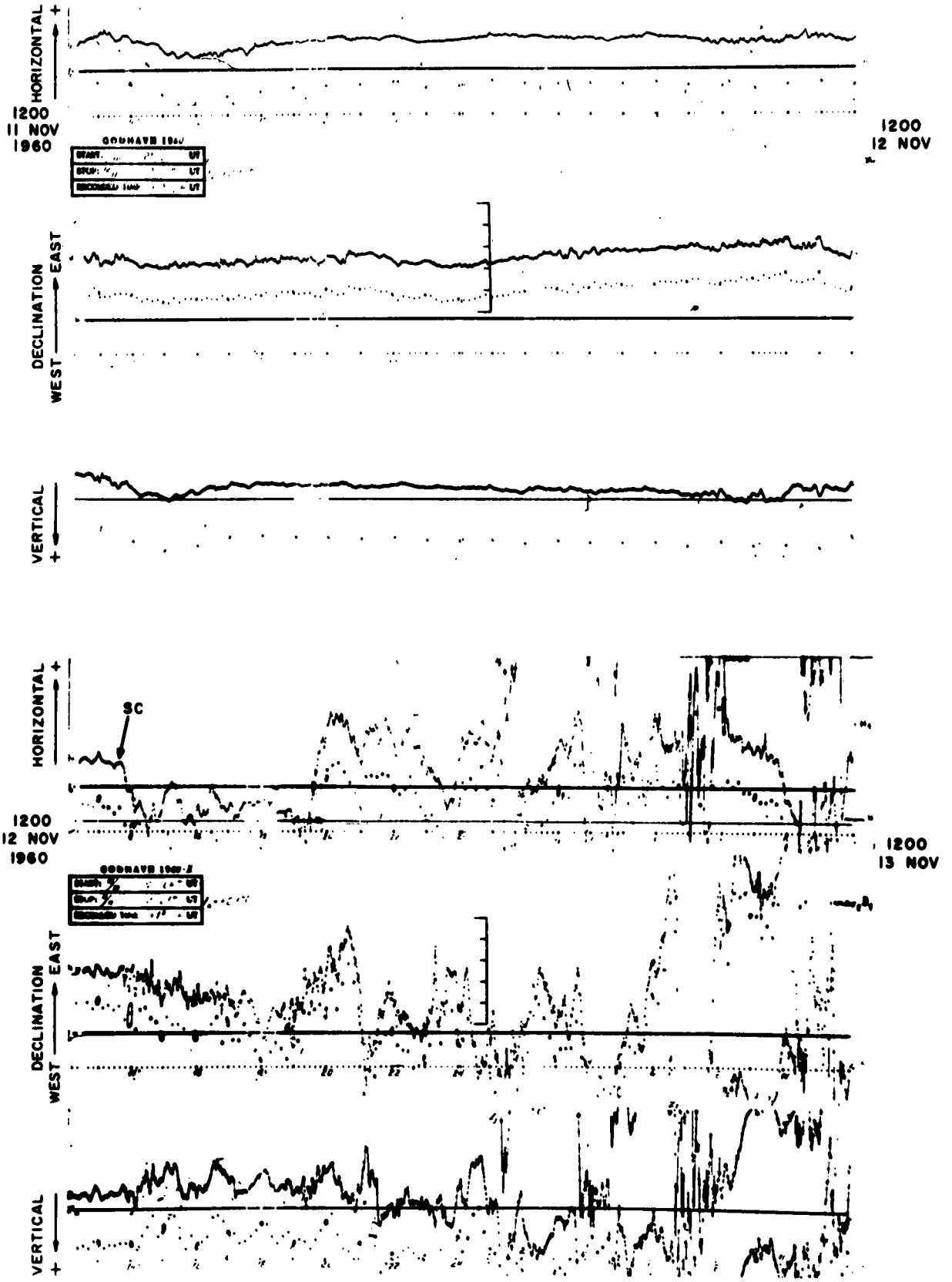

Figure 6-2. Magnetograms from Godhaven Showing Commencement of 12 November 1960 Event

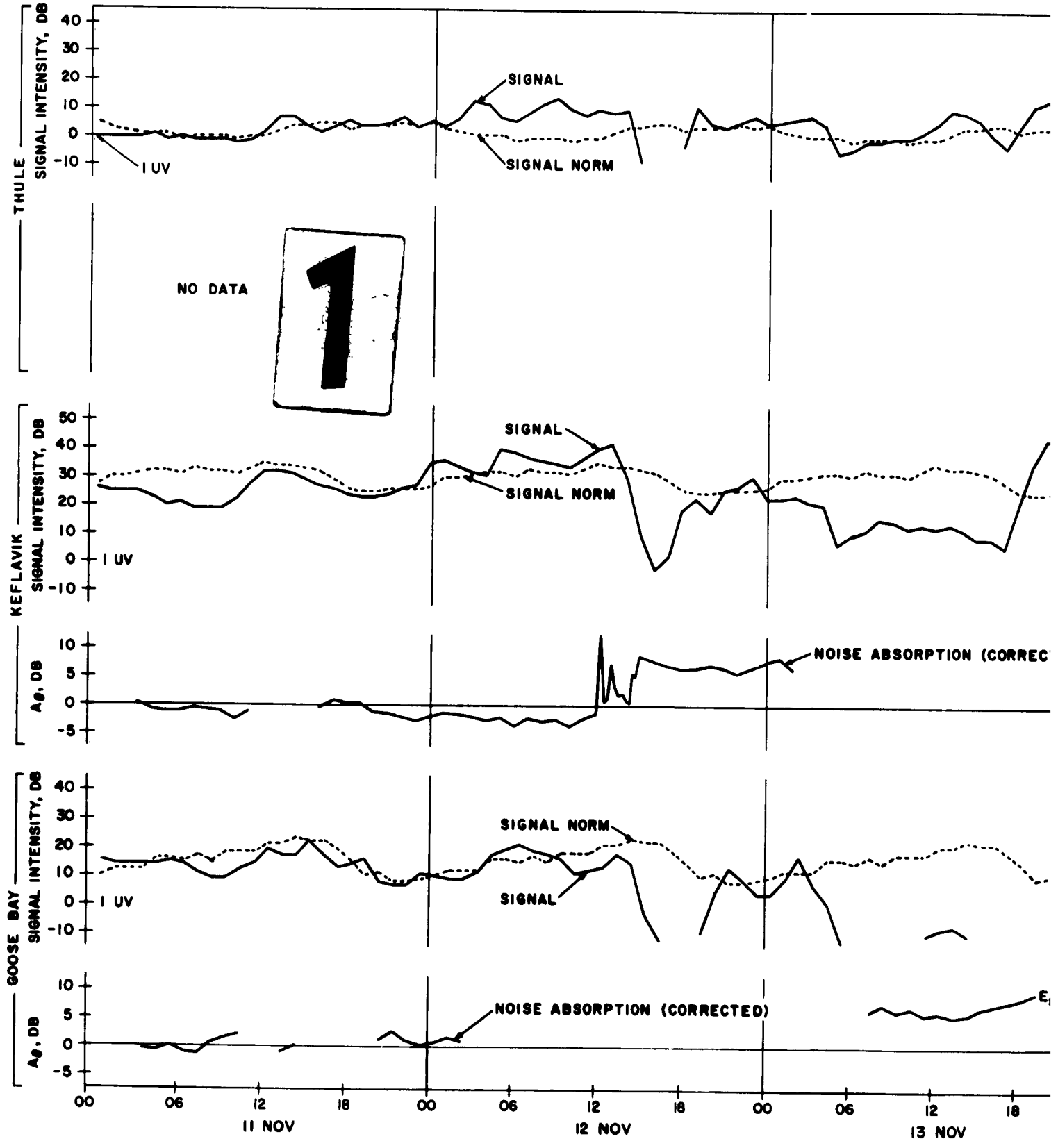
THULE
SIGNAL INTENSITY, DB
40
30
20
10
0
-10
SIGNAL
1 UV
SIGNAL NORM
NO DATA
1
KEFLAVIK
SIGNAL INTENSITY, DB
50
40
30
20
10
0
-10
SIGNAL
SIGNAL NORM
1 UV
Aø, DB
10
5
0
-5
NOISE ABSORPTION (CORREC
GOOSE BAY
SIGNAL INTENSITY, DB
40
30
20
10
0
-10
SIGNAL NORM
1 UV
SIGNAL
Aø, DB
10
5
0
-5
NOISE ABSORPTION (CORRECTED)
00
06
12
18
00
06
12
18
00
06
12
18
11 NOV
12 NOV
13 NOV

PCE-R-9063A

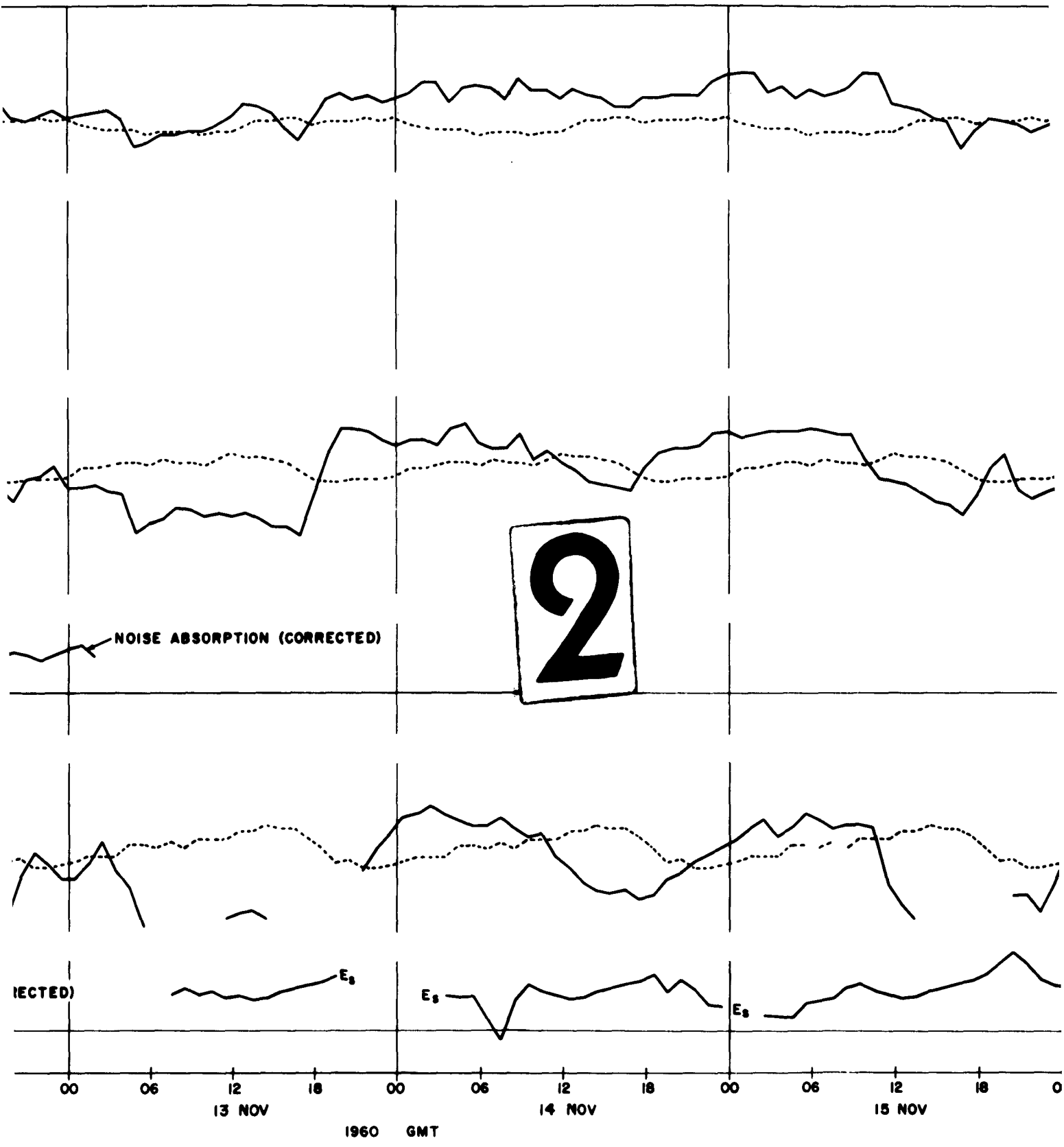

Figure 6-3.
Variations fo

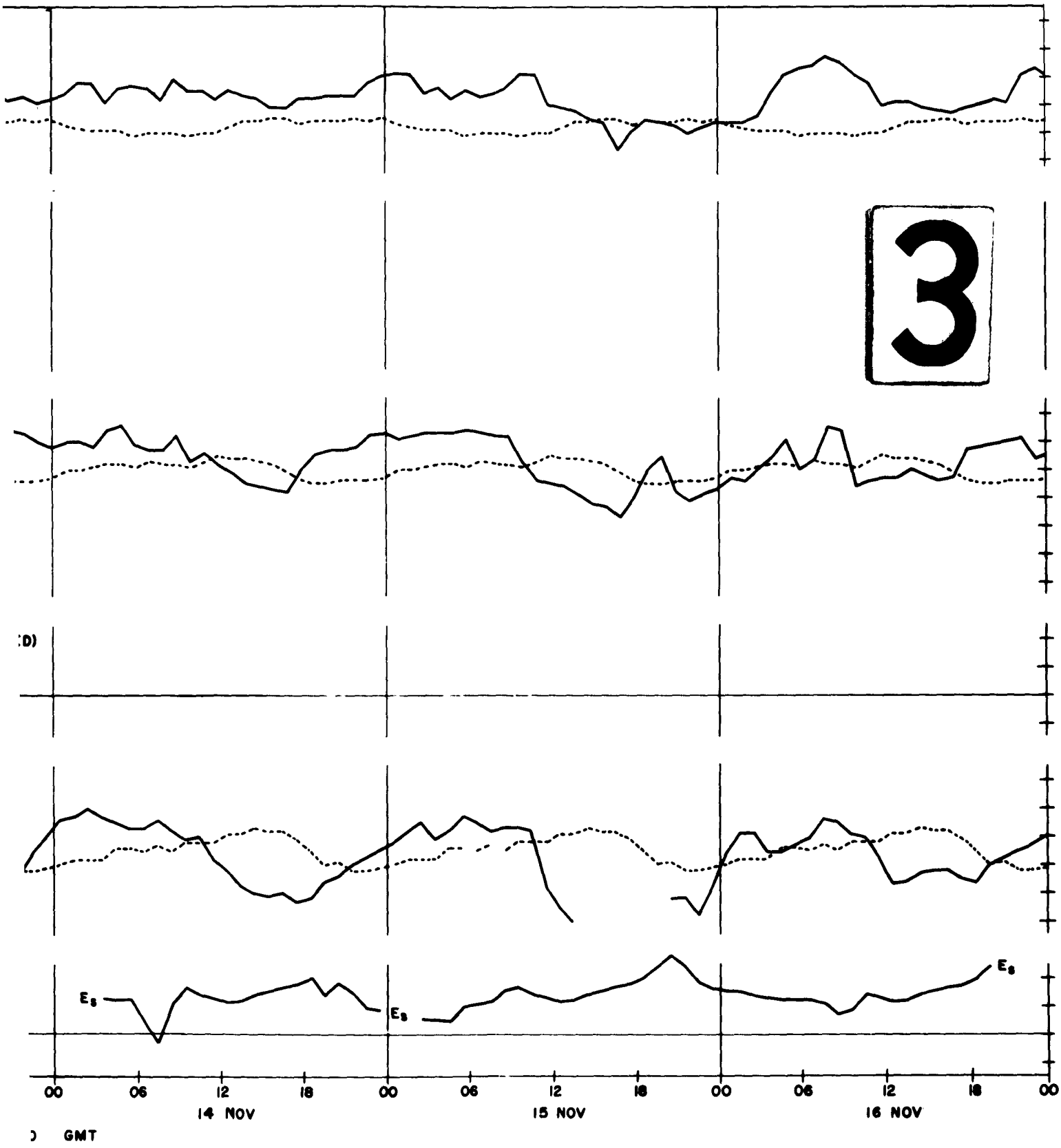

Figure 6-3. Signal and Noise Absorption Variations for the November 1960 Event (Sheet 1 of 2)

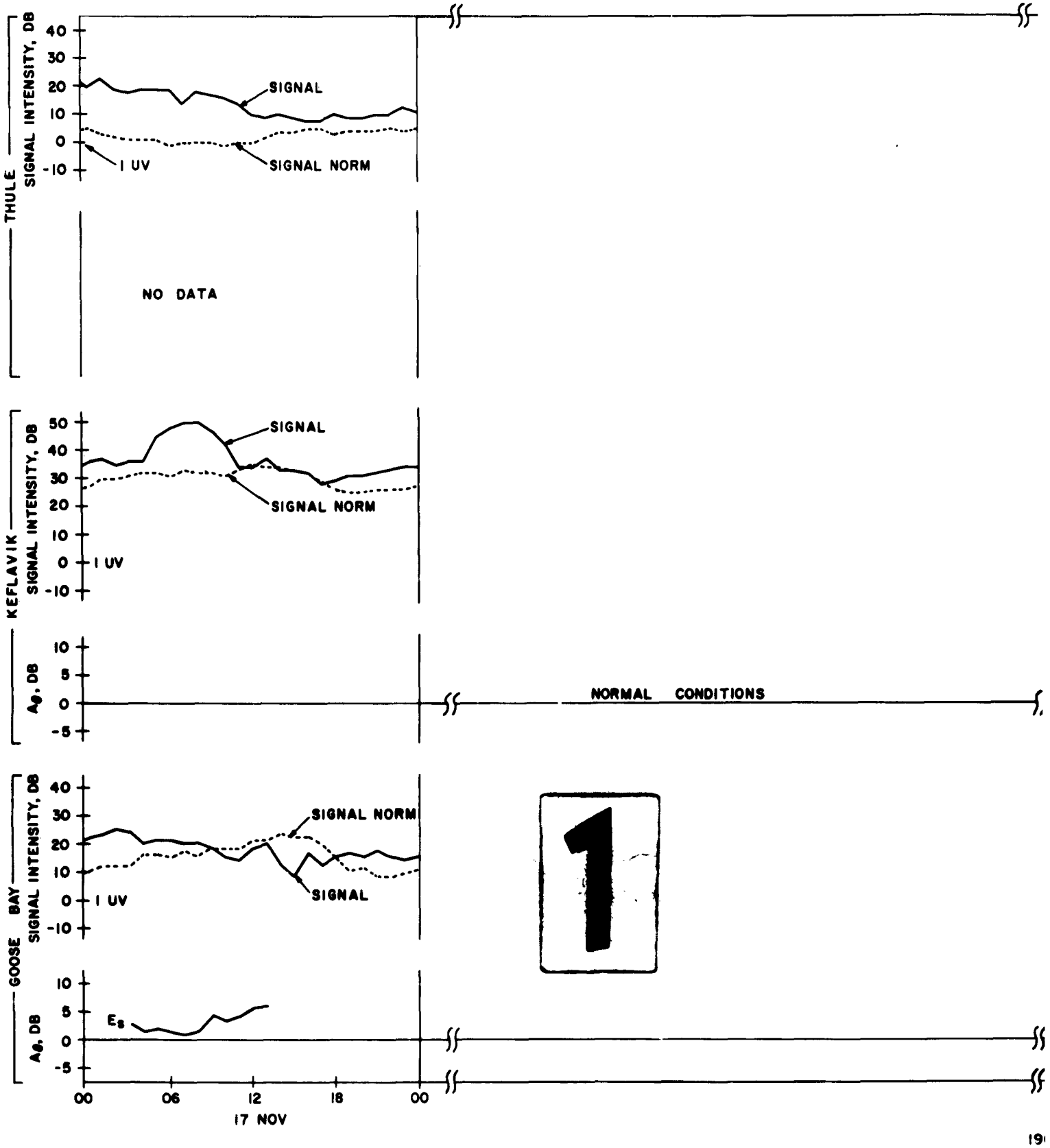
THULE
SIGNAL INTENSITY, DB
40
30
20
10
0
-10
SIGNAL
1 UV
SIGNAL NORM
NO DATA
KEFLAVIK
SIGNAL INTENSITY, DB
50
40
30
20
10
0
-10
SIGNAL
SIGNAL NORM
1 UV
Aφ, DB
10
5
0
-5
NORMAL CONDITIONS
GOOSE BAY
SIGNAL INTENSITY, DB
40
30
20
10
0
-10
SIGNAL NORM
1 UV
SIGNAL
Aφ, DB
10
5
0
-5
Es
00
06
12
18
00
17 NOV

1

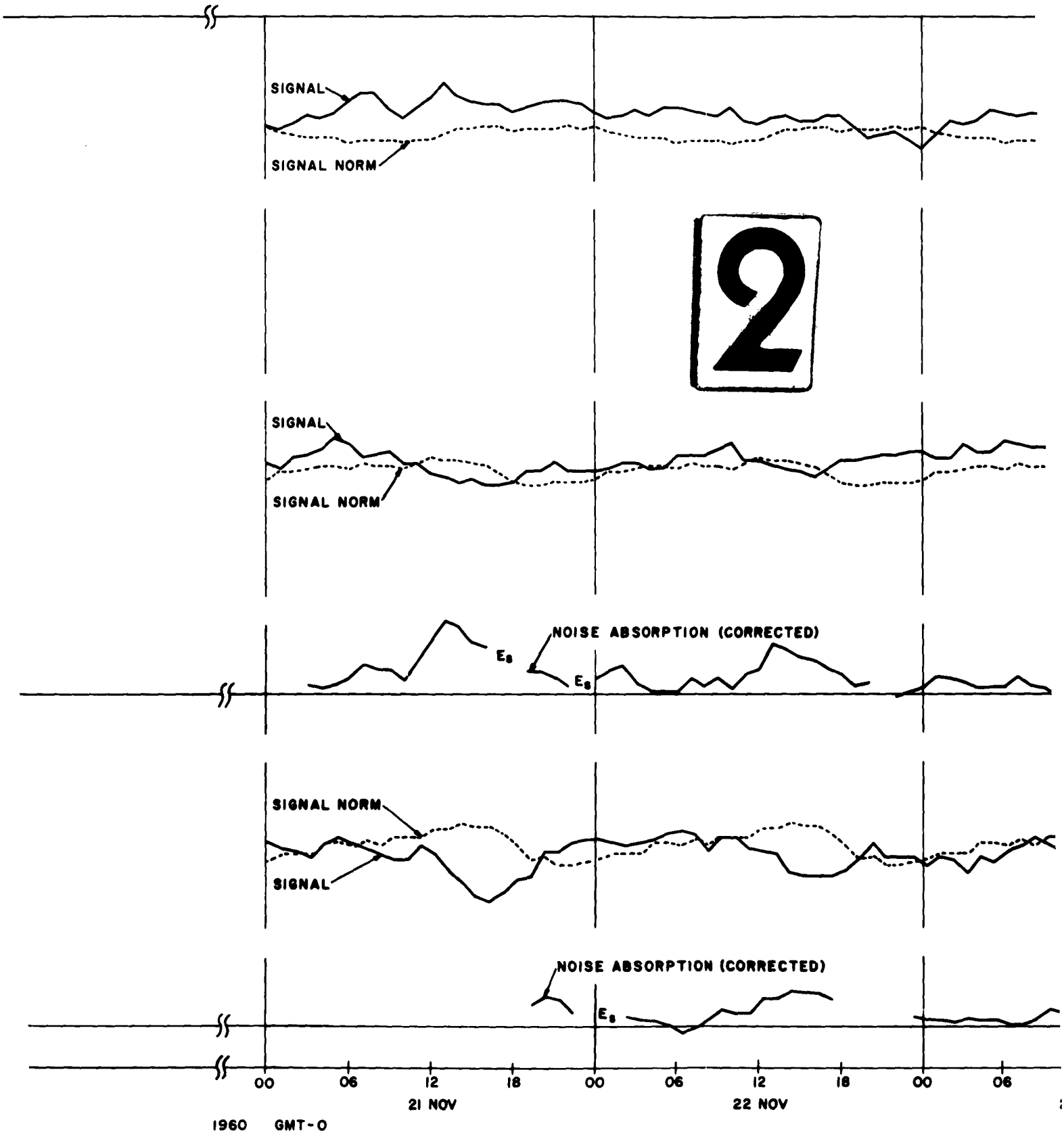

Figure 6-3. Signal and Noi
Variations for the Novembe
(Sheet 2 of 2)

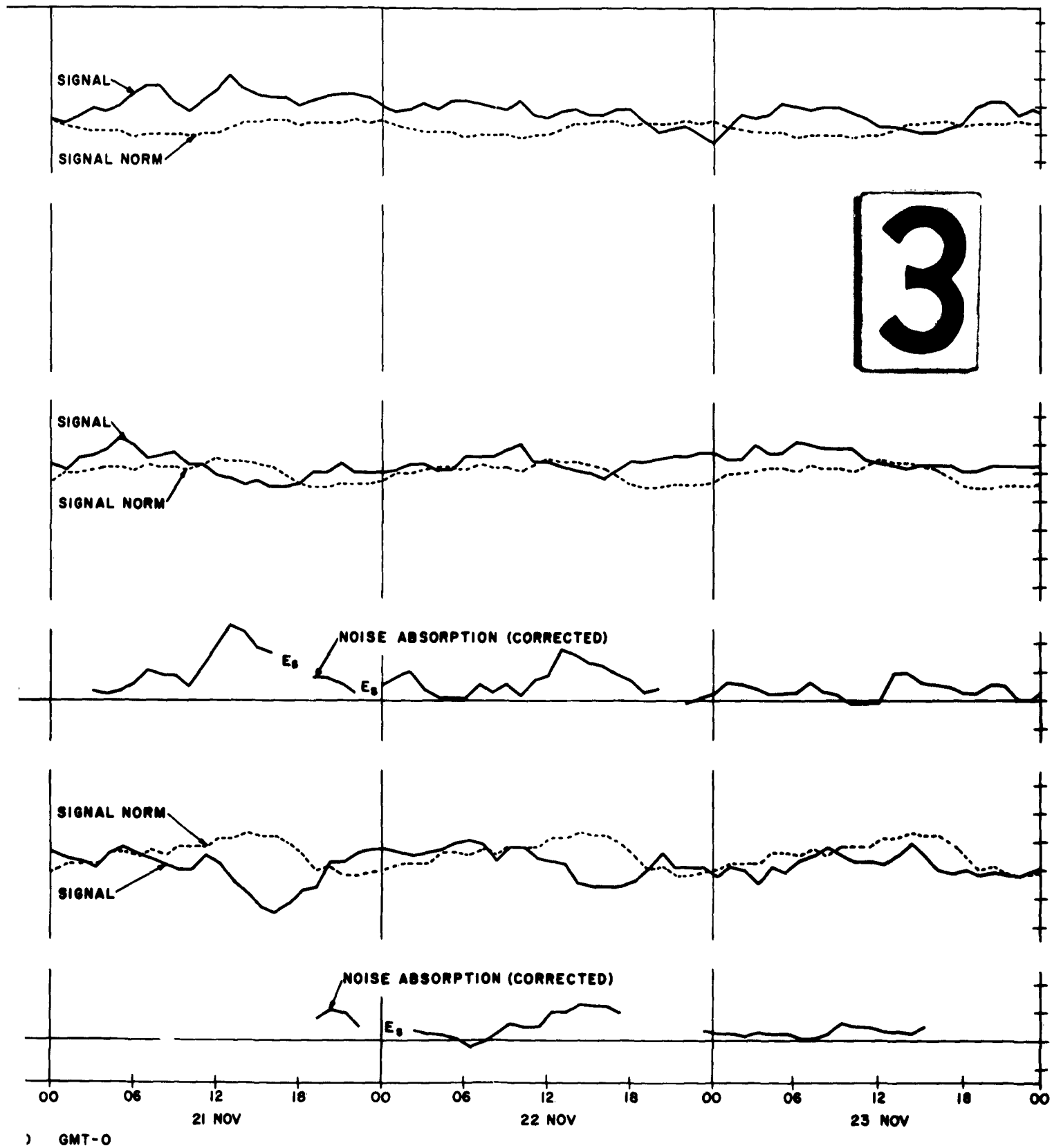

Figure 6-3. Signal and Noise Absorption Variations for the November 1960 Event (Sheet 2 of 2)

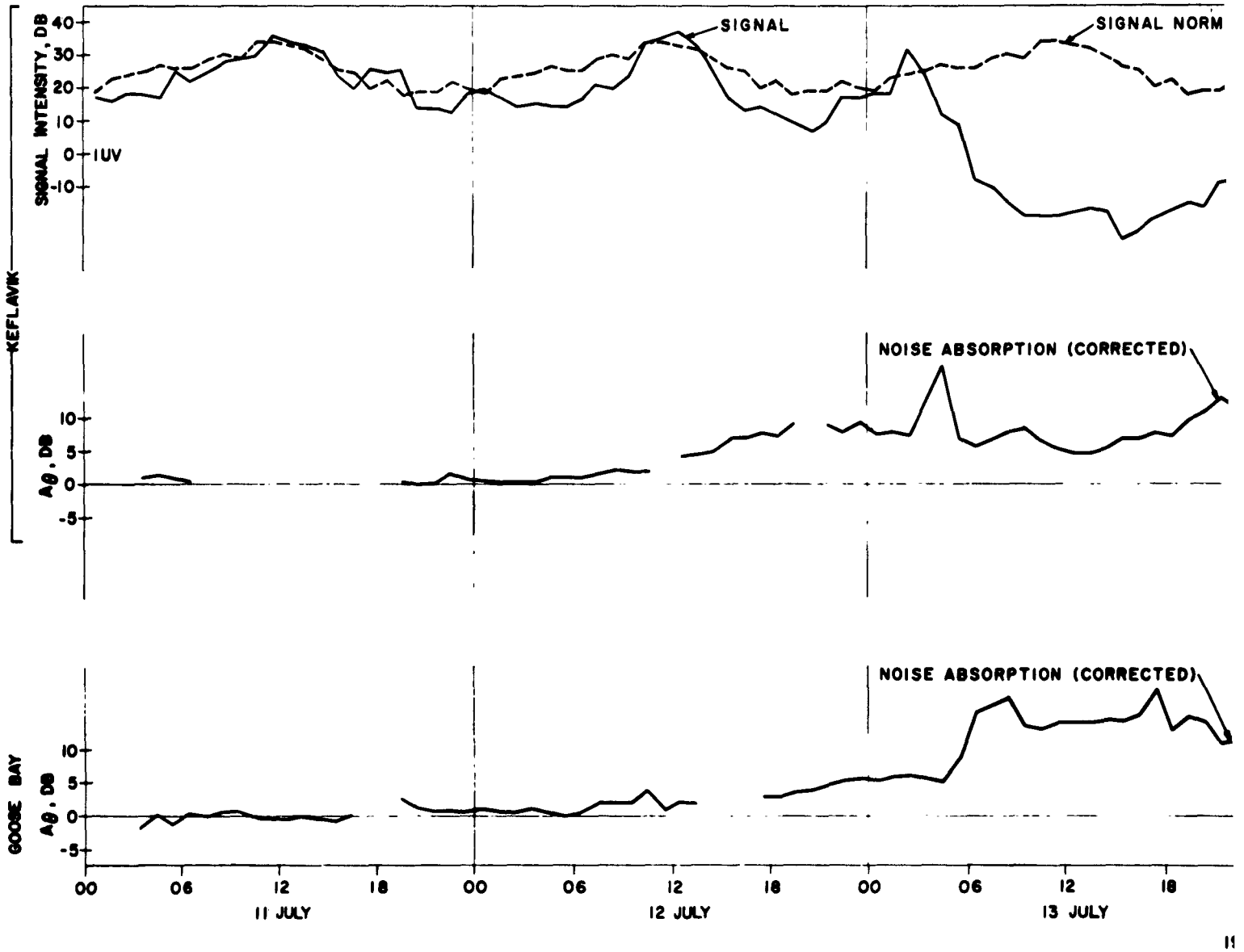
KEFLAVIK
SIGNAL INTENSITY, DB
40
30
20
10
0
-10
1UV
SIGNAL
SIGNAL NORM
NOISE ABSORPTION (CORRECTED)
Aθ, DB
10
5
0
-5
GOOSE BAY
NOISE ABSORPTION (CORRECTED)
Aθ, DB
10
5
0
-5
00
06
12
18
00
06
12
18
00
06
12
18
11 JULY
12 JULY
13 JULY

3

PCE-R-9063A

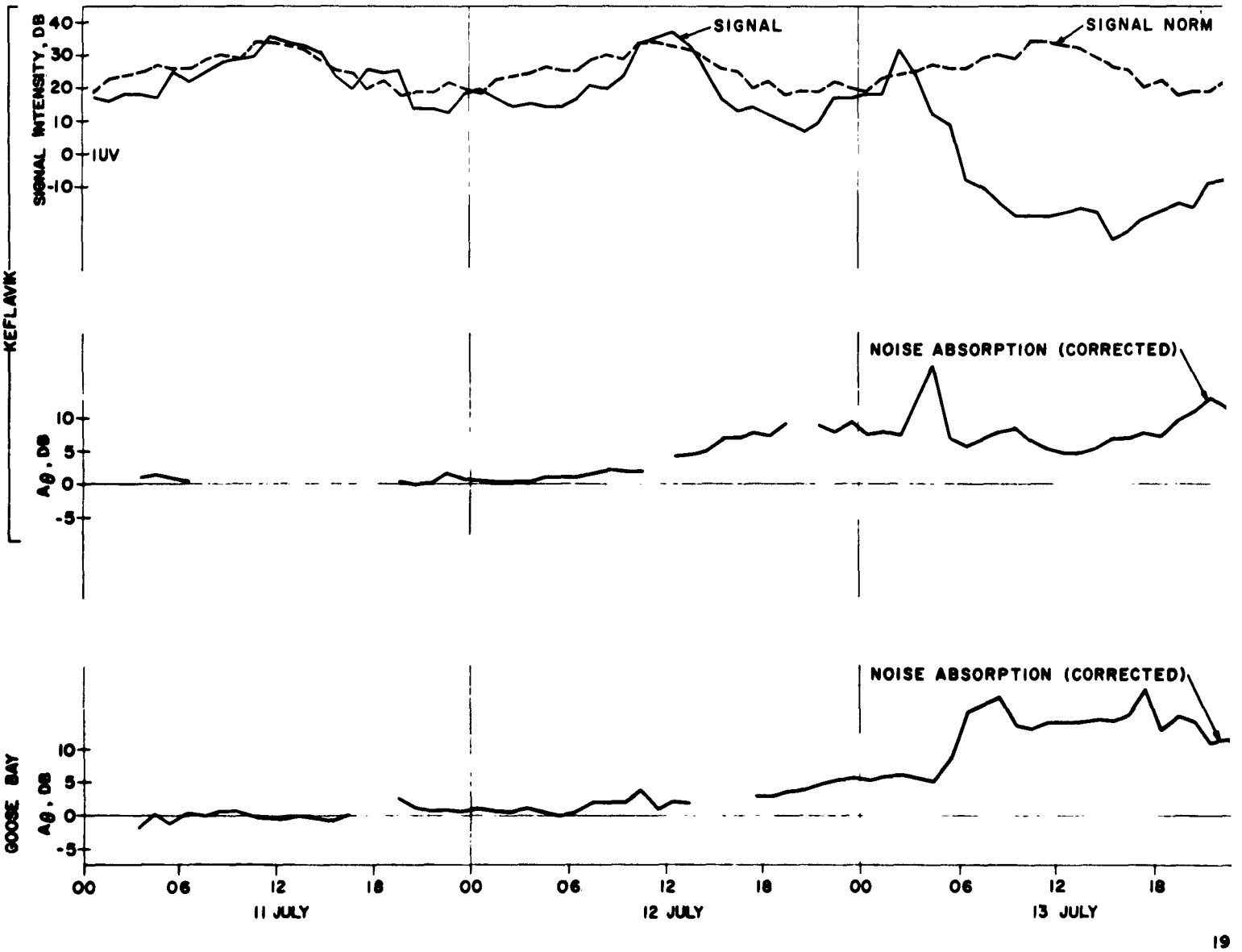
KEFLAVIK
SIGNAL INTENSITY, DB
40
30
20
10
0
-10
1UV
SIGNAL
SIGNAL NORM
NOISE ABSORPTION (CORRECTED)
Aθ, DB
10
5
0
-5
GOOSE BAY
NOISE ABSORPTION (CORRECTED)
Aθ, DB
10
5
0
-5
00
06
12
18
00
06
12
18
00
06
12
18
11 JULY
12 JULY
13 JULY
19

PCE-R-9063A

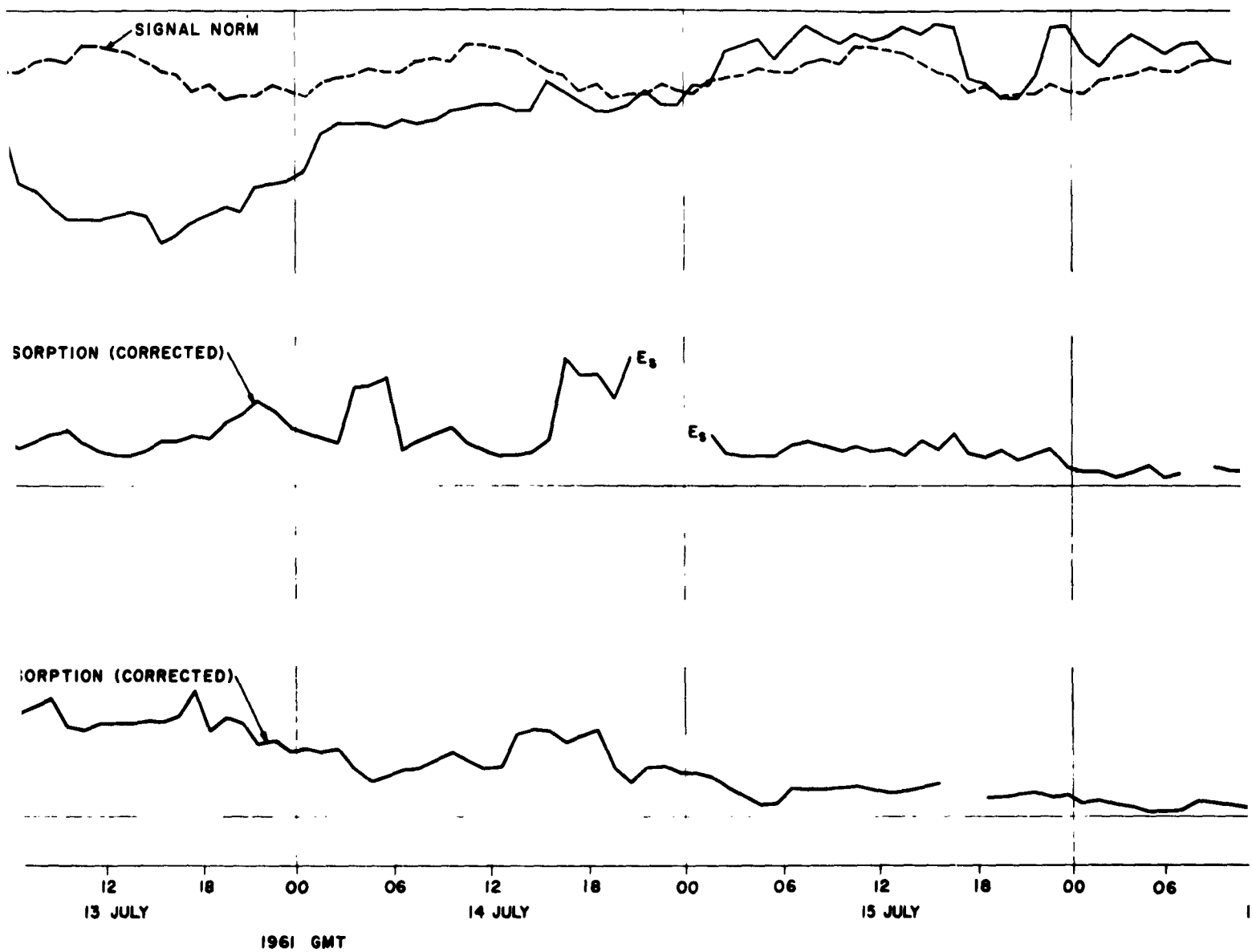

2

Figure 6-4. Signal and No
Variations for the July
(Sheet 1 of 2

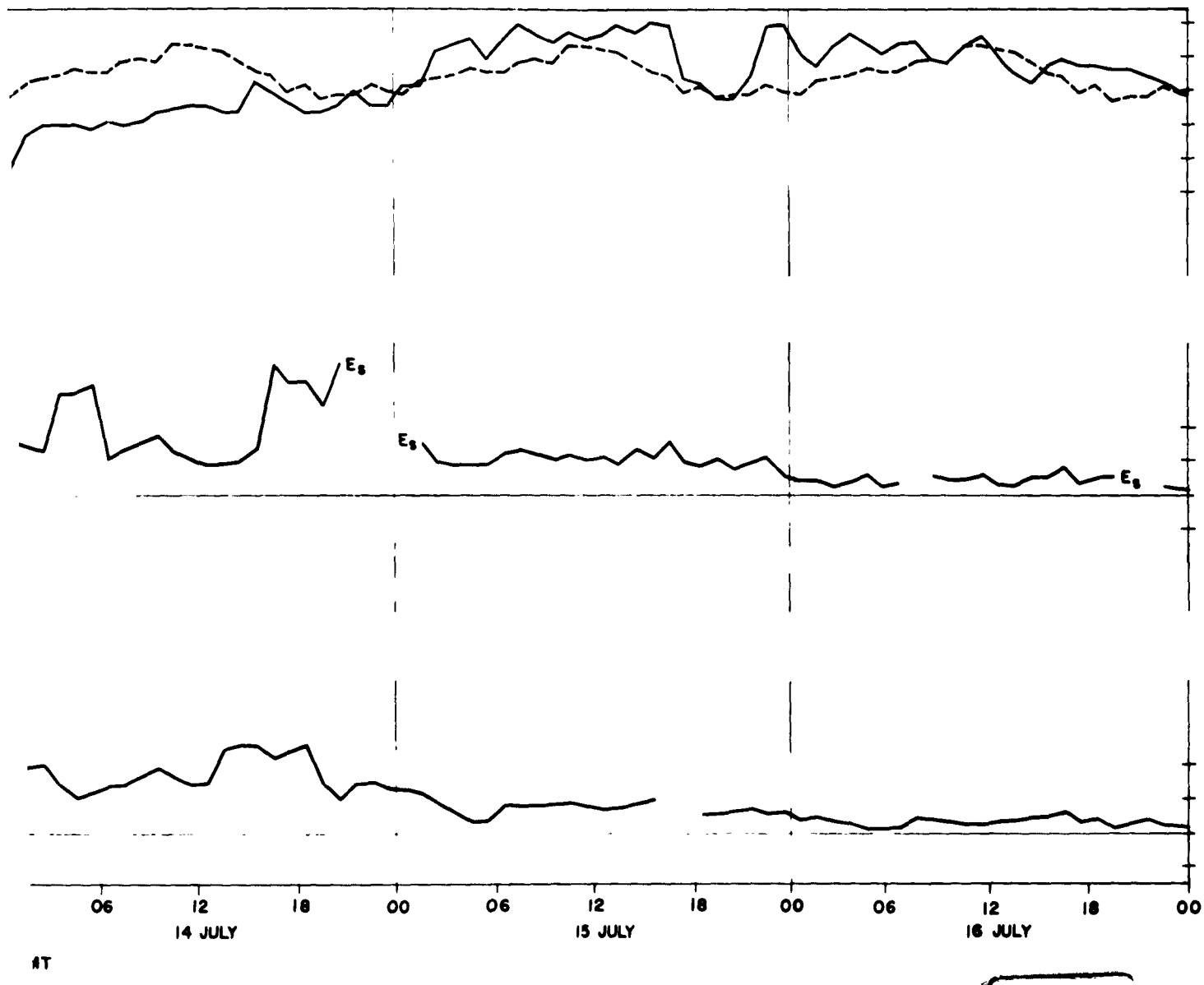

3

Figure 6-4. Signal and Noise Absorption Variations for the July 1961 Event
(Sheet 1 of 2)

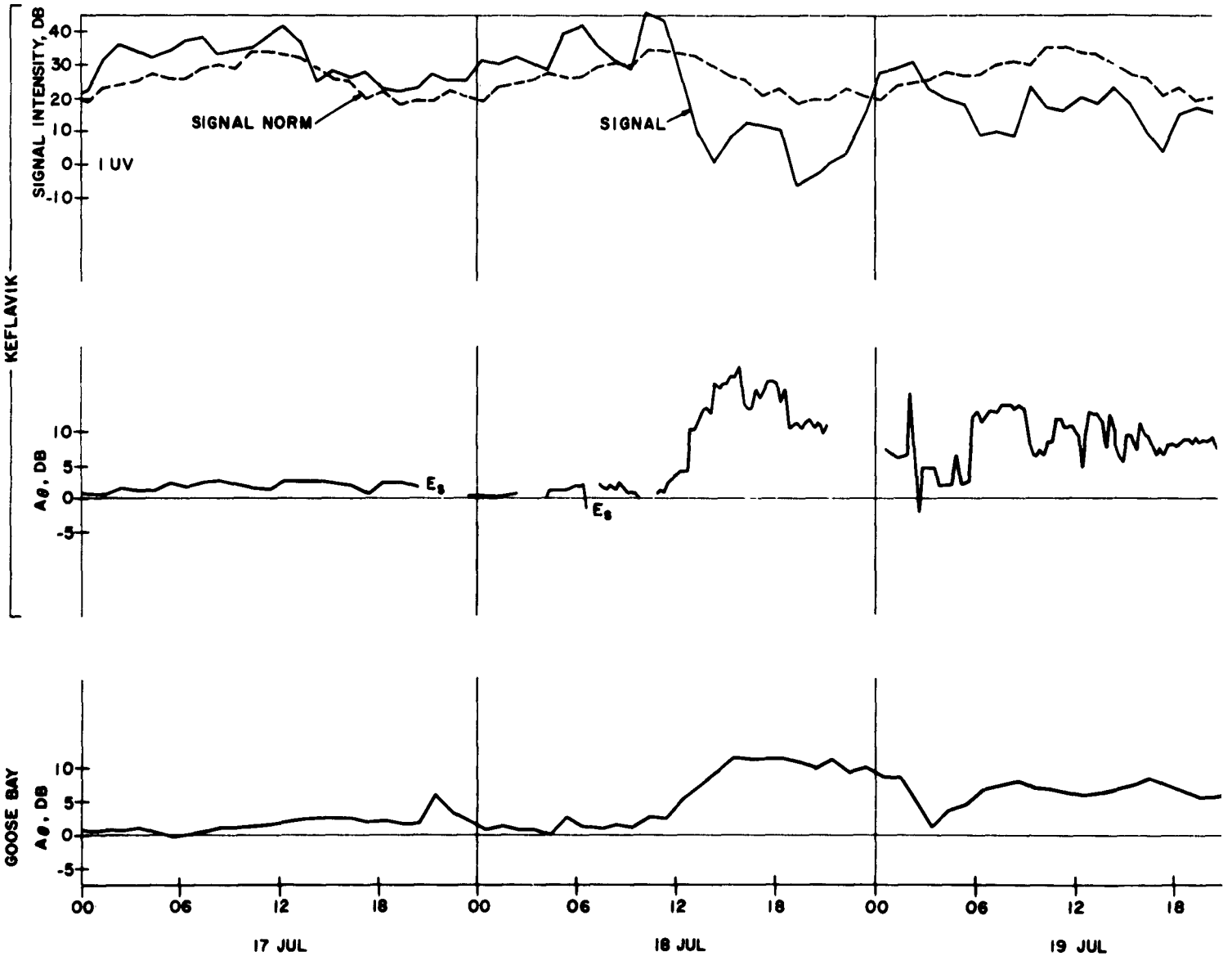
KEFLAVIK
SIGNAL INTENSITY, DB
40
30
20
10
0
-10
1 UV
SIGNAL NORM
SIGNAL
Aθ, DB
10
5
0
-5
Es
Es
GOOSE BAY
Aθ, DB
10
5
0
-5
00
06
12
18
00
06
12
18
00
06
12
18
17 JUL
18 JUL
19 JUL

1

PCE-R-9063A

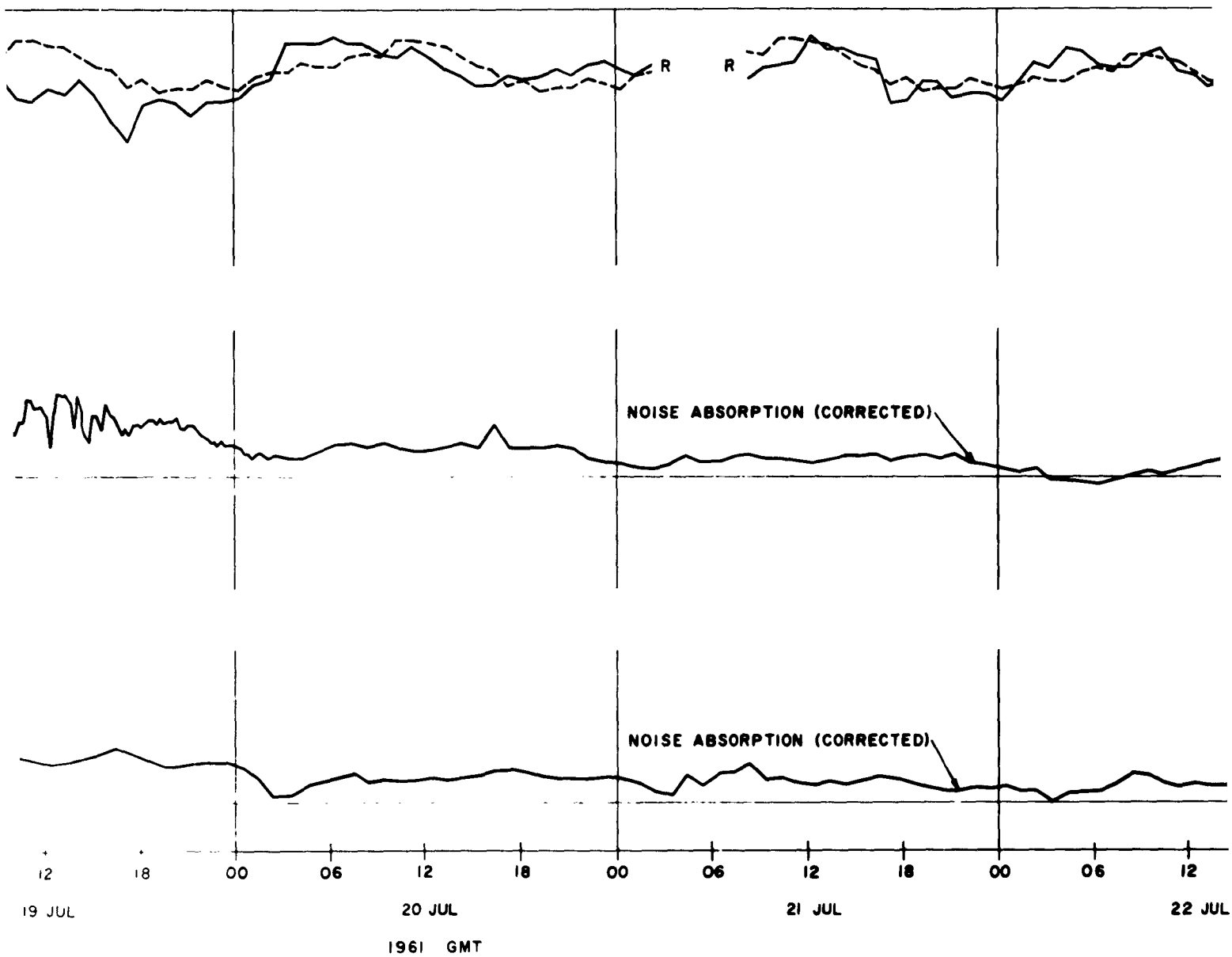
R
R
NOISE ABSORPTION (CORRECTED)
NOISE ABSORPTION (CORRECTED)
12
18
00
06
12
18
00
06
12
18
00
06
12
19 JUL
20 JUL
21 JUL
22 JUL
1961 GMT

2

Figure 6-4.

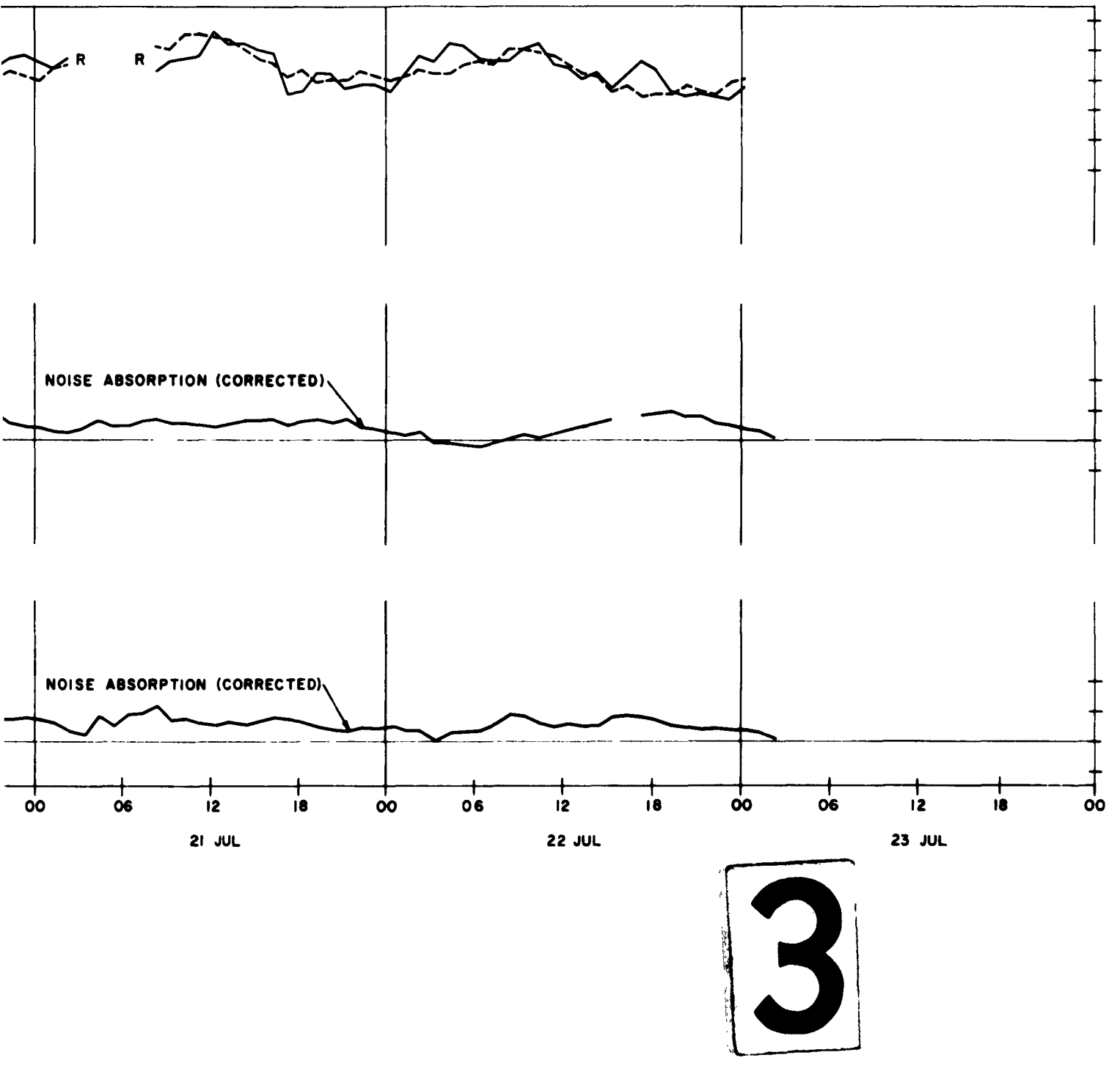

3

Figure 6-4. Signal and Noise Absorption Variations for the July 1961 Event
(Sheet 2 of 2)

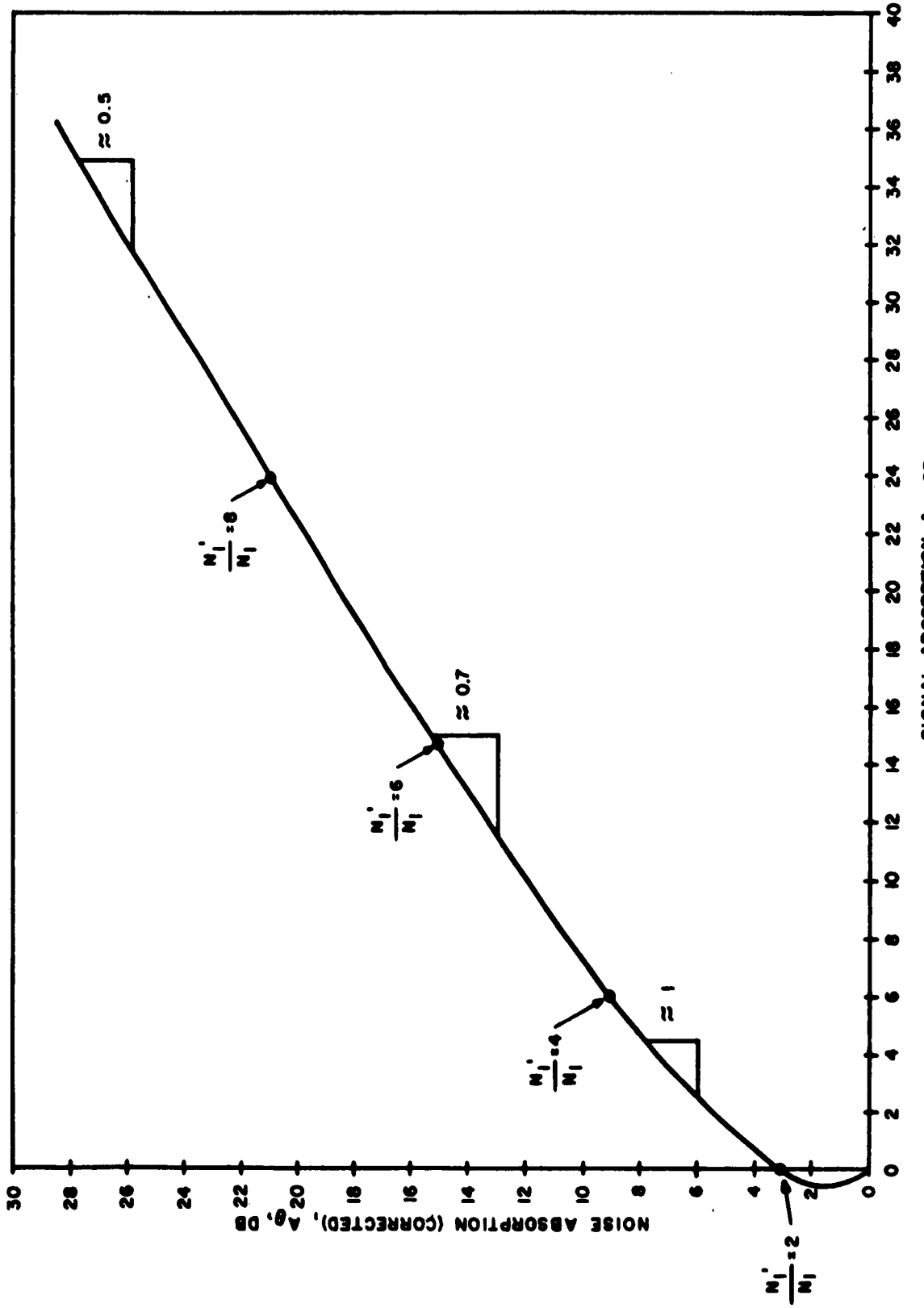

Figure 6-5. Calculated Signal vs Noise Absorption for the Simple Model

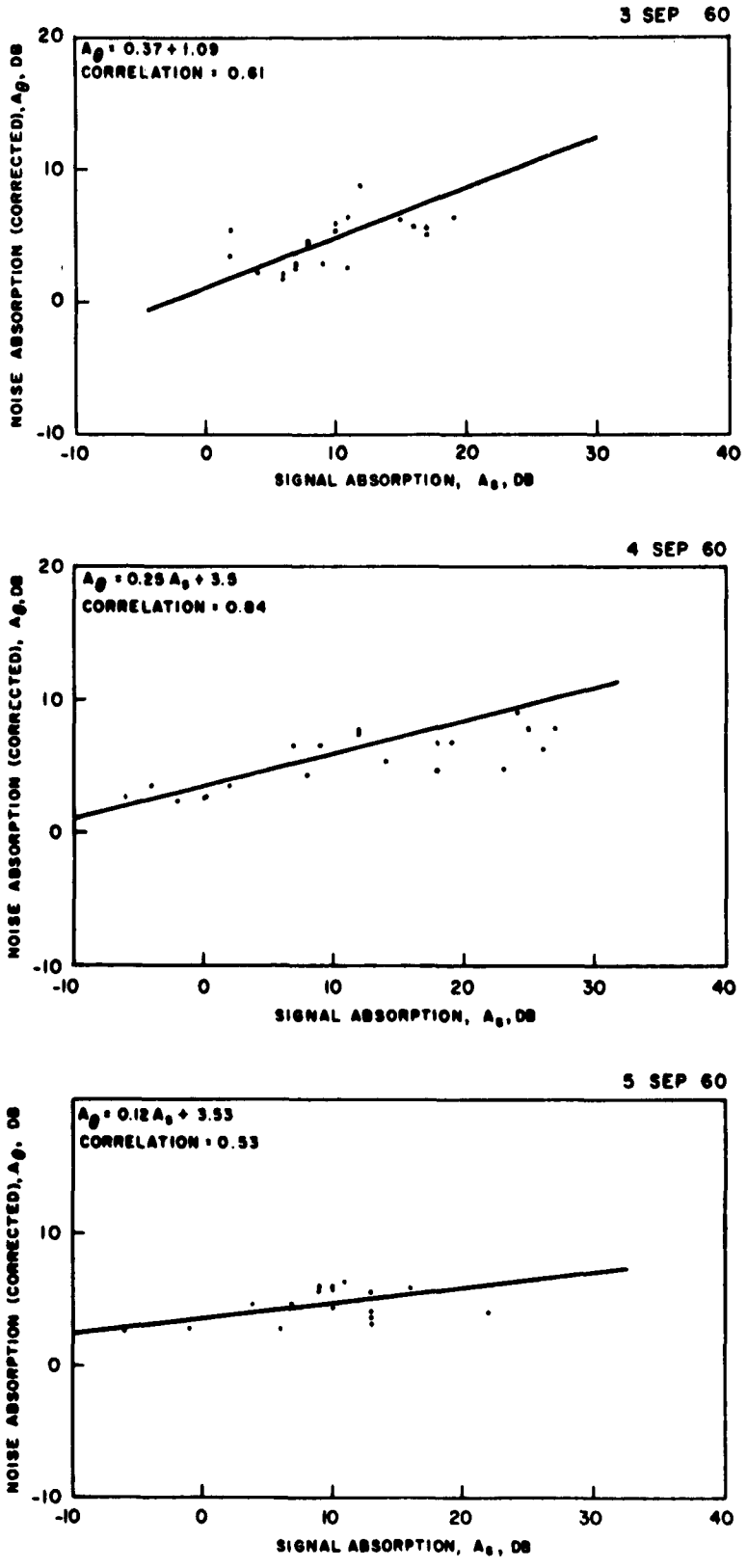

Figure 6-6. Signal vs Noise Absorption on the Keflavik Antenna for 3, 4, 5 September 1960

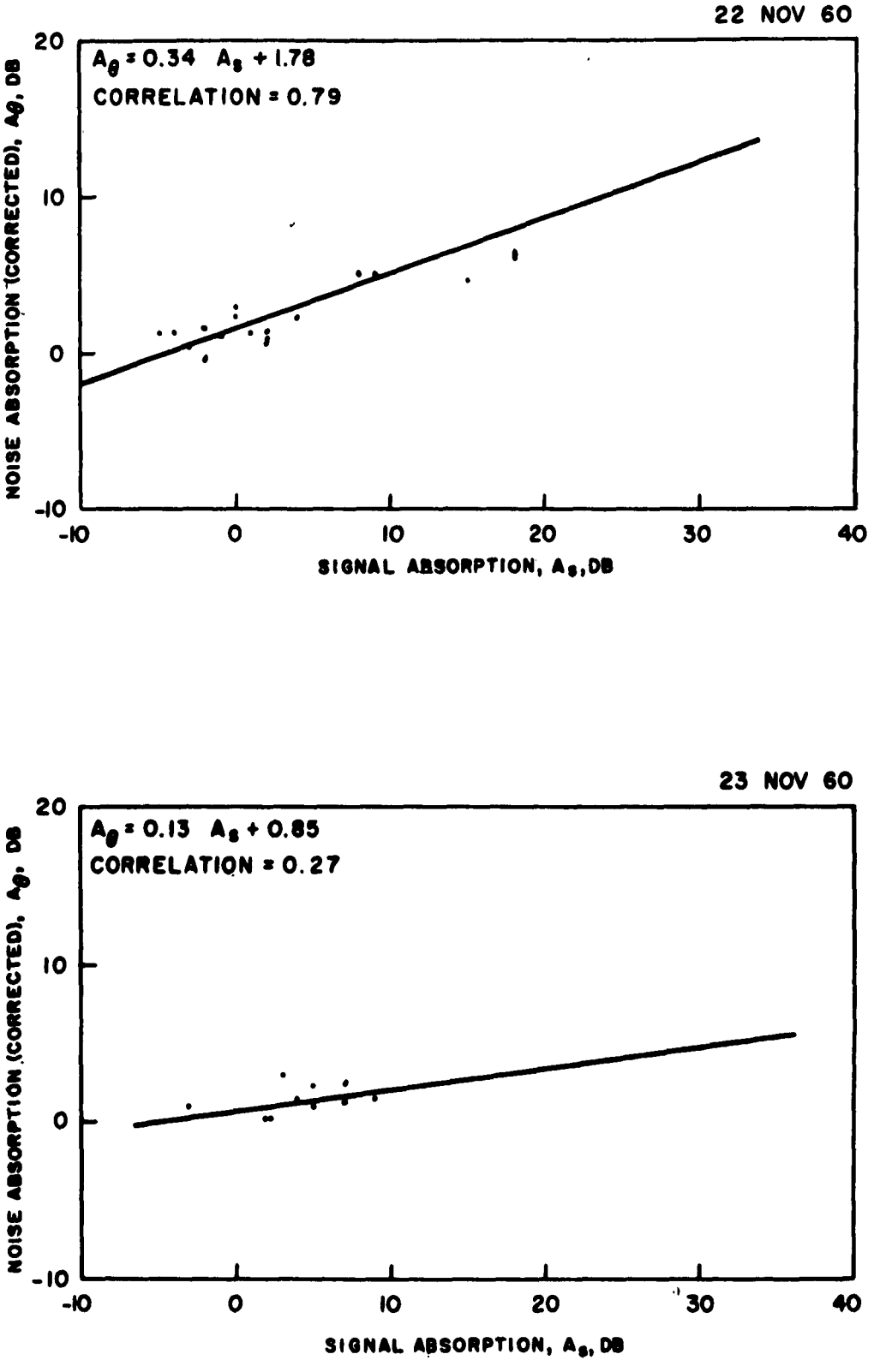

Figure 6-7. Signal vs Noise Absorption on the Keflavik Antenna for 22, 23 November

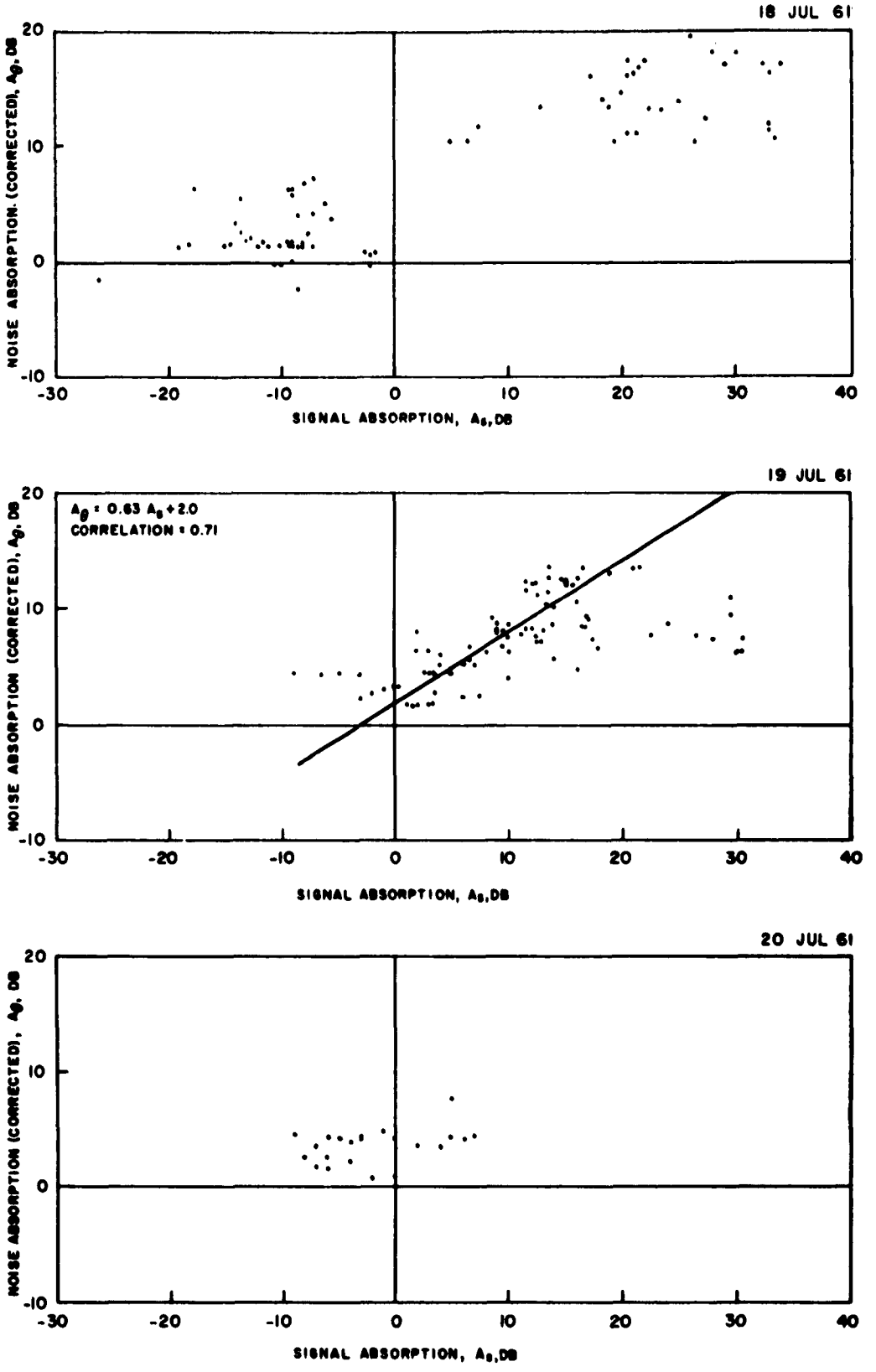

Figure 6-8. Signal vs Noise Absorption on the Keflavik Antenna for 18, 19, 20 July

SECTION VII

CONCLUSIONS

Some features of the normal components of ionospheric absorption in the arctic have been measured. Normal D-region absorption measurements during daylight resulted in values consistent with expectations. Normal F-layer absorption was inferred from vertical sounder data from Narsarssuak and included in the analysis.

Five polar cap absorption events have been studied. The absorption observed during these events frequently exceeded the resolution capability of the equipment, i.e., about 15 db on the riometer and 30 db on the signal. Data are presented showing the variation of absorption during the test period.

The results of this program indicate that nighttime absorption during an event may occur largely above the scattering region, while the daytime absorption is below the scattering level. No data were available relative to possible changes in the height of the scattering region during the events, but it is considered likely that this is more variable than the height of the absorption.

As far as could be determined, the commencement of polar cap absorption events is essentially simultaneous in the regions under study. The absorption appears more intense in the auroral zone than at the higher latitudes, although the effects persist longer at the higher latitudes. The absorption exhibits no appreciable movement except for an apparent movement due to a strong dependence on solar zenith angle.

Auroral absorption measurements were often obscured by the simultaneous presence of strongly enhanced signals over the path, desensitizing the recording equipment. It is felt, however, that the considerable size of the oblique antenna beam at the auroral heights tended to obscure the effects of the discrete auroral absorption regions. Since auroral absorption is frequently observed on vertical riometers, the size of typical auroral absorption areas is therefore thought to not usually exceed 10,000 km^2. The reasons set forth in paragraphs 5.3 and 6.2.2 support the suggestion that aurorally generated noise was present and affected the measurements.

SECTION VIII

ACKNOWLEDGEMENTS

This program was sponsored by the USAF Office of Aerospace Research. The cooperation of the personnel of the NORLANT Air Force Communications Region (AFCR), who permitted the installation and operation of the equipment at their sites and who provided valuable aid to the technician in Sondrestrom, is also acknowledged.

Private communications from D. K. Bailey in clarifying the objectives and results of the program are gratefully acknowledged. Data were also generously made available by Dr. Karl Anderson, Director, Det Danske Meteorologiske Institute, and the Central Radio Propagation Laboratory of the National Bureau of Standards.

SECTION IX

BIBLIOGRAPHY

1. D. K. Bailey and J. M. Harrington, "The Occurrence of Polar Cap Absorption," AGARD Symposium, Naples, 1961.

2. D. K. Bailey, R. Bateman, and R. C. Kirby, "Radio Transmission at VHF by Scattering and Other Processes in the Lower Ionosphere," Proc. IRE, Vol. 43, No. 10, pp. 1181-1230, (1955).

3. C. G. Little and H. Leinbach, "Some Measurements of High Latitude Ionospheric Absorption Using Extraterrestrial Radio Waves," Proc. IRE, Jan 1958, p. 334.

4. E. V. Appleton, "Wireless Studies of the Ionosphere," JIEE, Vol. 71, p. 642.

5. C. G. Little and R. Silberstein, "A Comparison of Arctic HF Transmission Loss and VHF Riometer Data," NBS Report 6743.

6. A. P. Mitra and C. A. Shain, "The Measurements of Ionospheric Absorption Using Observations of 18.3 Mc/s Cosmic Radio Noise," J. Atmos. Terr. Phys., 4, 204-218, (1953).

7. Bruce Lusignan, "Cosmic Noise Absorption Measurements at Stanford, California, and Pullman, Washington," J. Geophys. Res., Vol. 65, Dec., p. 3895, (1960).

8. K. R. Ramanathan, R. V. Bhonsle, and S. S. Degaonkar, "Effect of Electron-Ion Collisions in the F-region of the Ionosphere on the Absorption of Cosmic Radio Noise at 25 Mc/s at Ahmedabad," J. Geophys. Res., Vol. 66, No. 9, p. 2763, (1961).

9. K. R. Ramanathan and R. V. Bhonsle, "Cosmic Radio Noise Absorption on 25 Mc/s and F-Scatter," J. Geophys. Res., Vol. 64, No. 10, (1959).

10. Ionospheric Radio Propagation, NBS Circular 462, (1948).

11. R. D. Egan and A. M. Peterson, "Auroral Noise at HF," J. Geophys. Res., Vol. 65, No. 11, p. 3830, (1960).

12. Physics of the Upper Atmosphere, Edit. J. A. Ratcliffe, Academic Press, New York and London, p. 105, (1960).

APPENDIX A

The following pages show scaled riometer data taken from the three antennas at Sondrestrom, Greenland, pointing respectively in the directions of Goose Bay, Labrador; Keflavik, Iceland; and Thule, Greenland.

The hourly noise values were scaled from the recording charts and compared with the temporary norms shown in the body of this report. The differences in noise intensities are shown, minus values representing absorption relative to the norm. Norm comparisons were made by adjusting for sidereal time variations in hourly increments. This results in some extraneous excursions about the norm even on quiet days because of the rapidly varying normal noise intensities during the daily galactic-noise maxima. For example, the plus and minus oscillations about 0400 GMT on 28, 29, and 30 May 1961 on the Goose Bay data are caused by this rather than by absorption variations. These plots are useful in scanning data to determine periods to be studied in detail. All detailed studies in the body of this report used daily sidereal time corrections, when determining absorption, to avoid these errors.

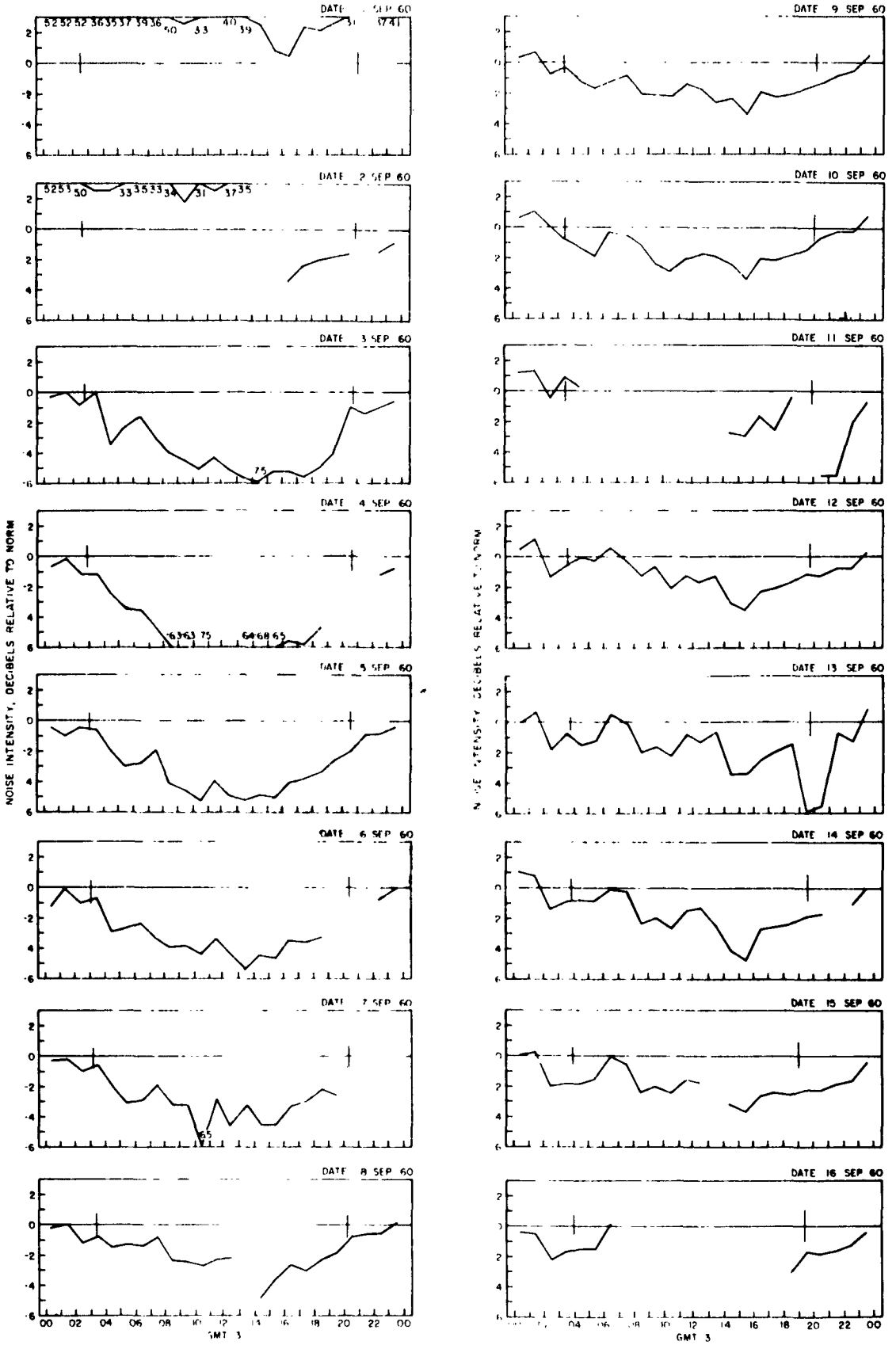

Keflavik, September 1960

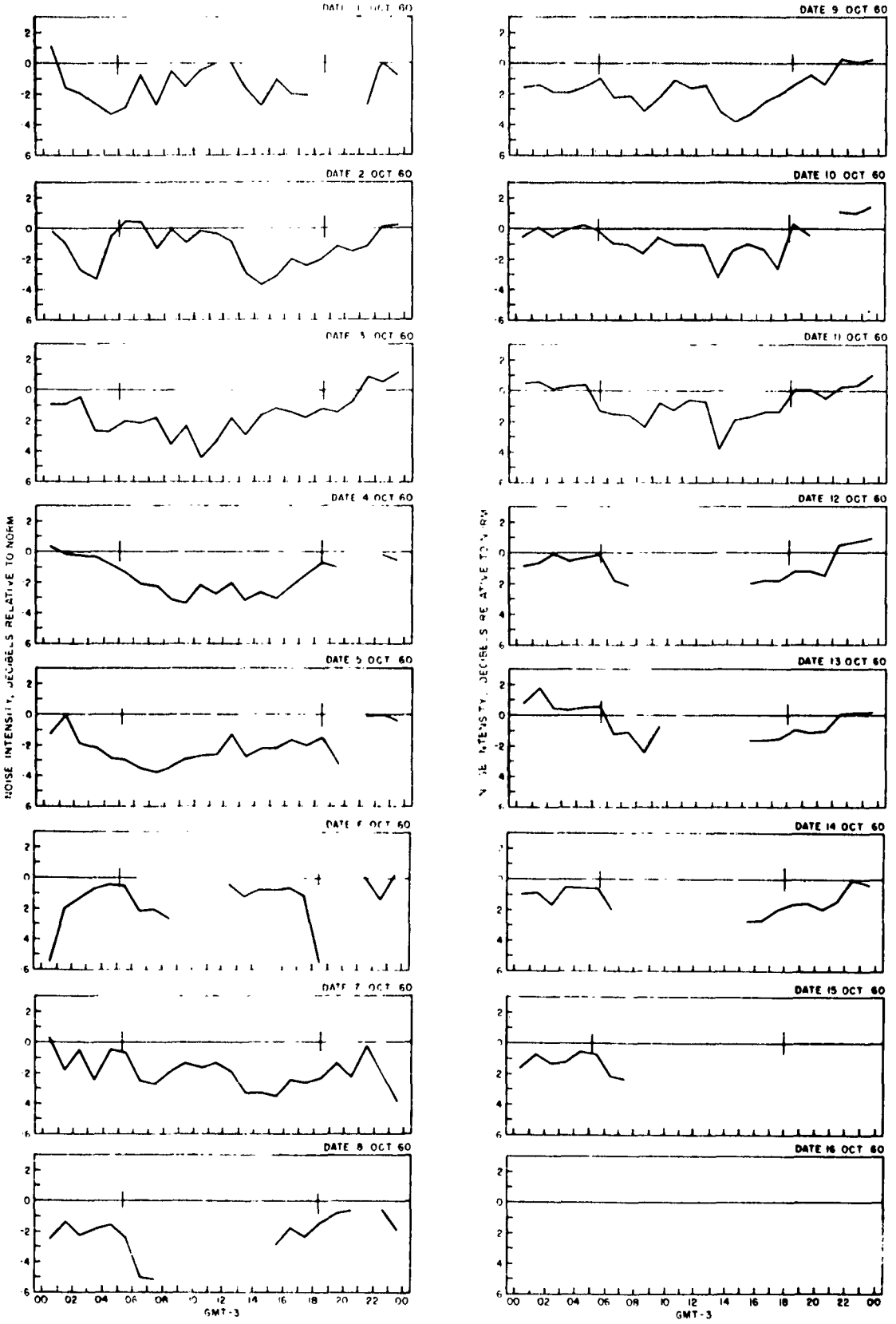

Keflavik, October 1960

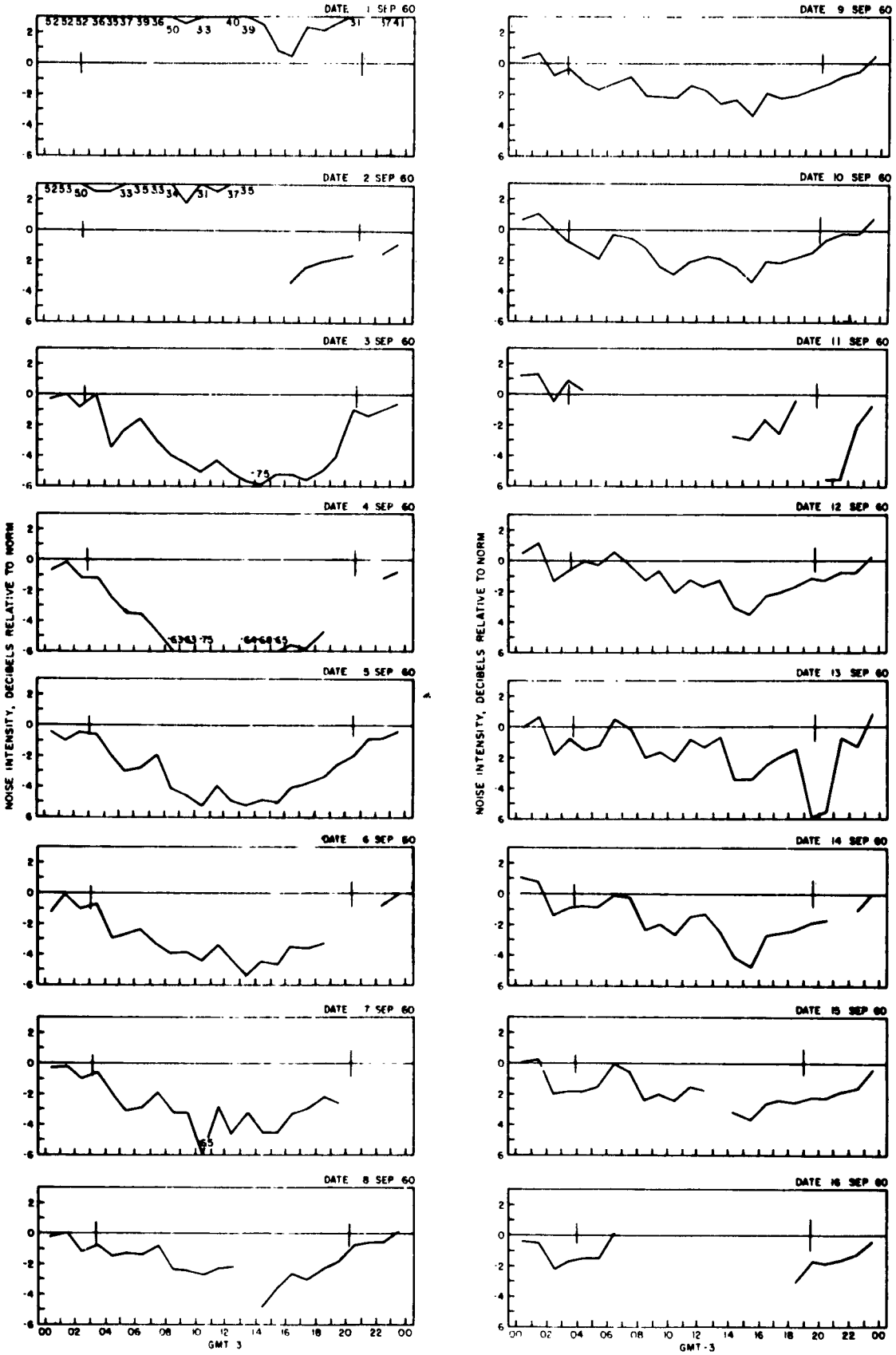

Keflavik, September 1960

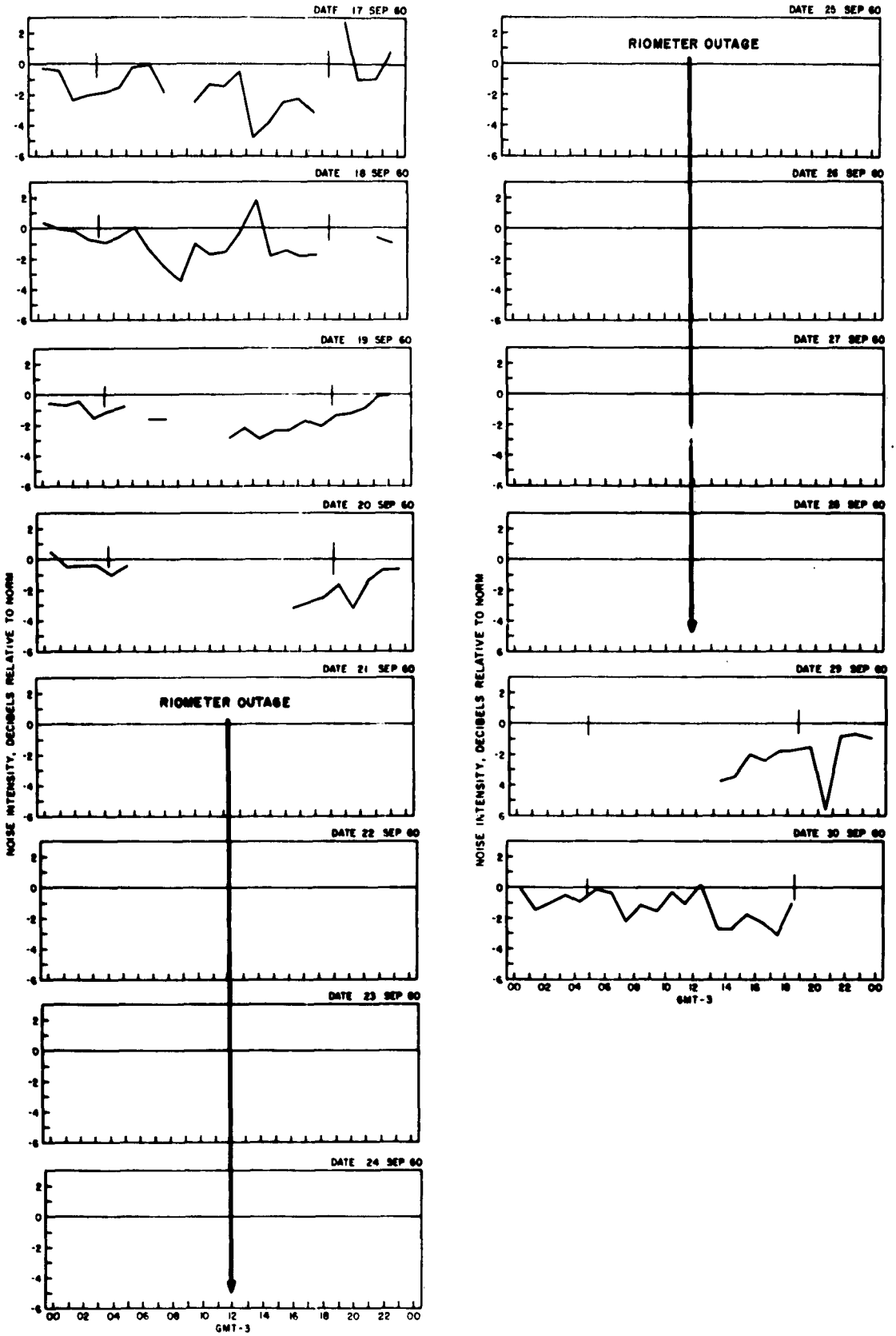

Keflavik, September 1960

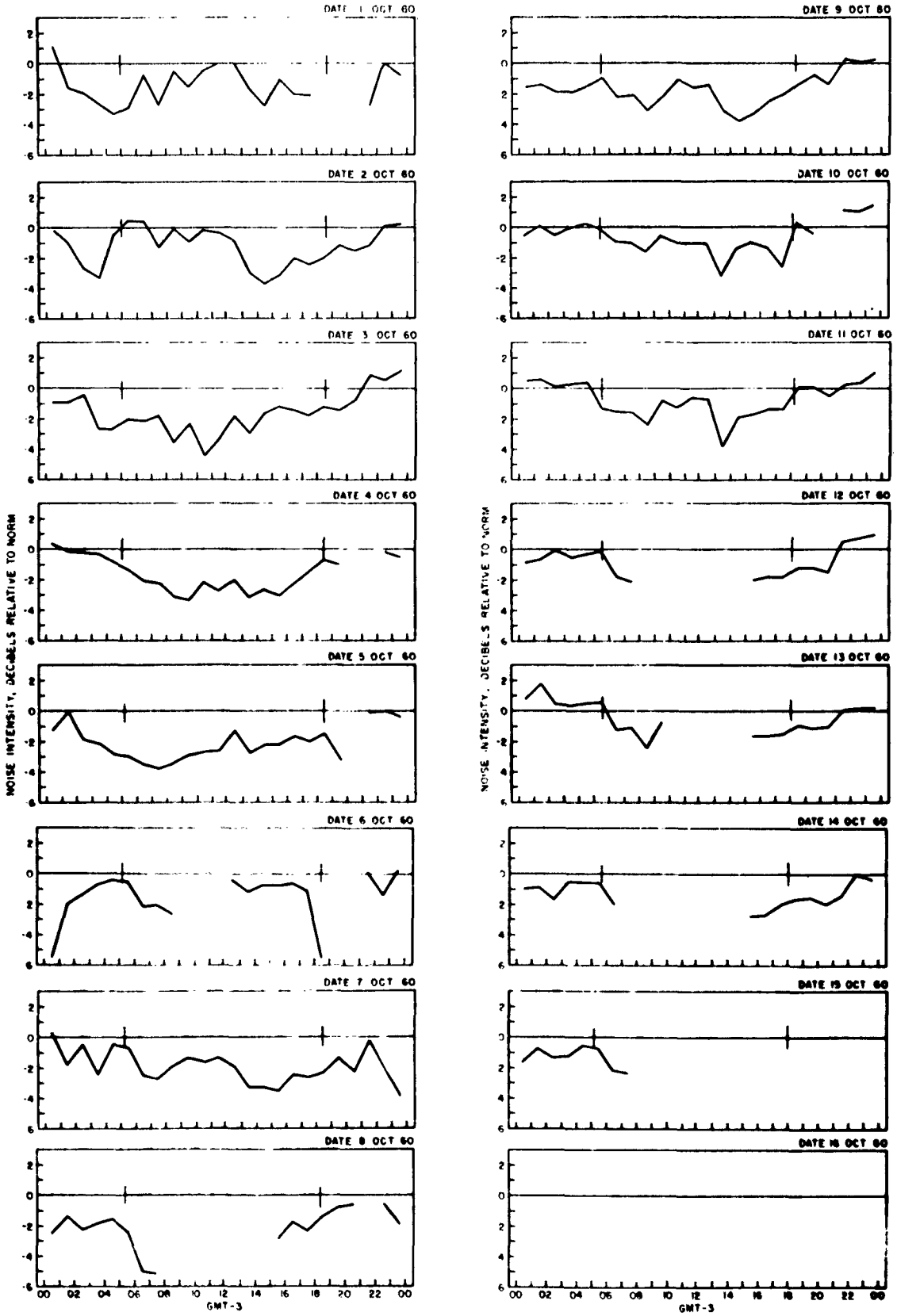

Keflavik, October 1960

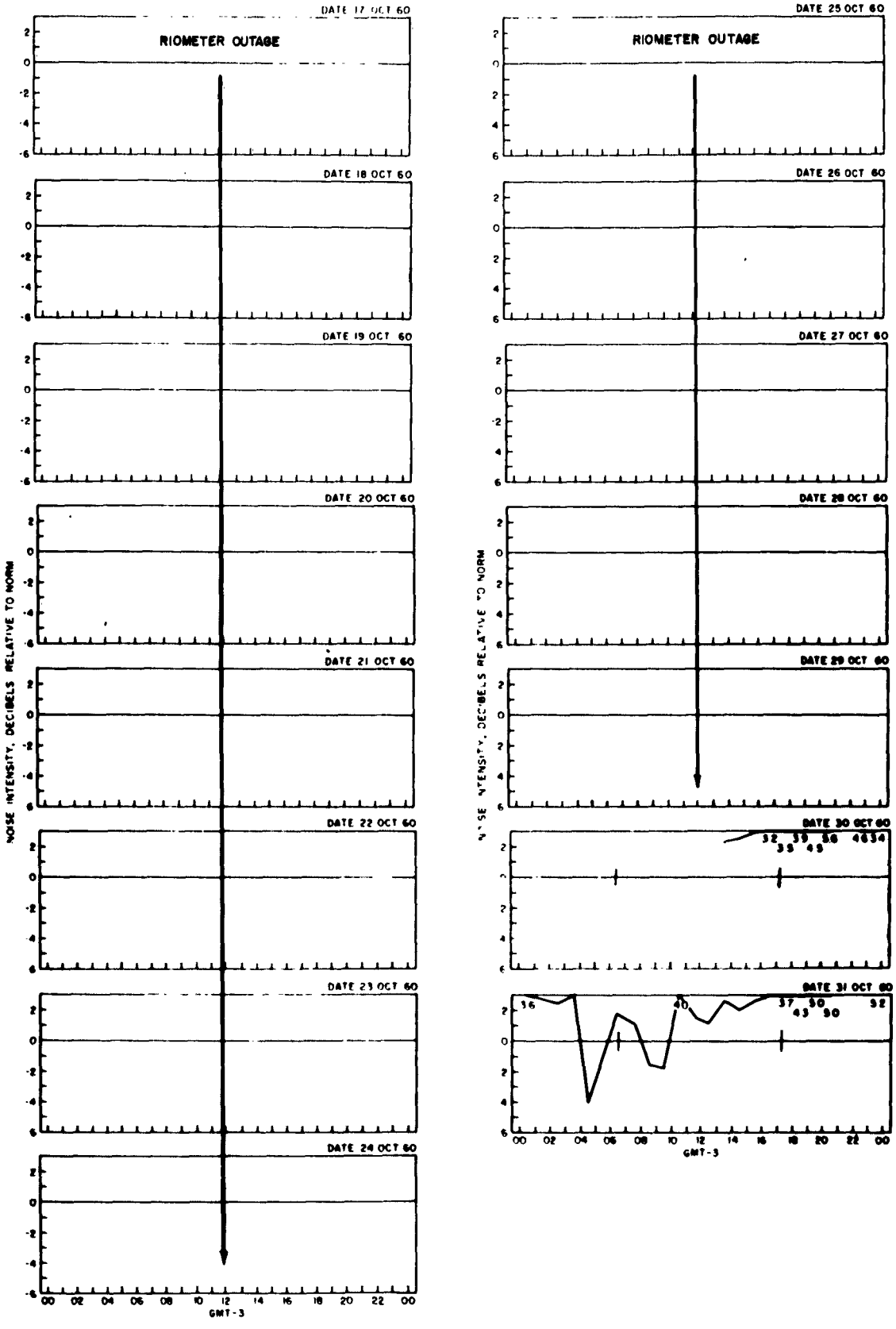

Keflavik, October 1960

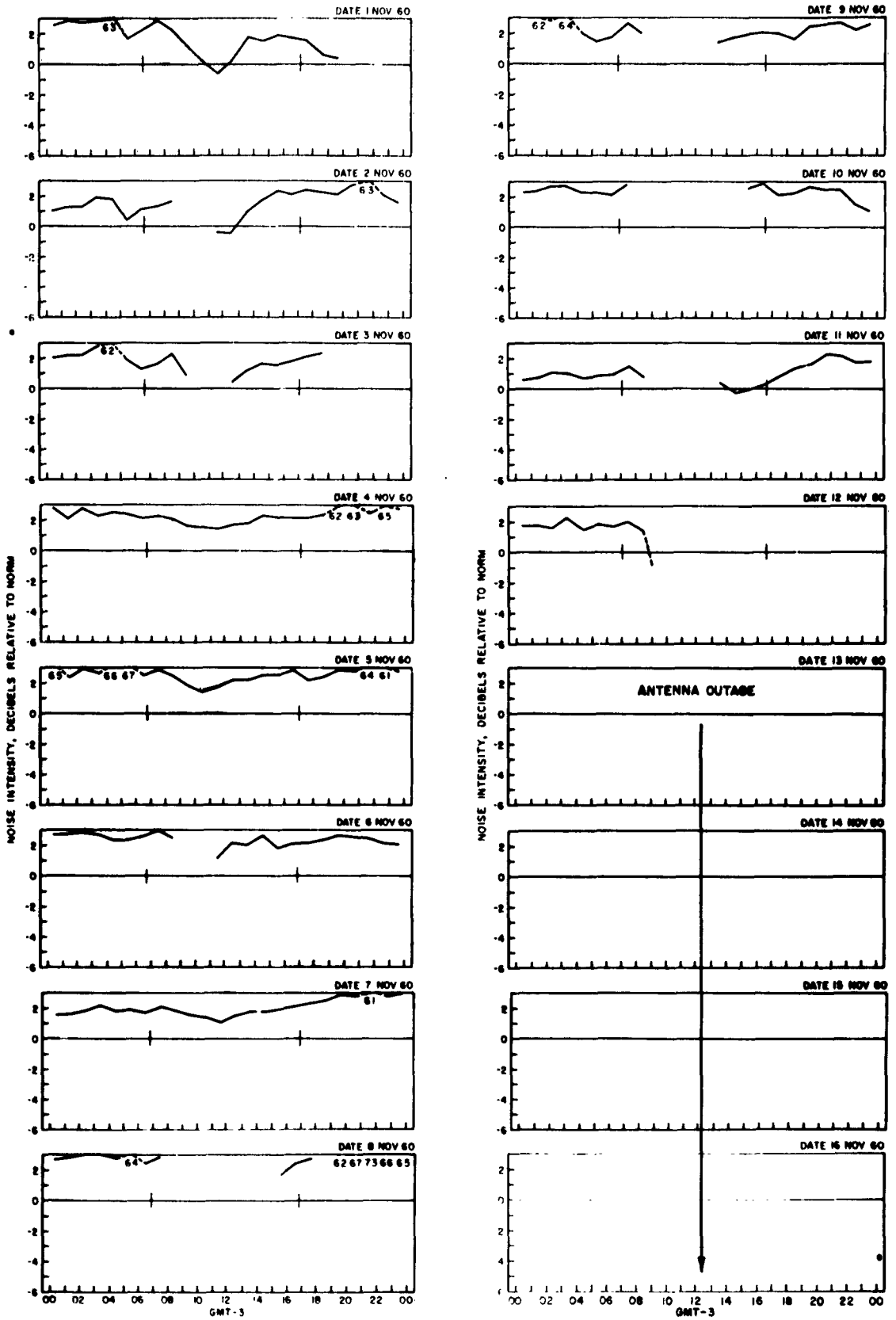

Keflavik, October 1960

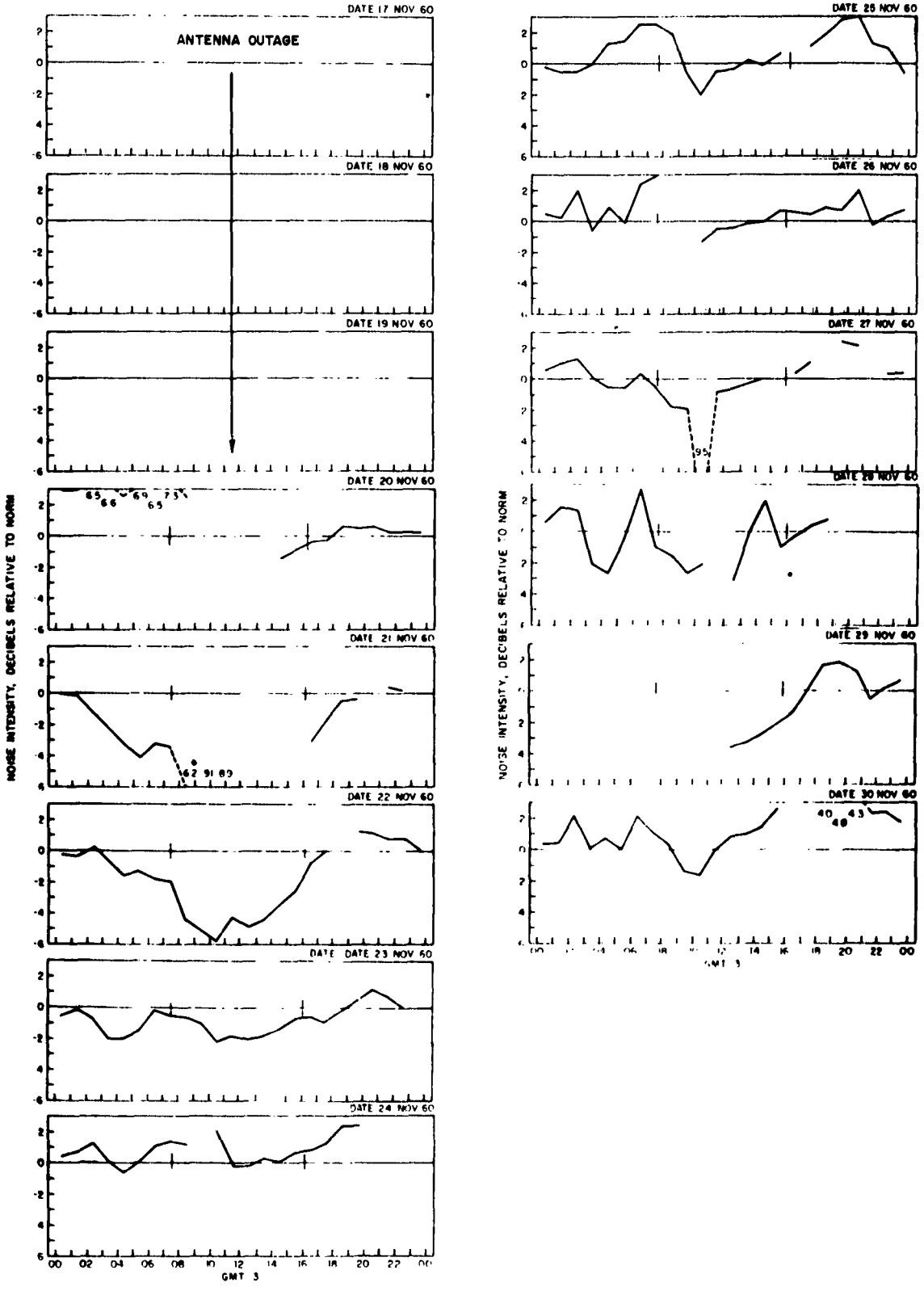

Keflavik, November 1960

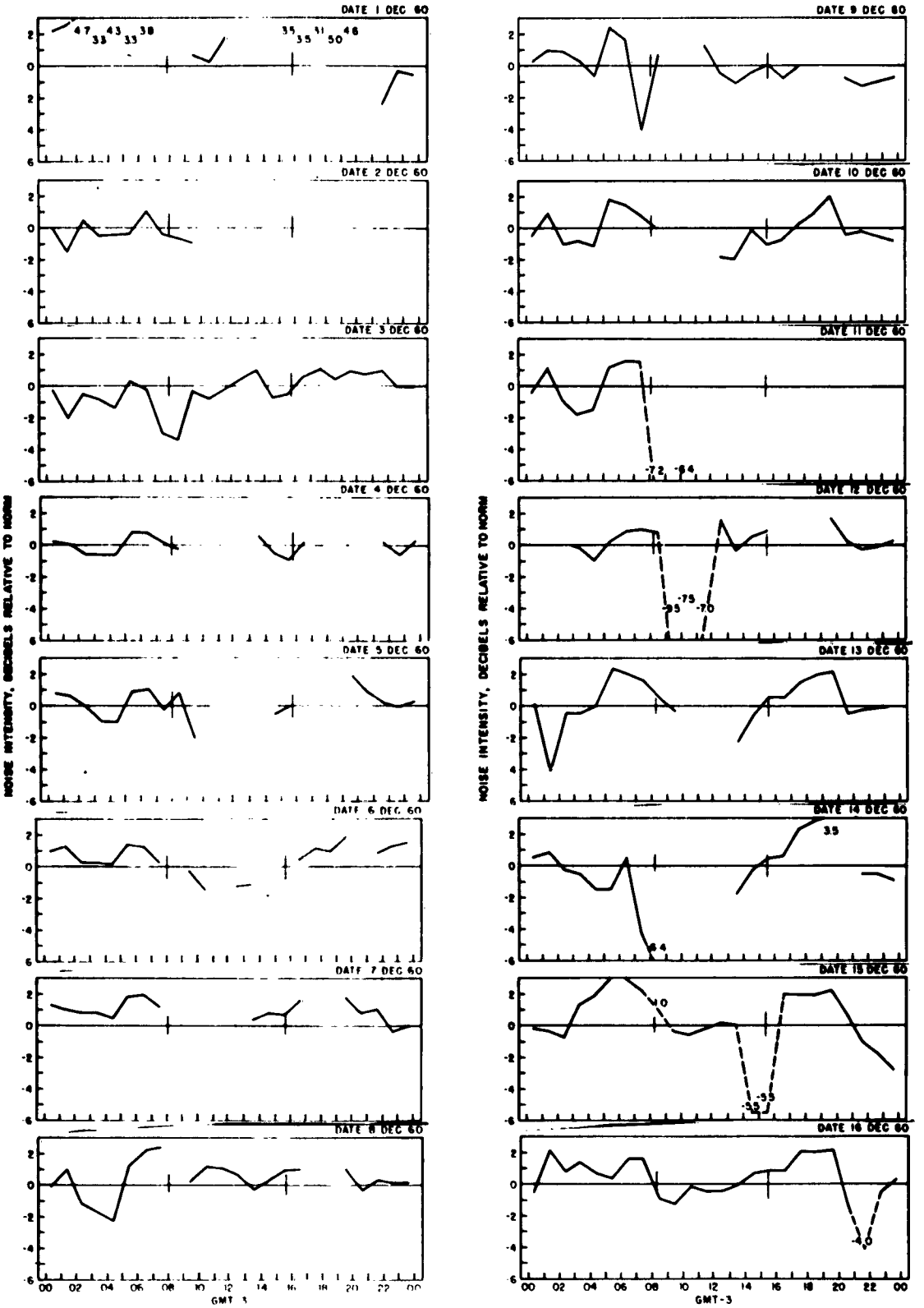

Keflavik, December 1960

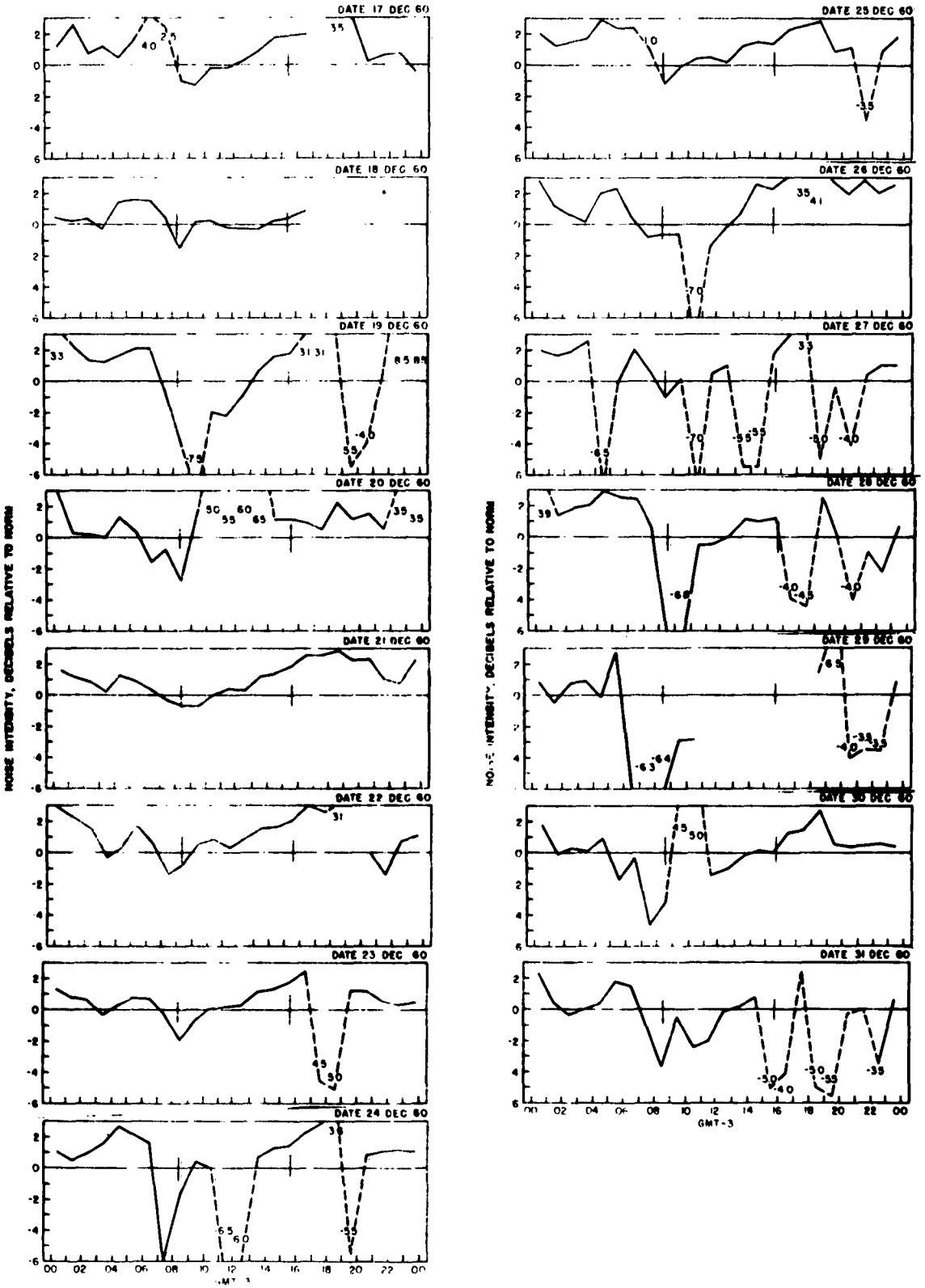

Keflavik, December 1960

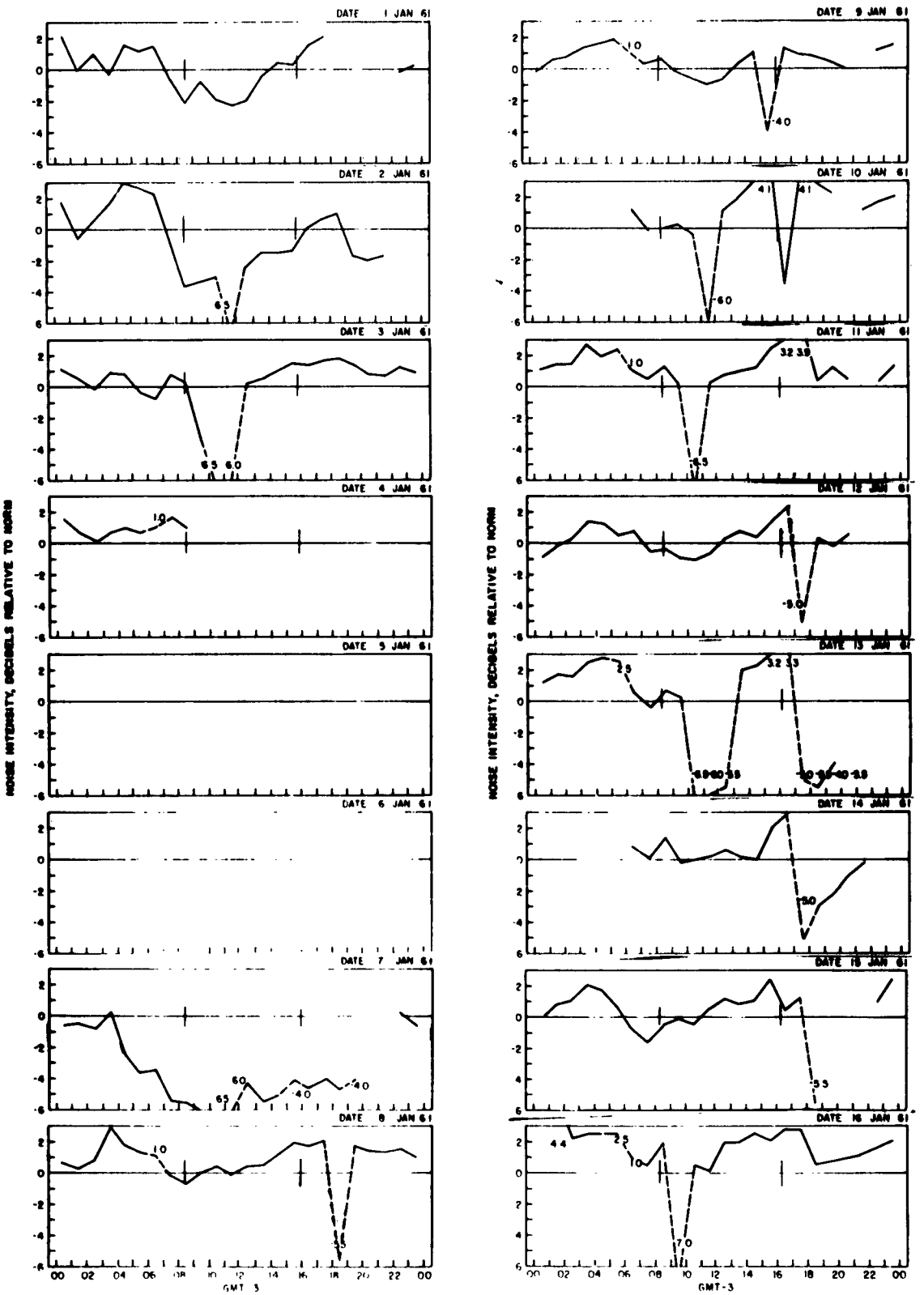

Keflavik, January 1961

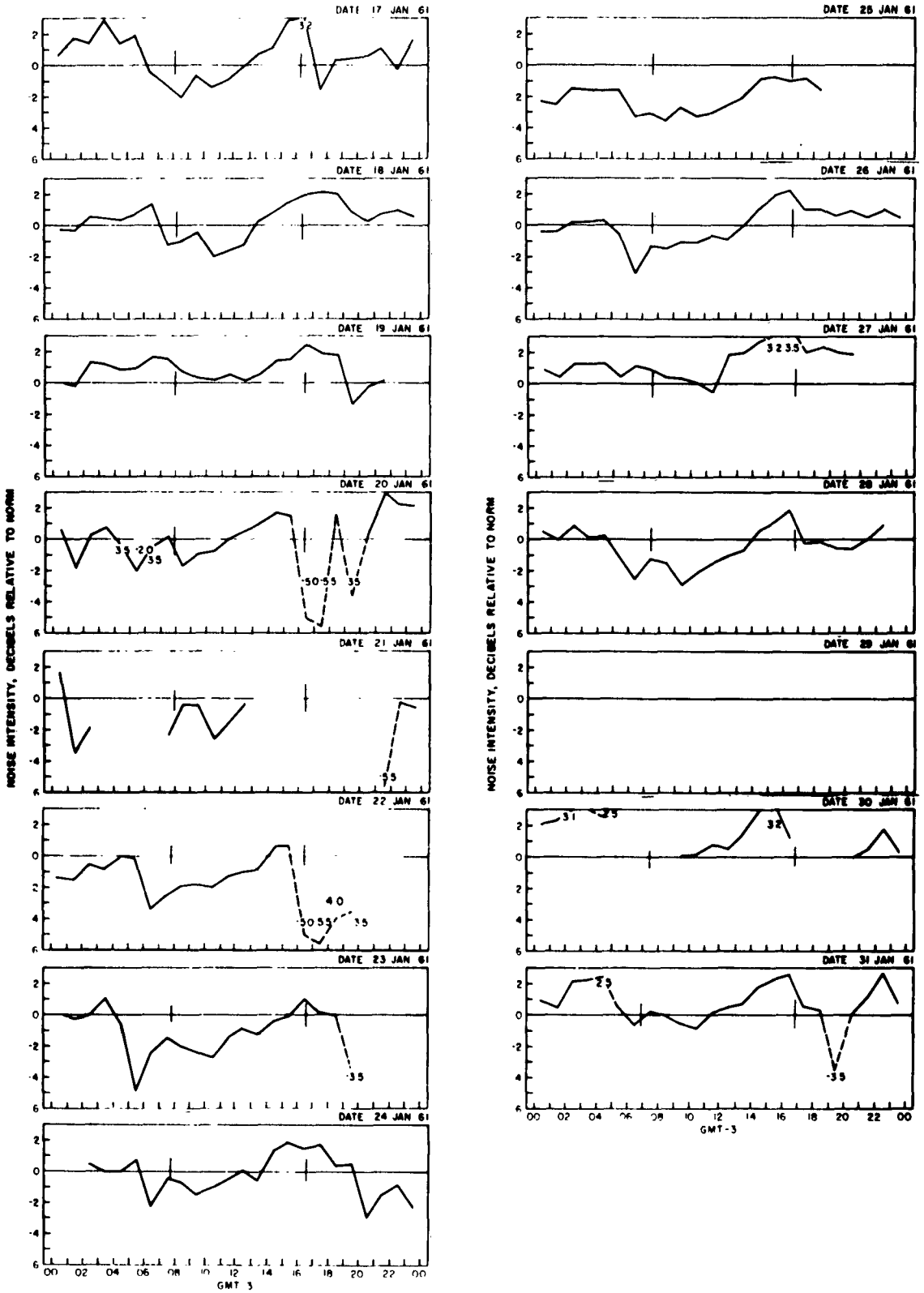

Keflavik, January 1961

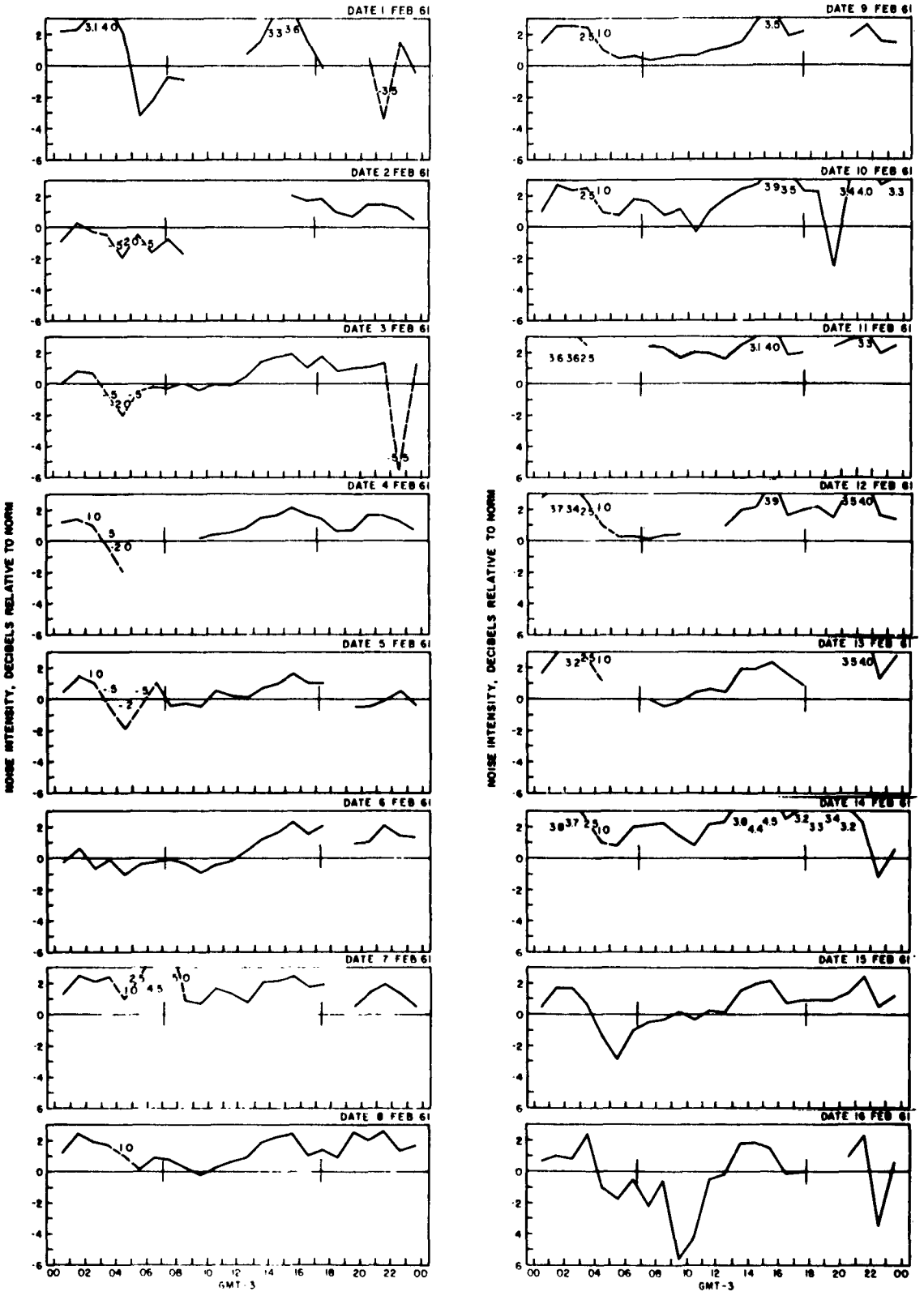

Keflavik, February 1961

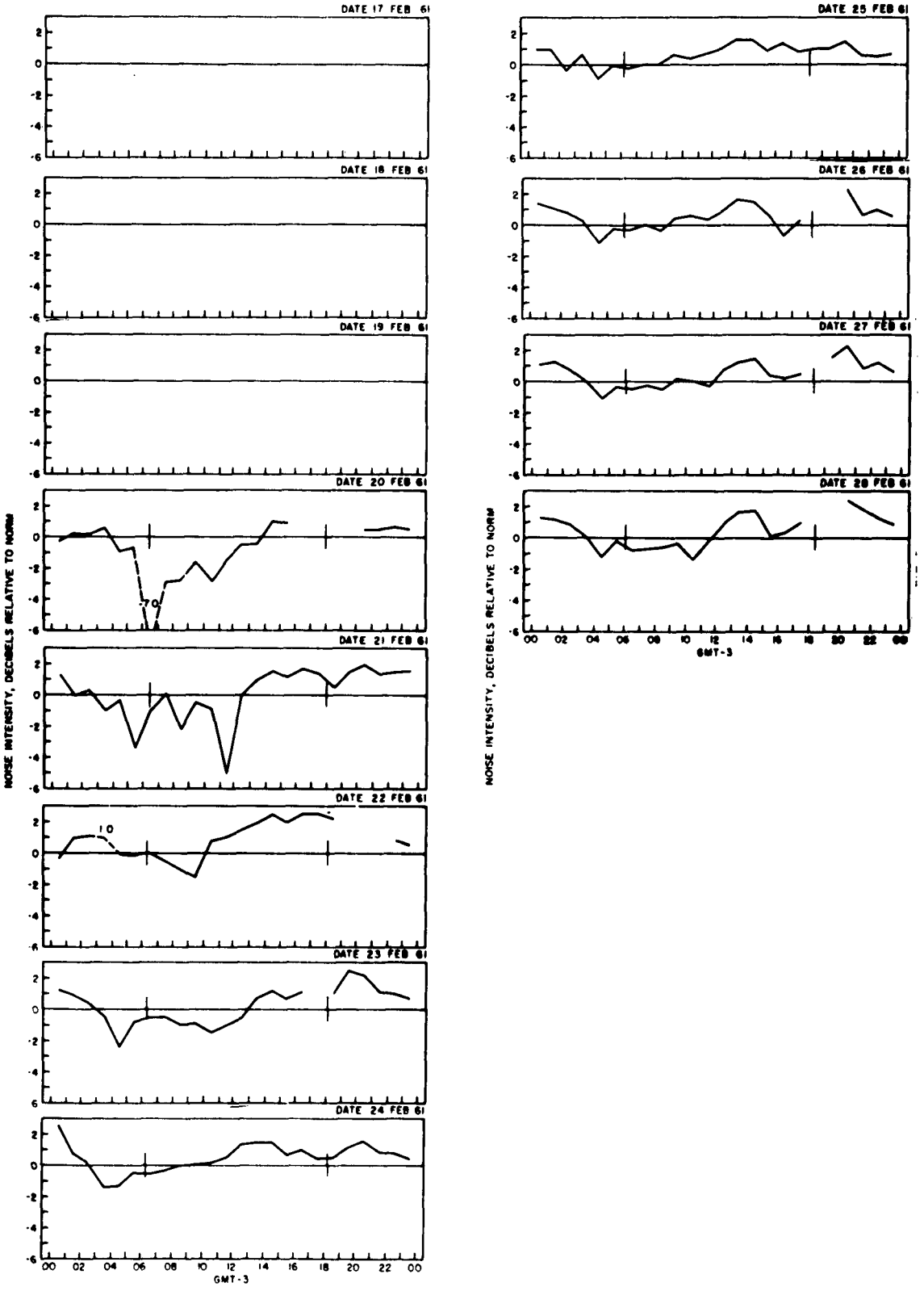

Keflavik, February 1961

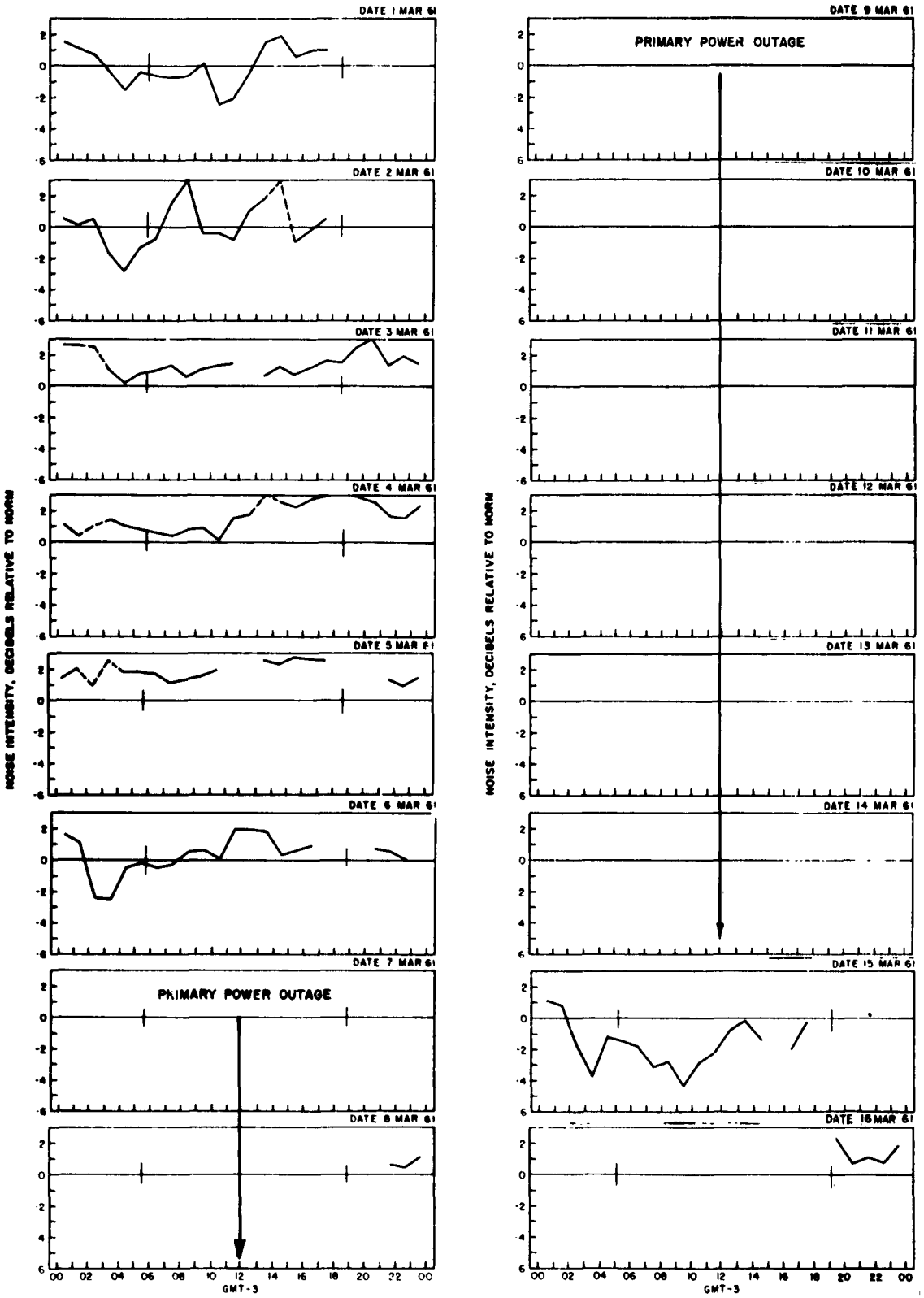

Keflavik, March 1961

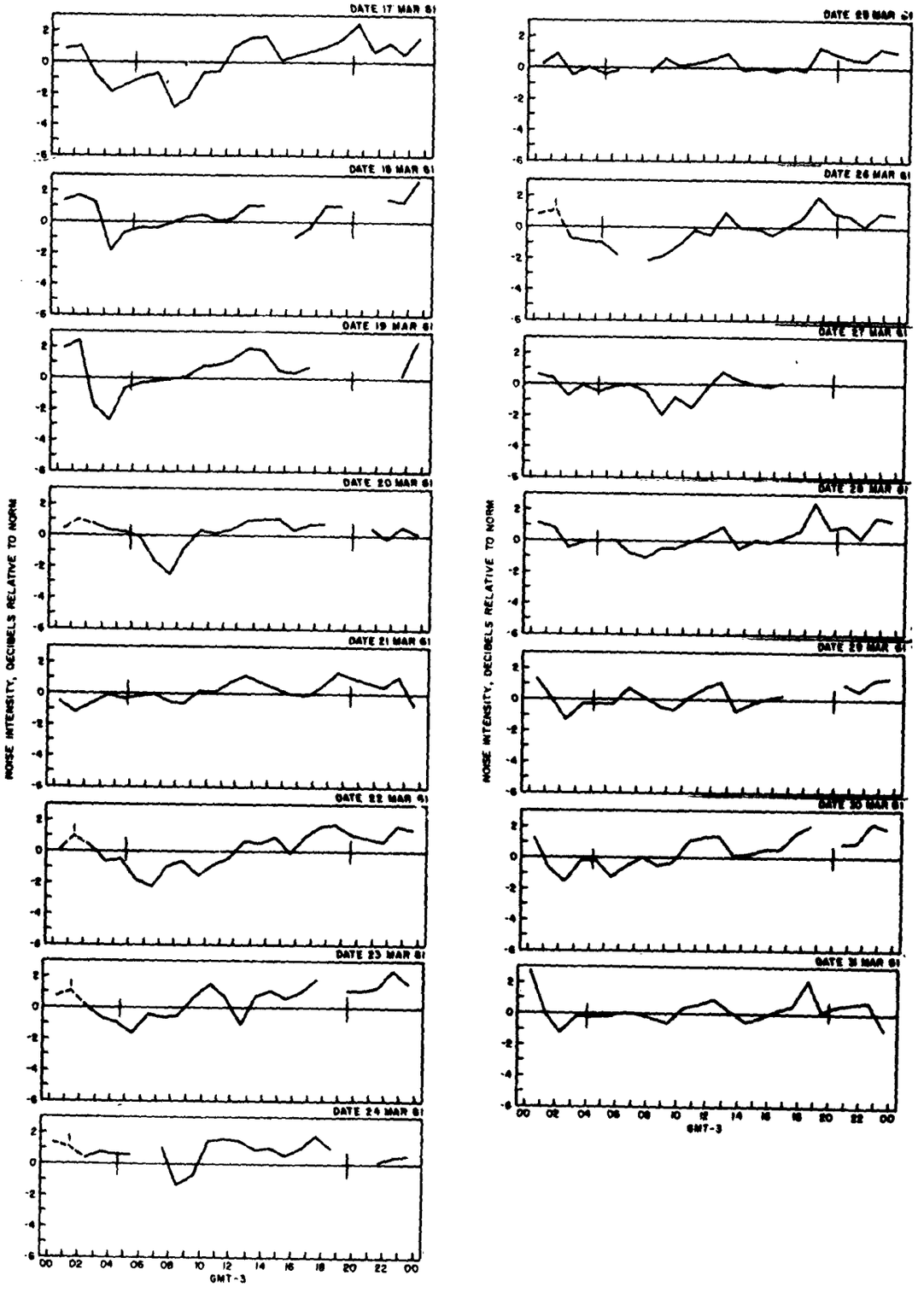

Keflavik, March 1961

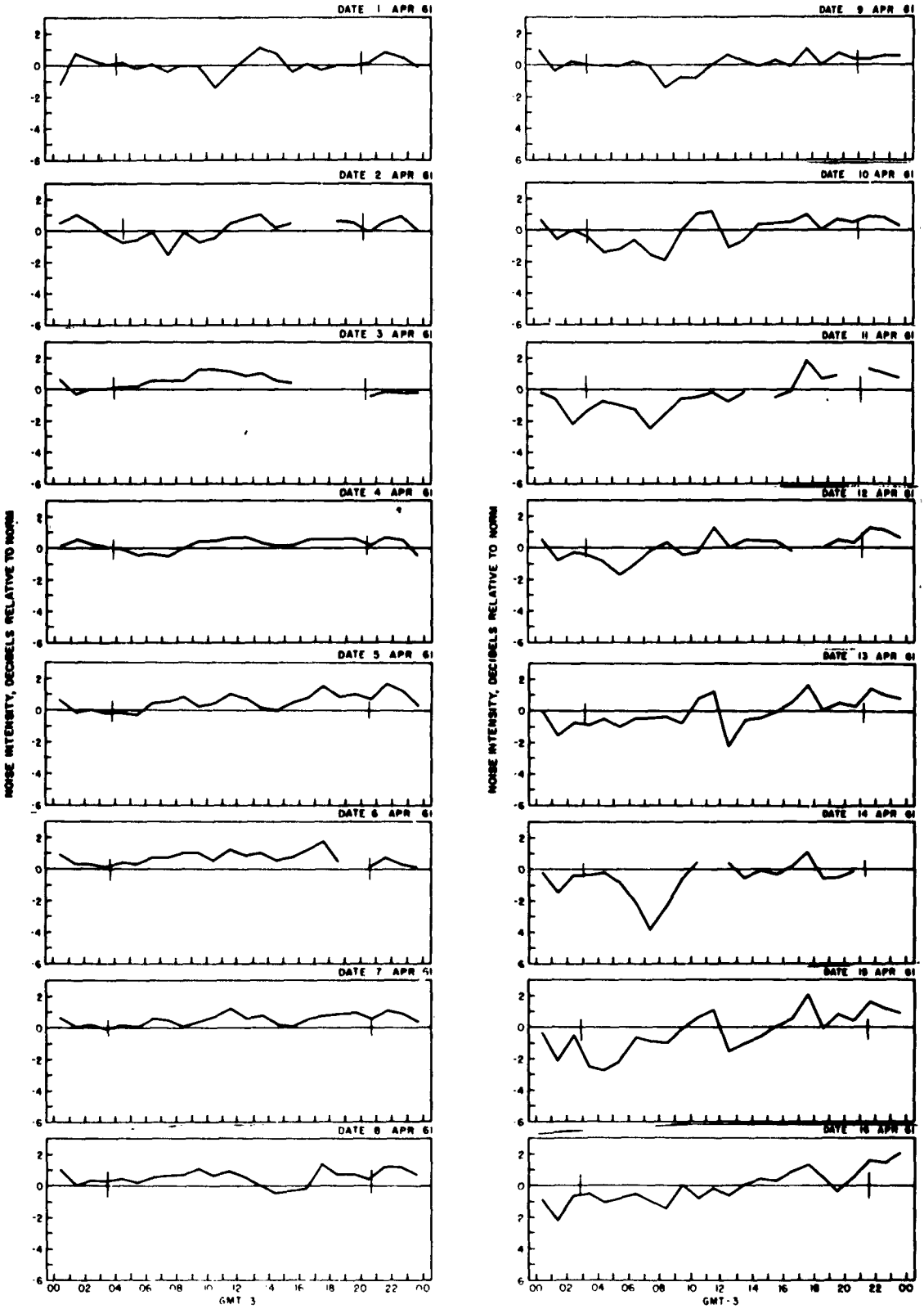

Keflavik, April 1961

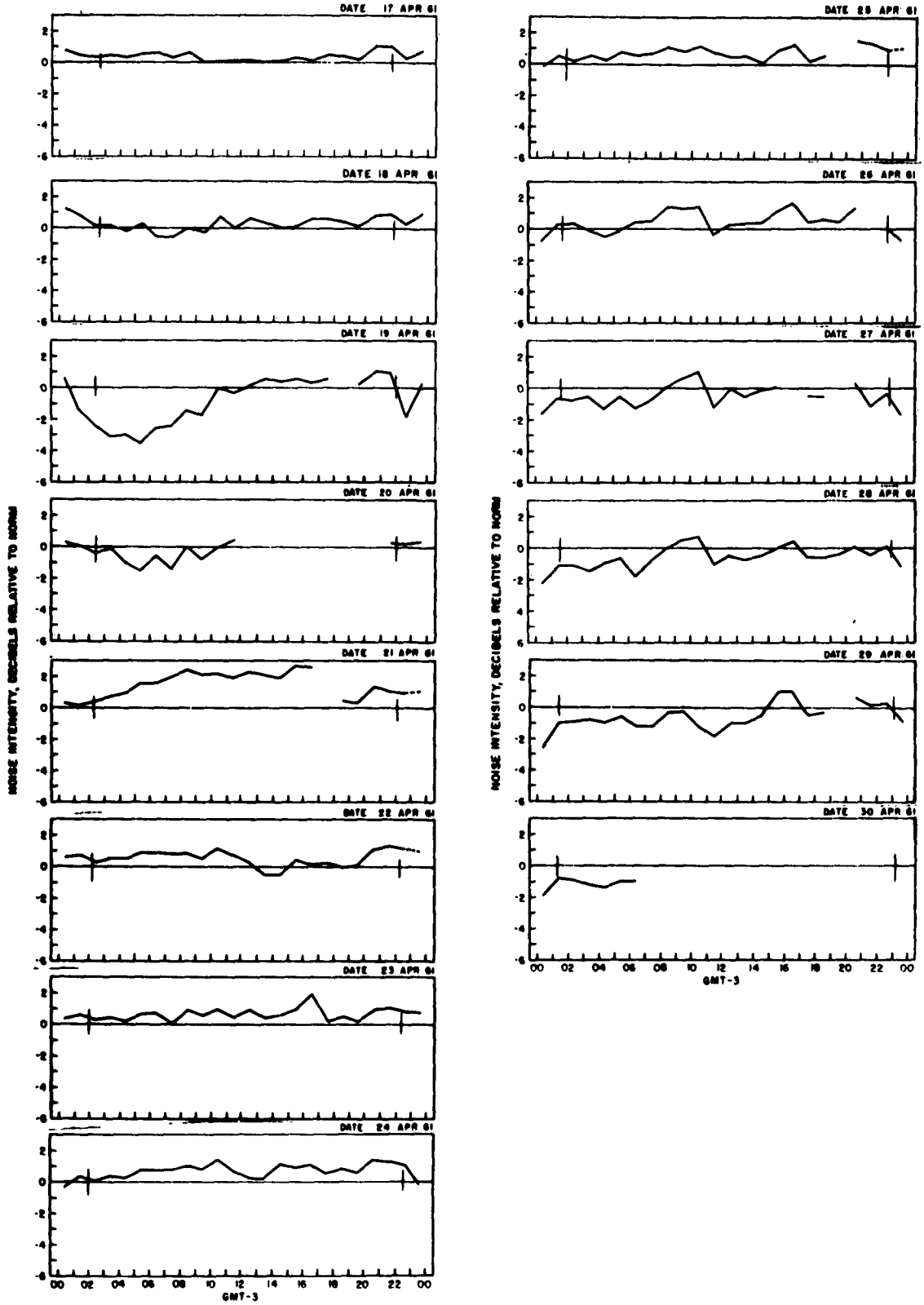

Keflavik, April 1961

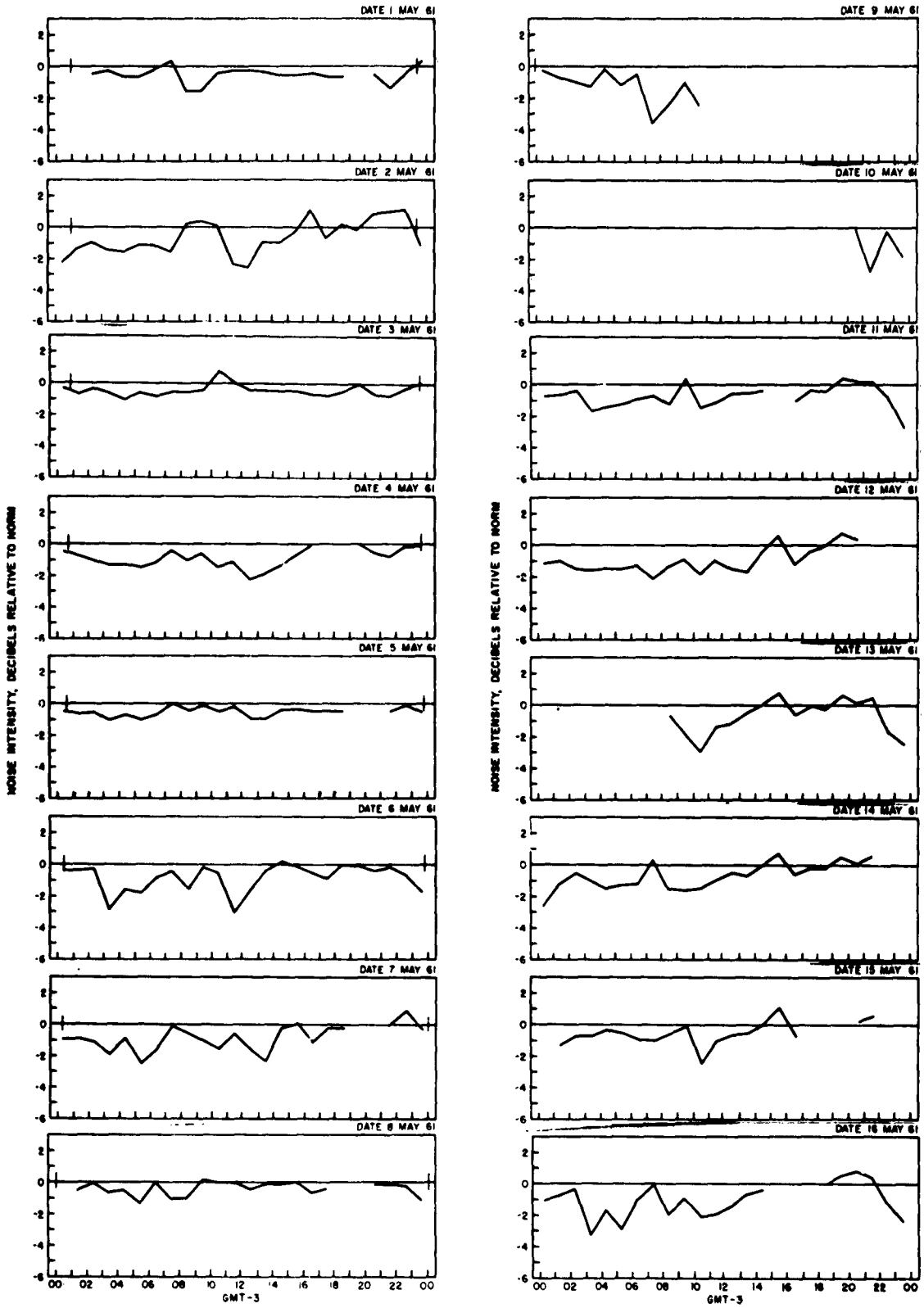

Keflavik, May 1961

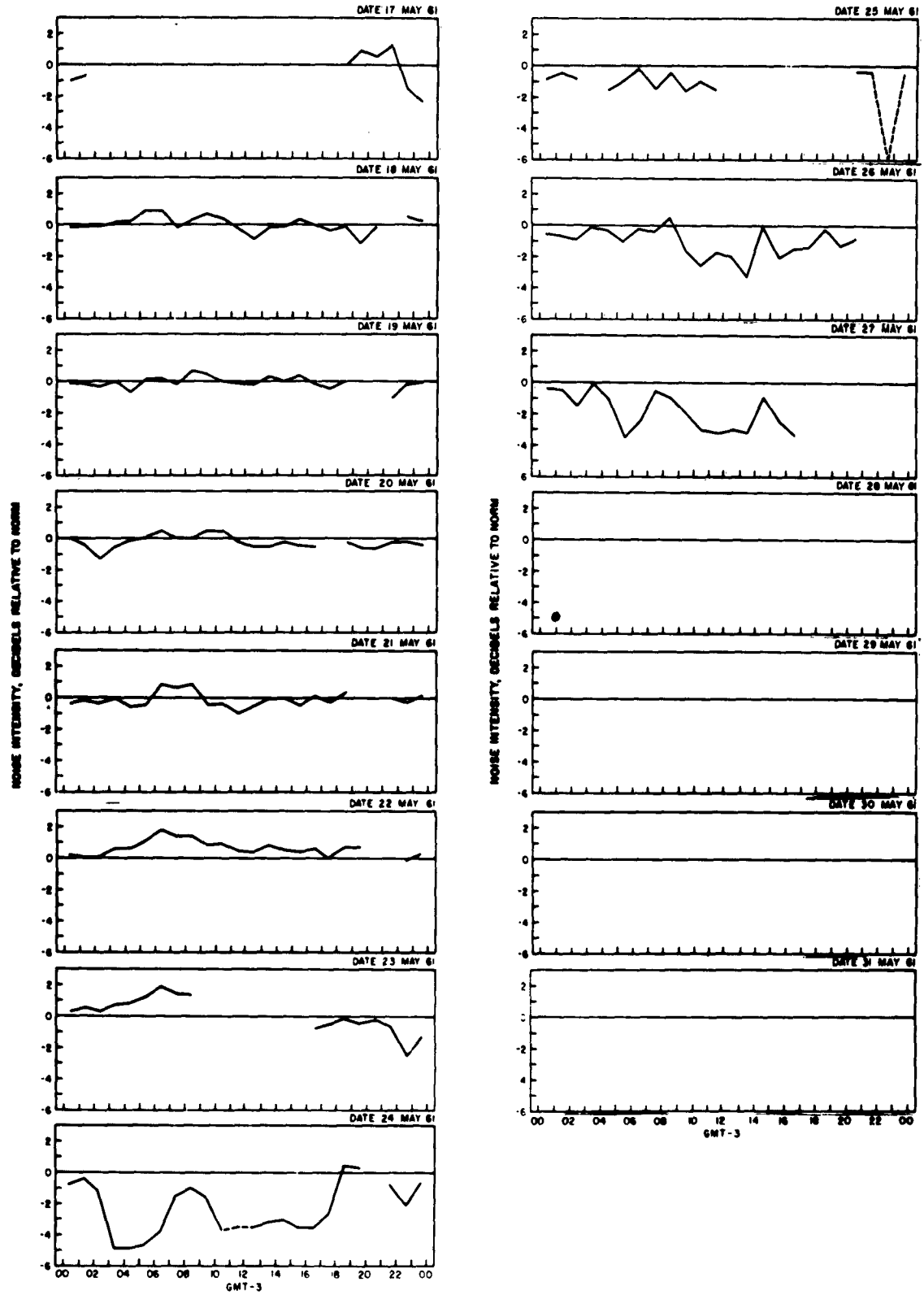

Keflavik, May 1961

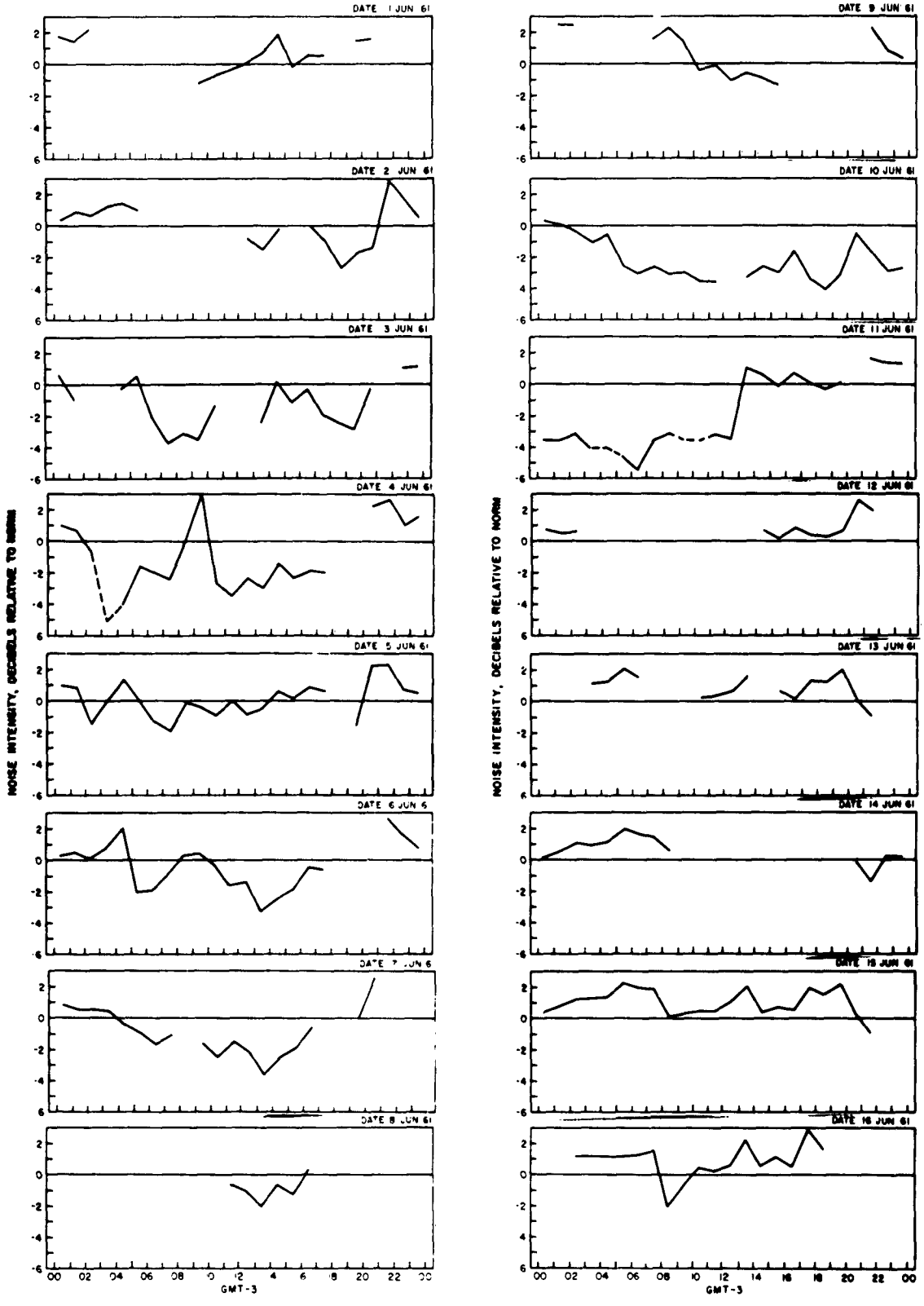

Keflavik, June 1961

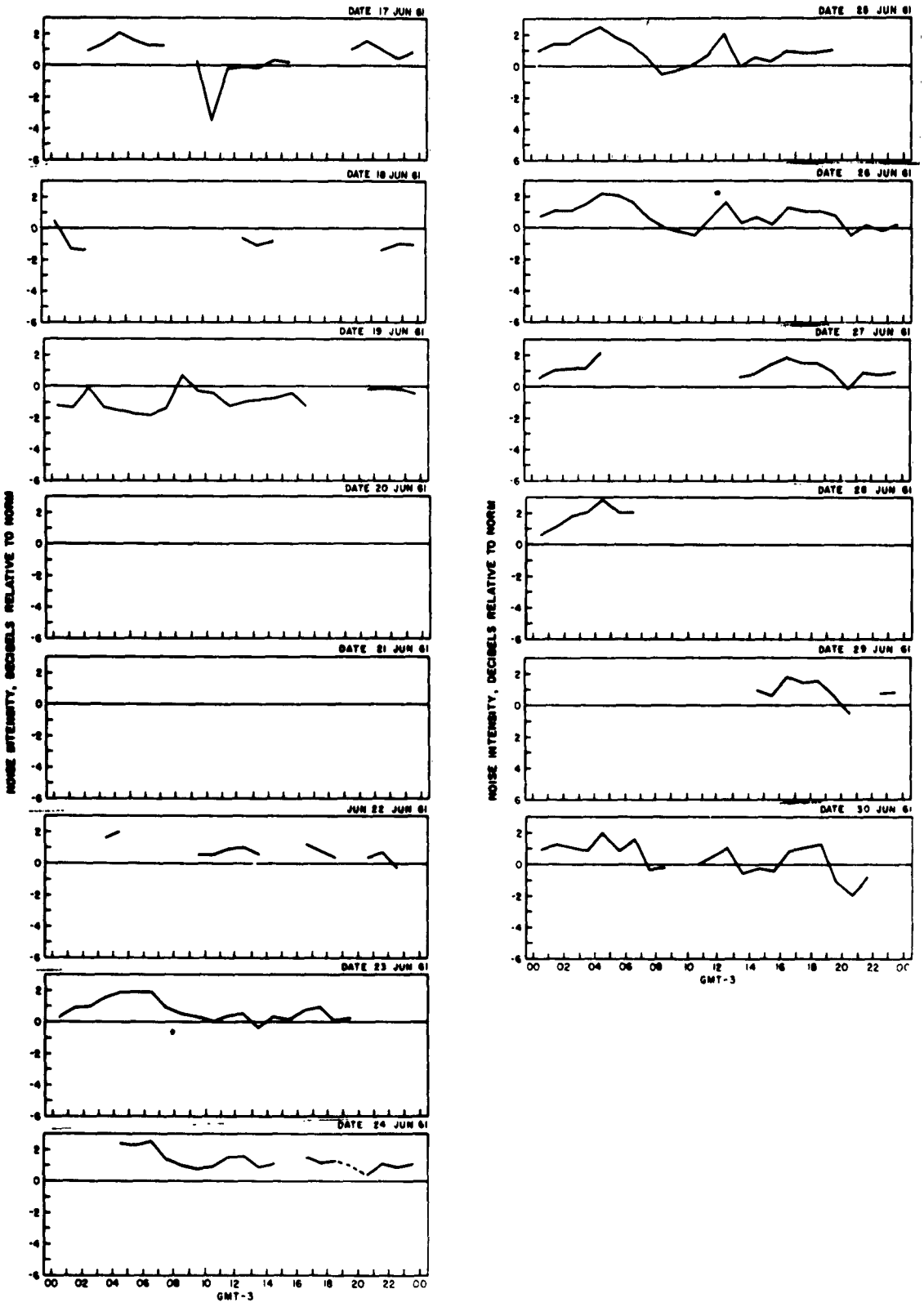

Keflavik, June 1961

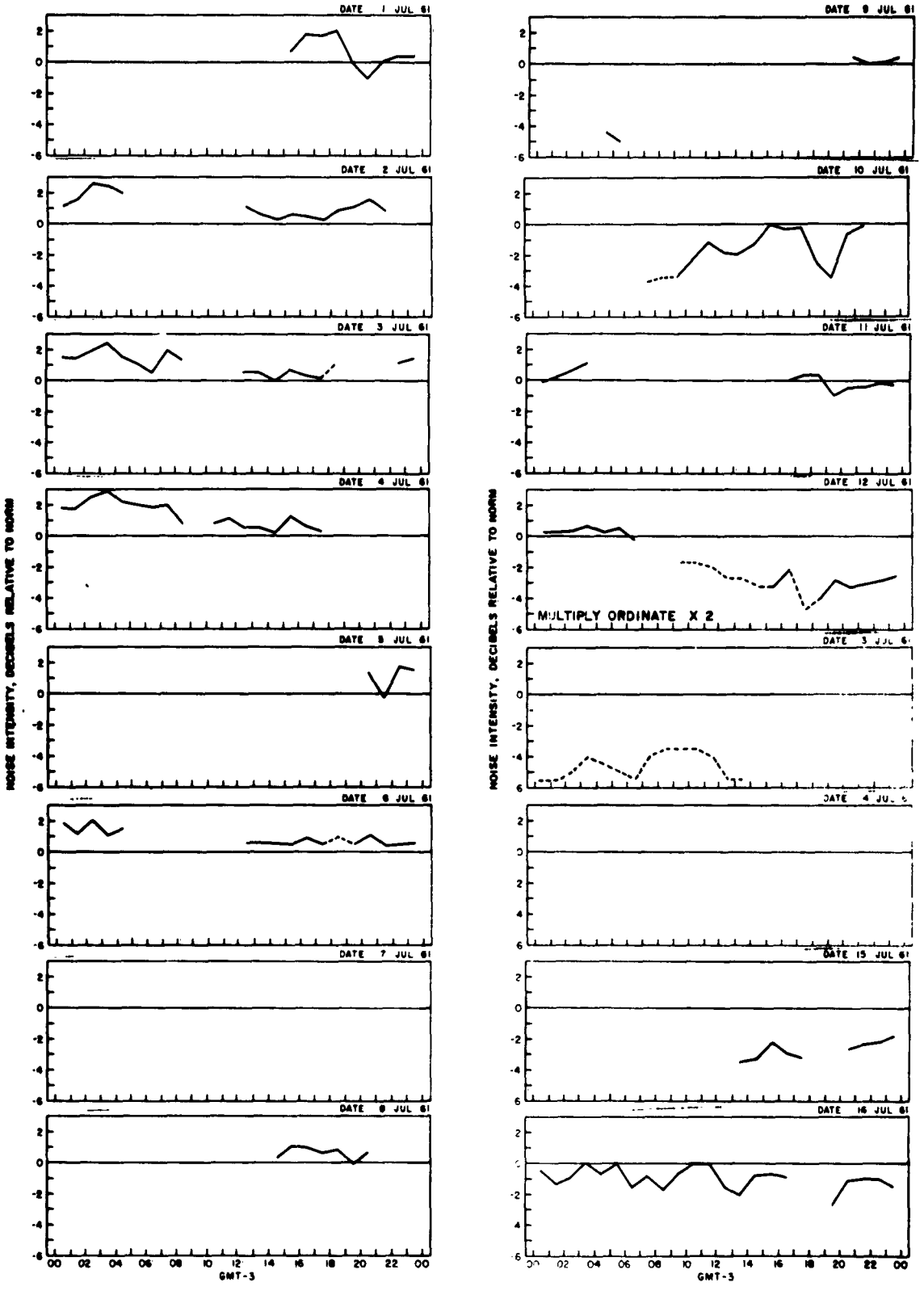

Keflavik, July 1961

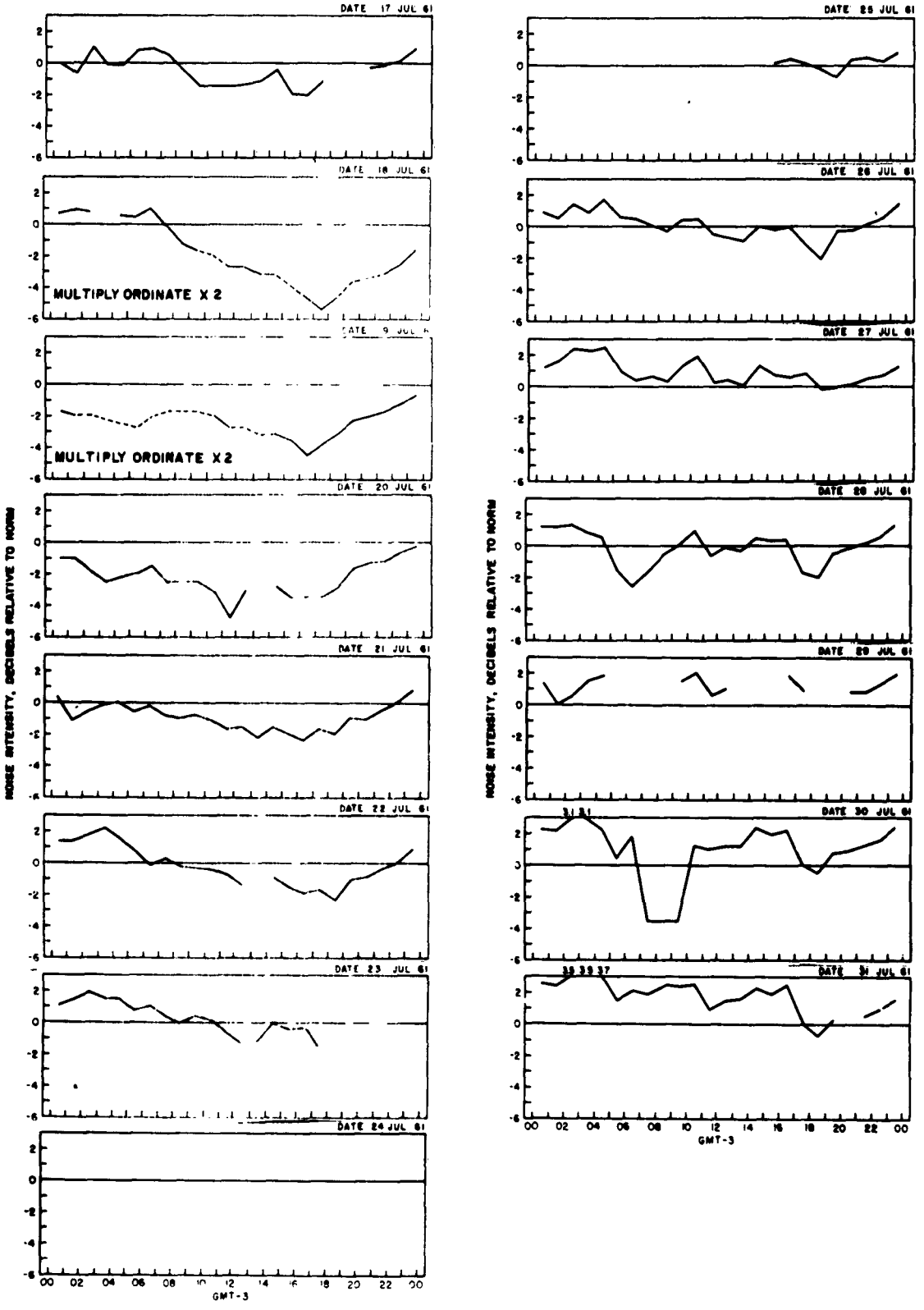

Keflavik, July 1961

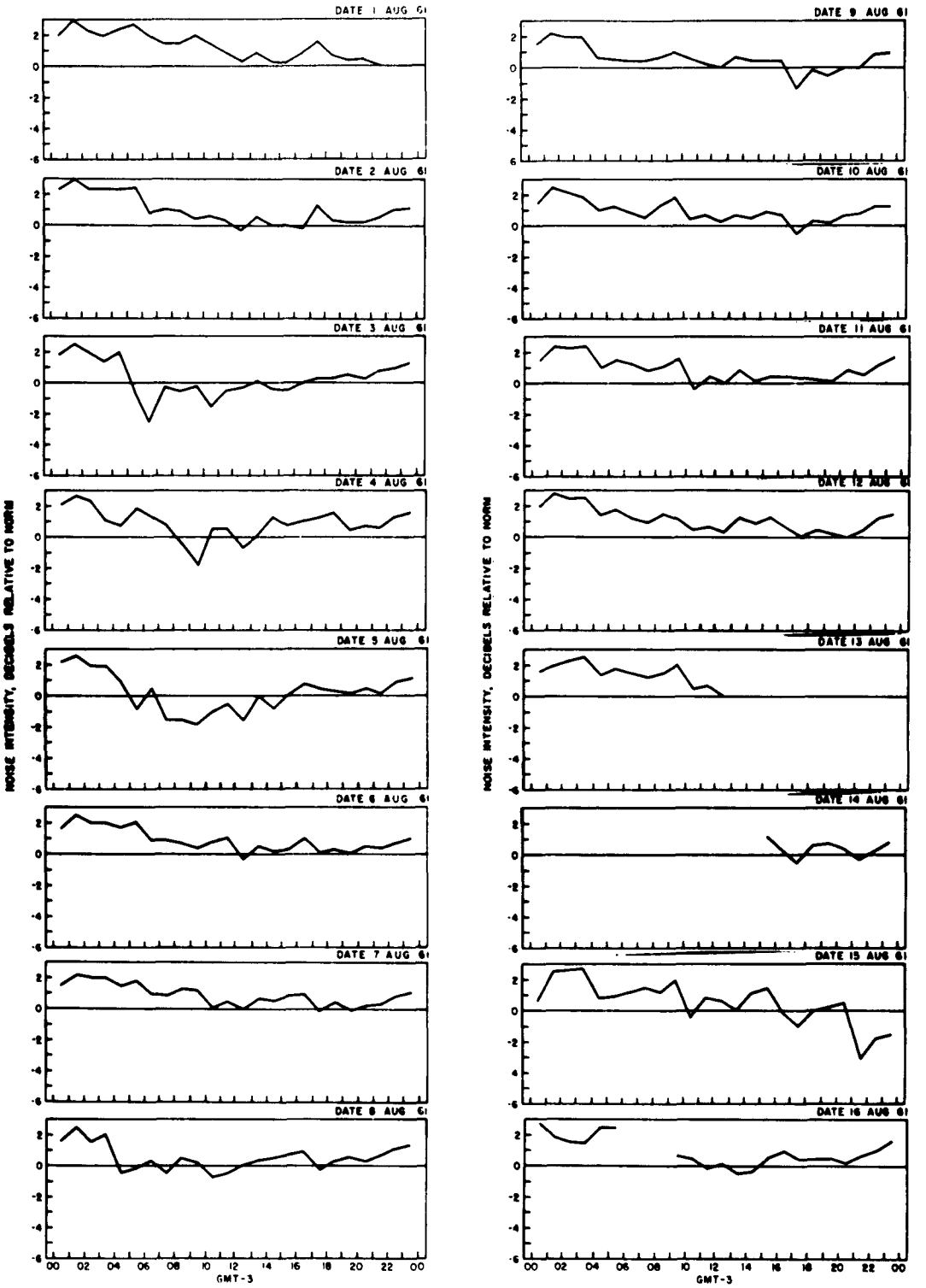

Keflavik, August 1961

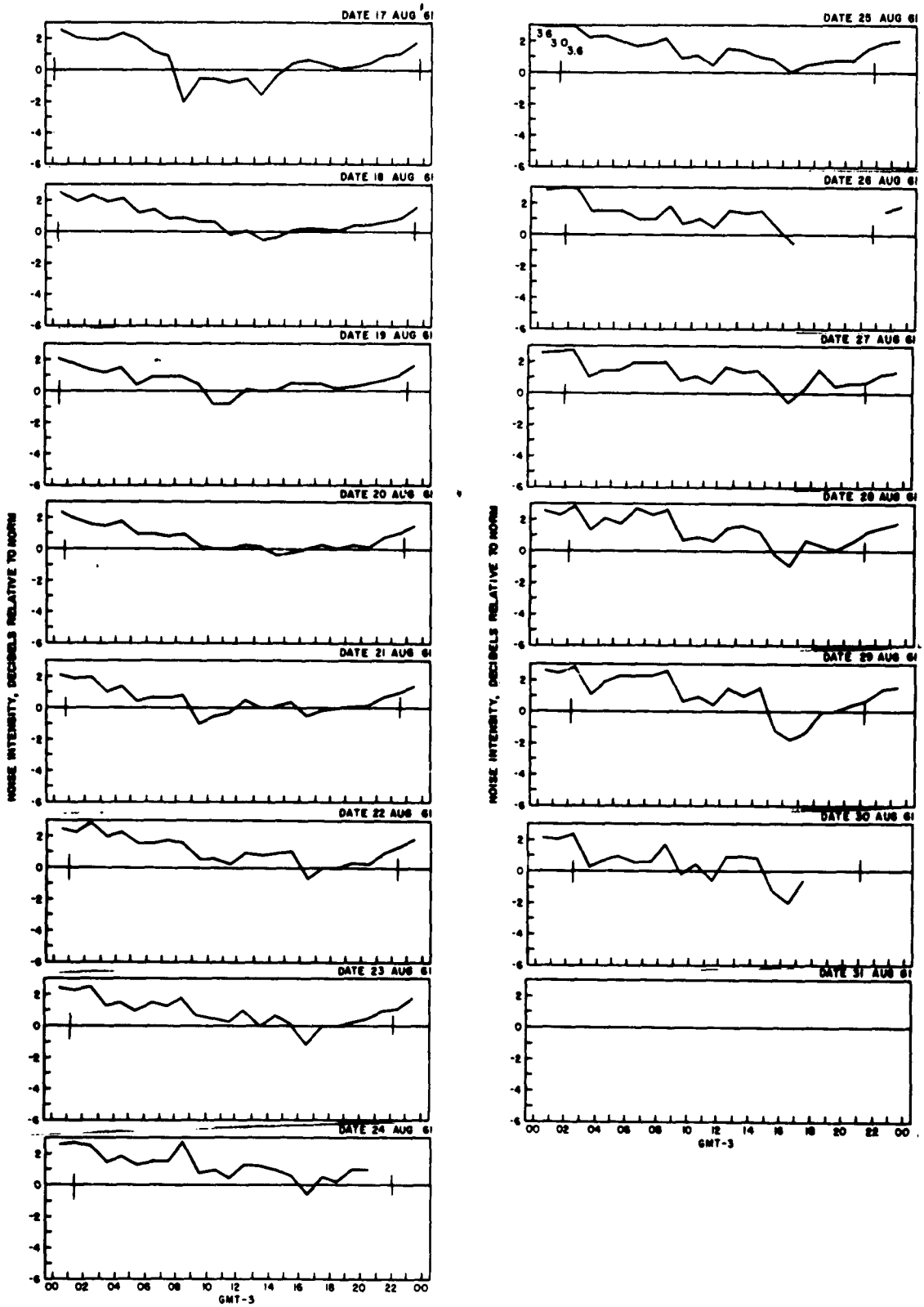

Keflavik, August 1961

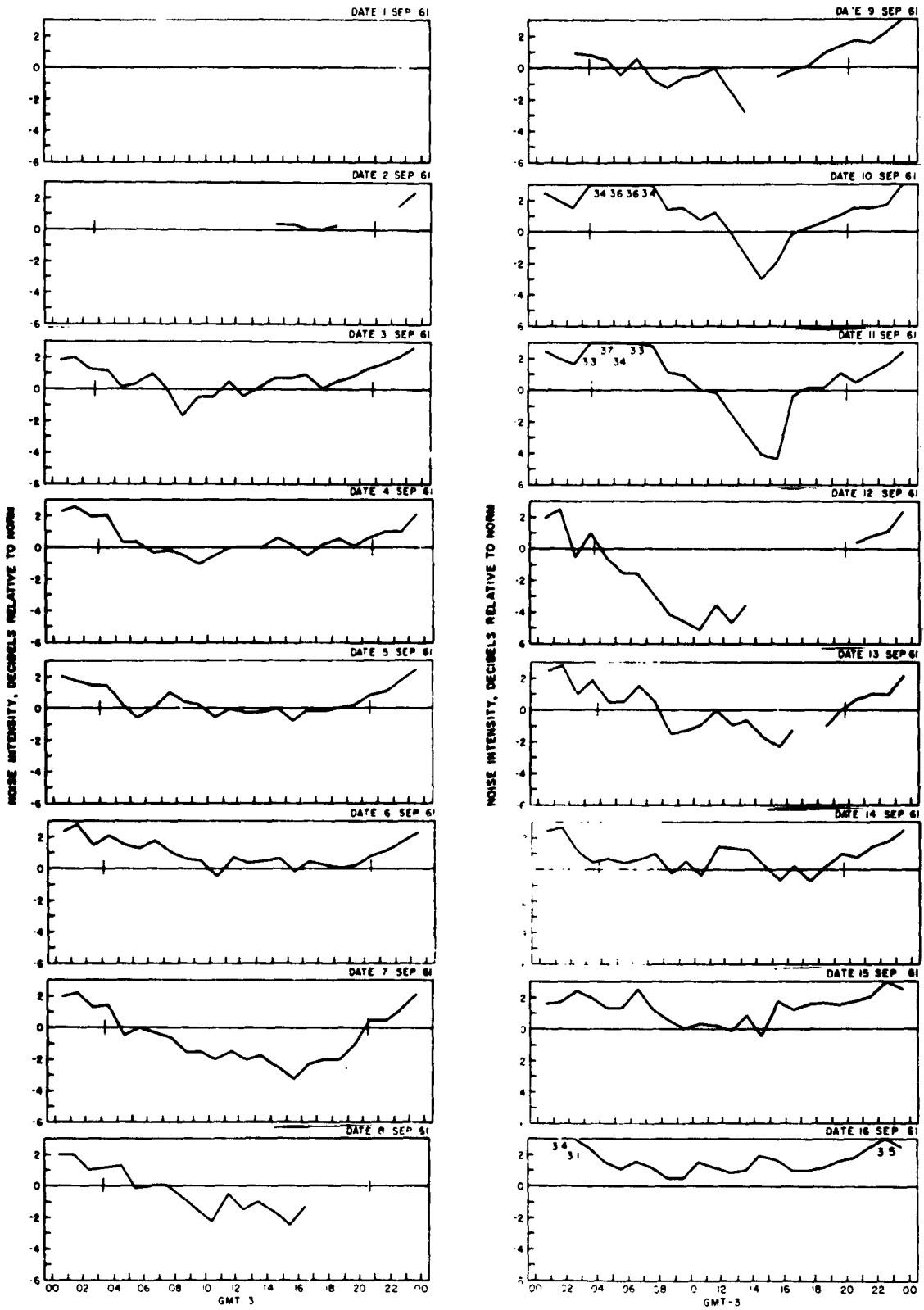

Keflavik, September 1961

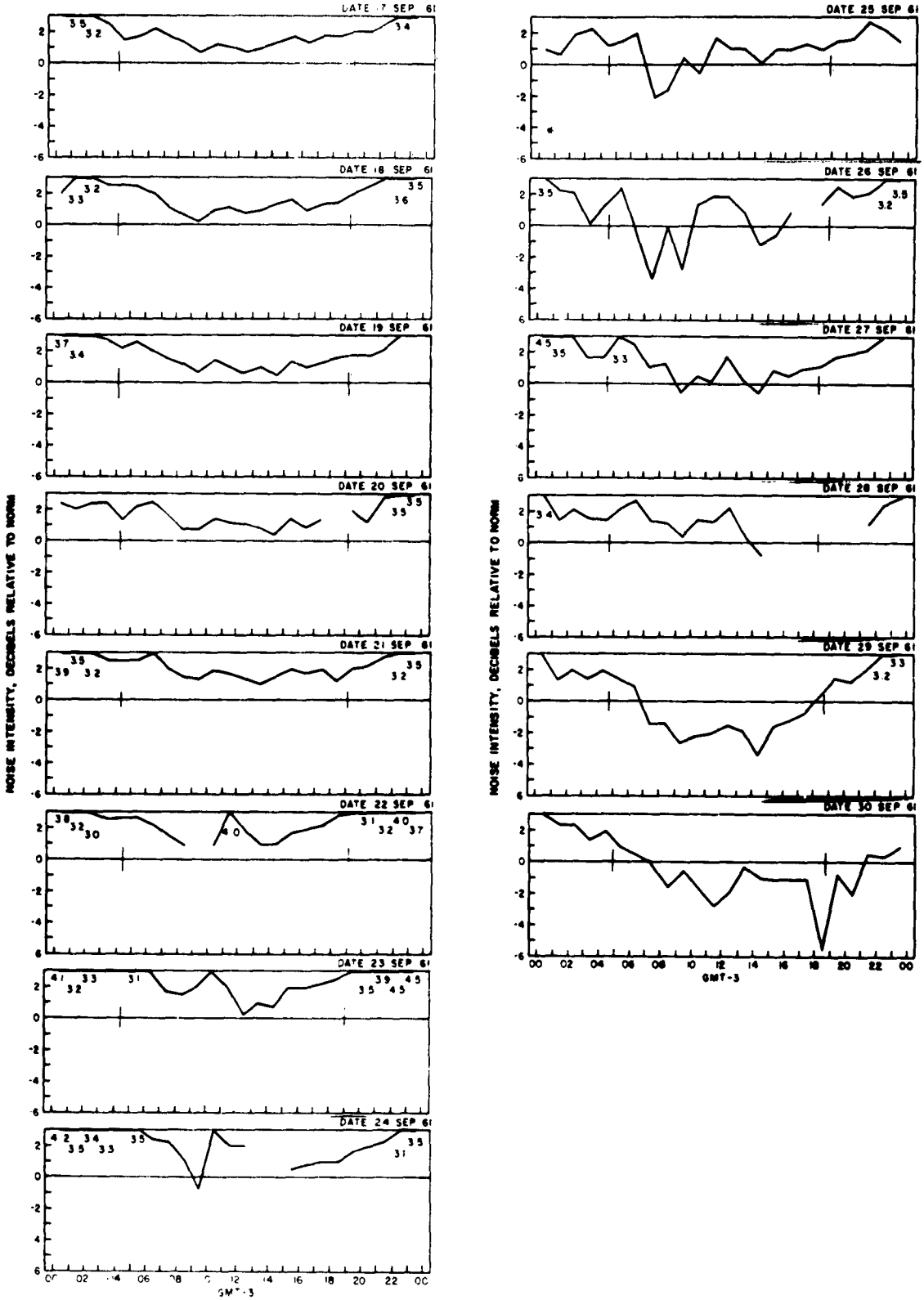

Keflavik, September 1961

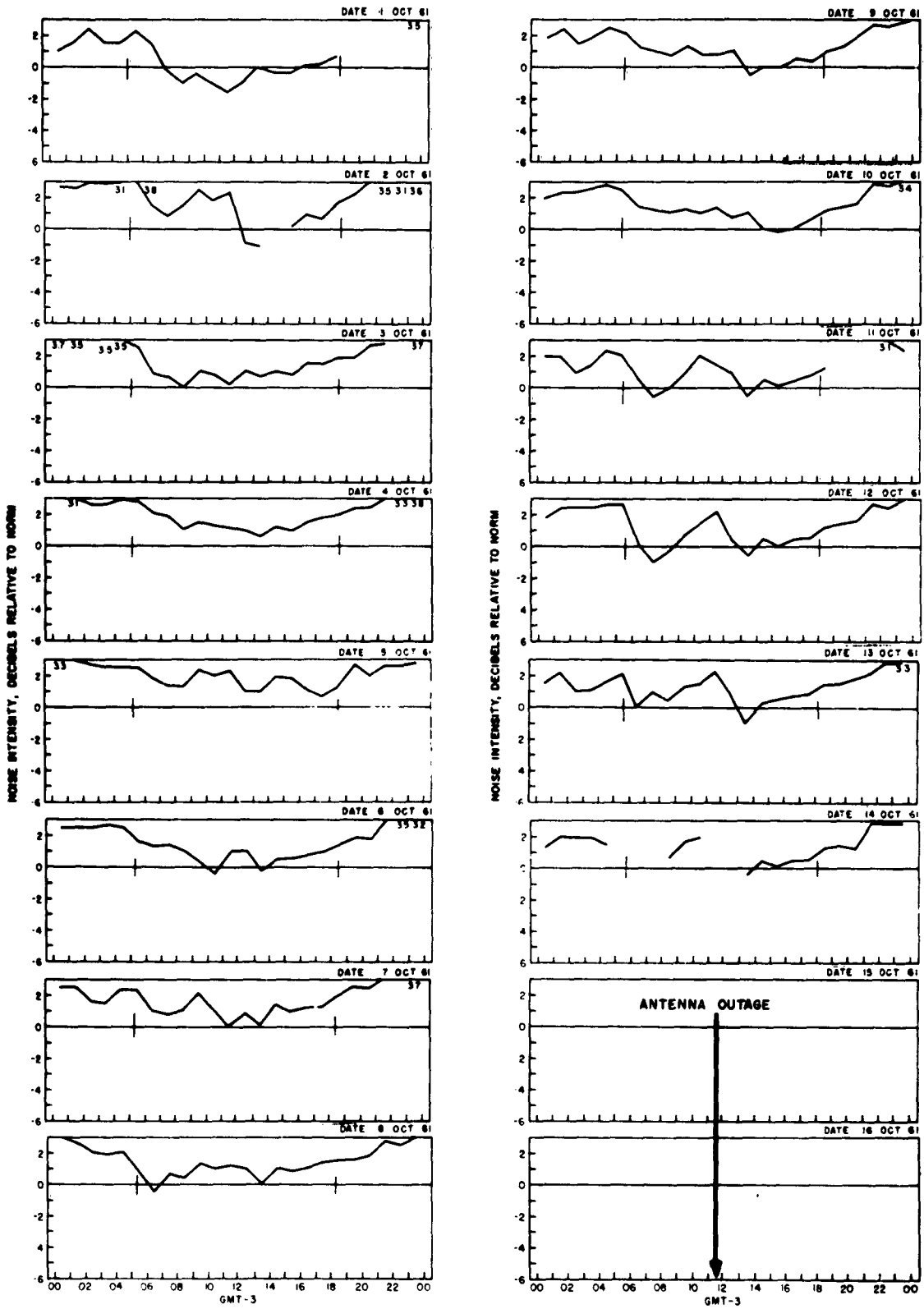

Keflavik, October 1961

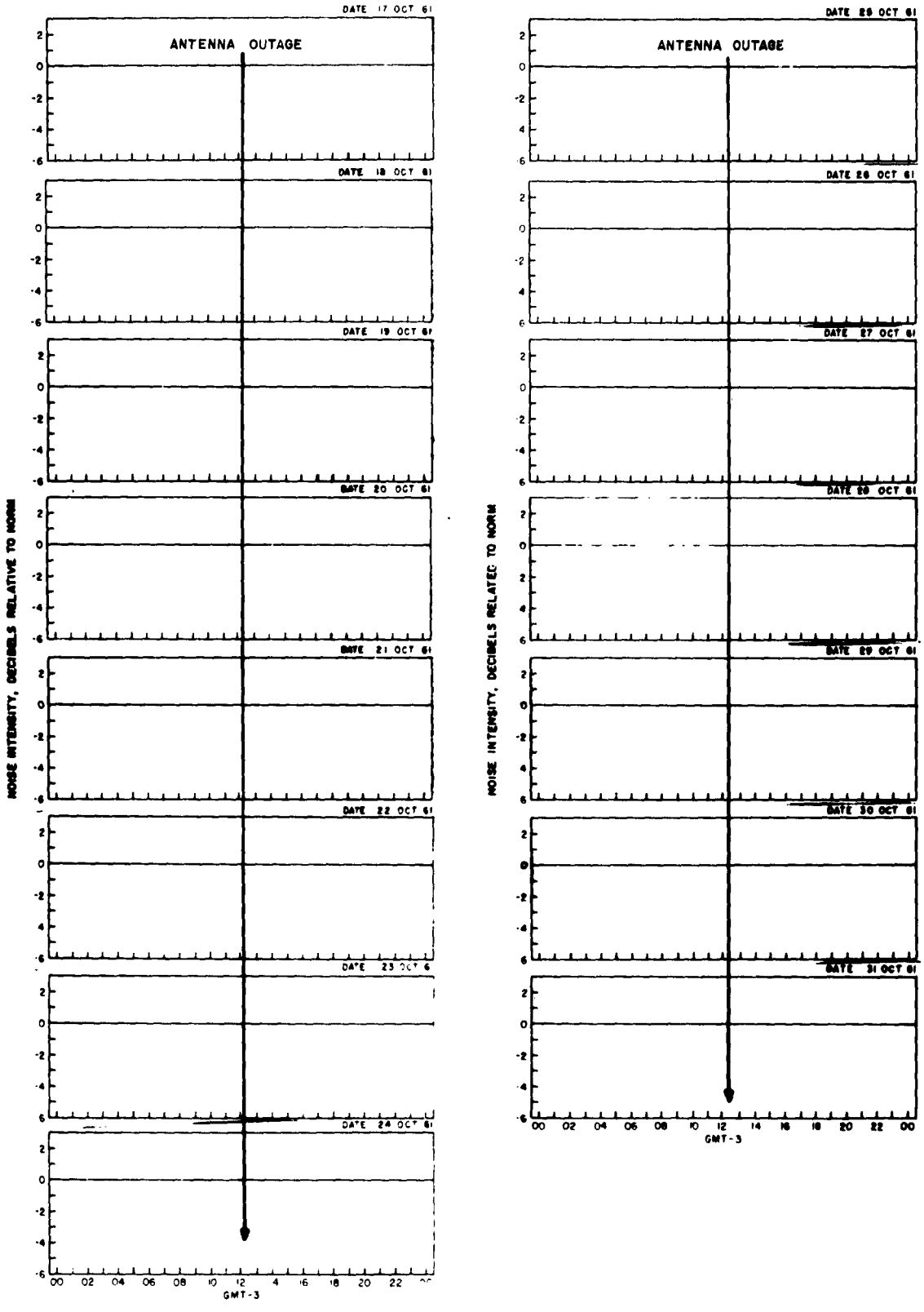

Keflavik, October 1961

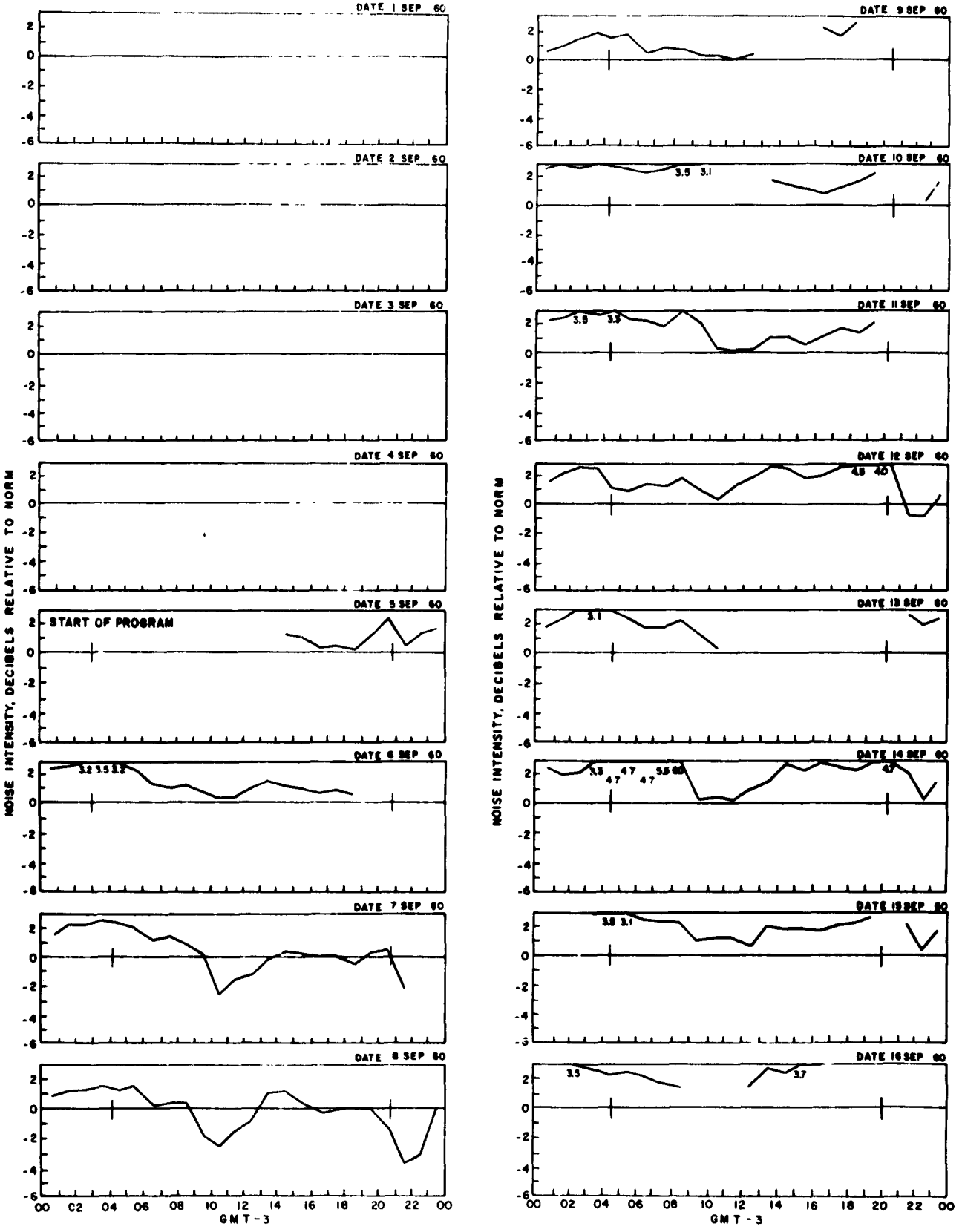

Goose Bay, September 1960

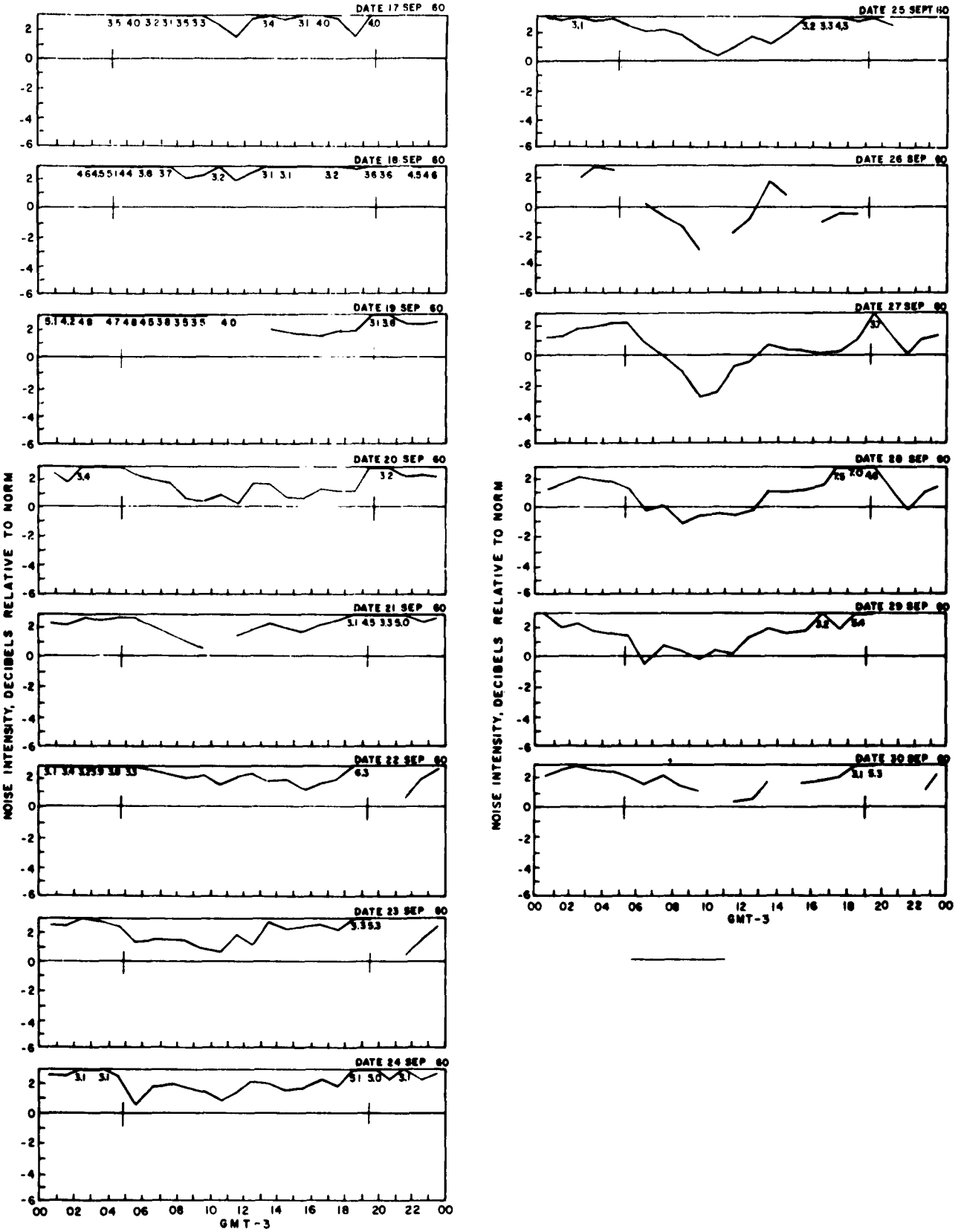

Goose Bay, September 1960

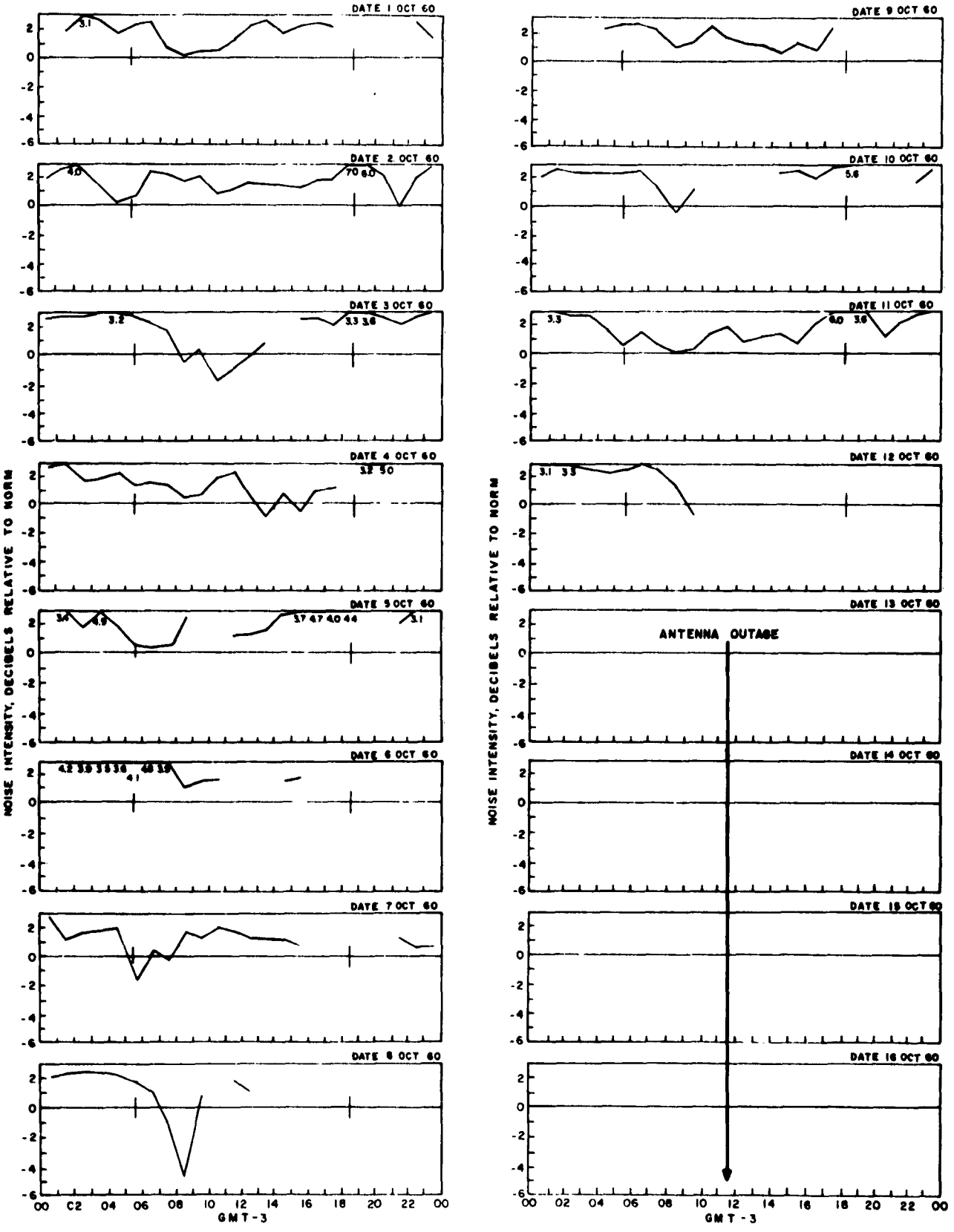

Goose Bay, October 1960

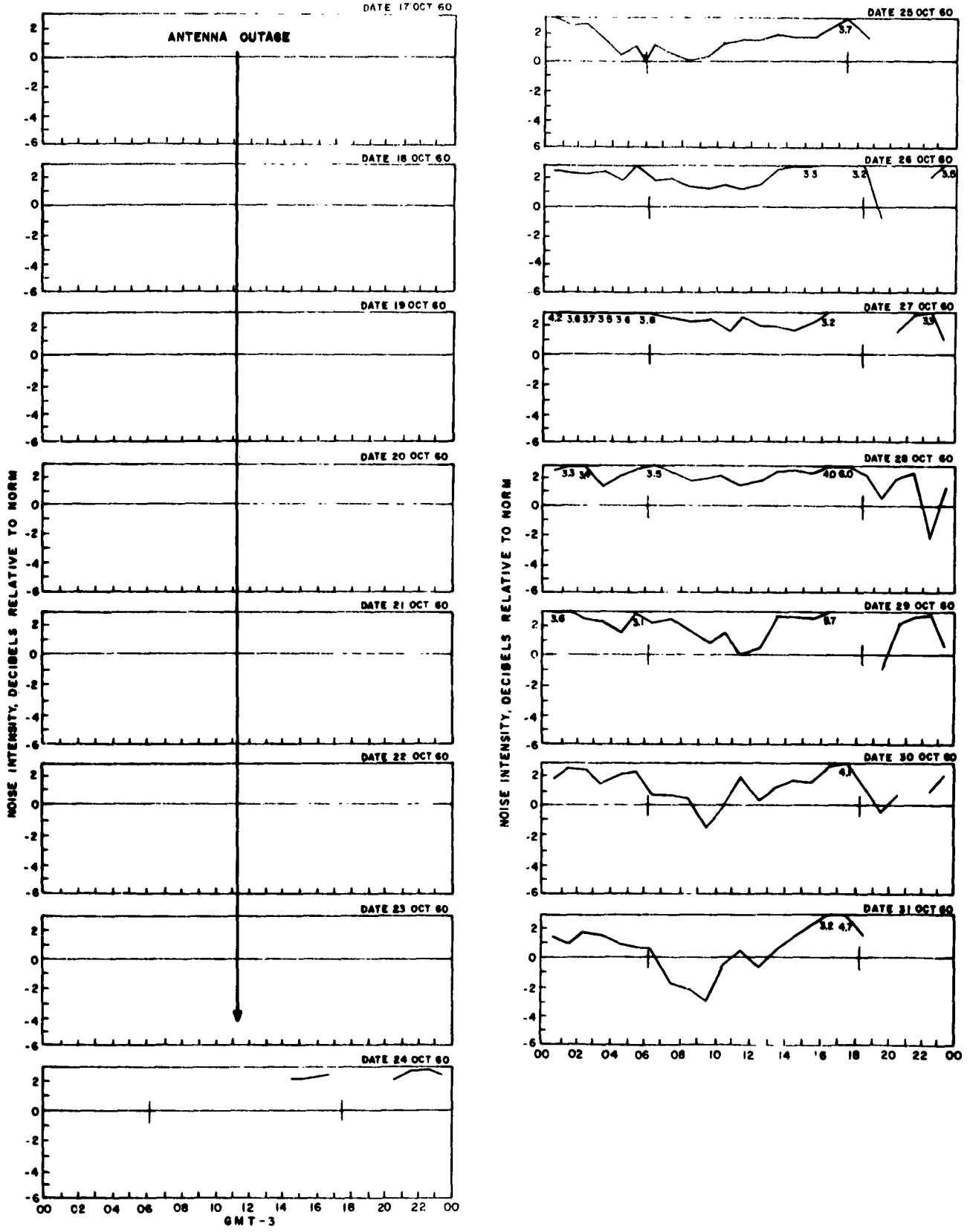

Goose Bay, October 1960

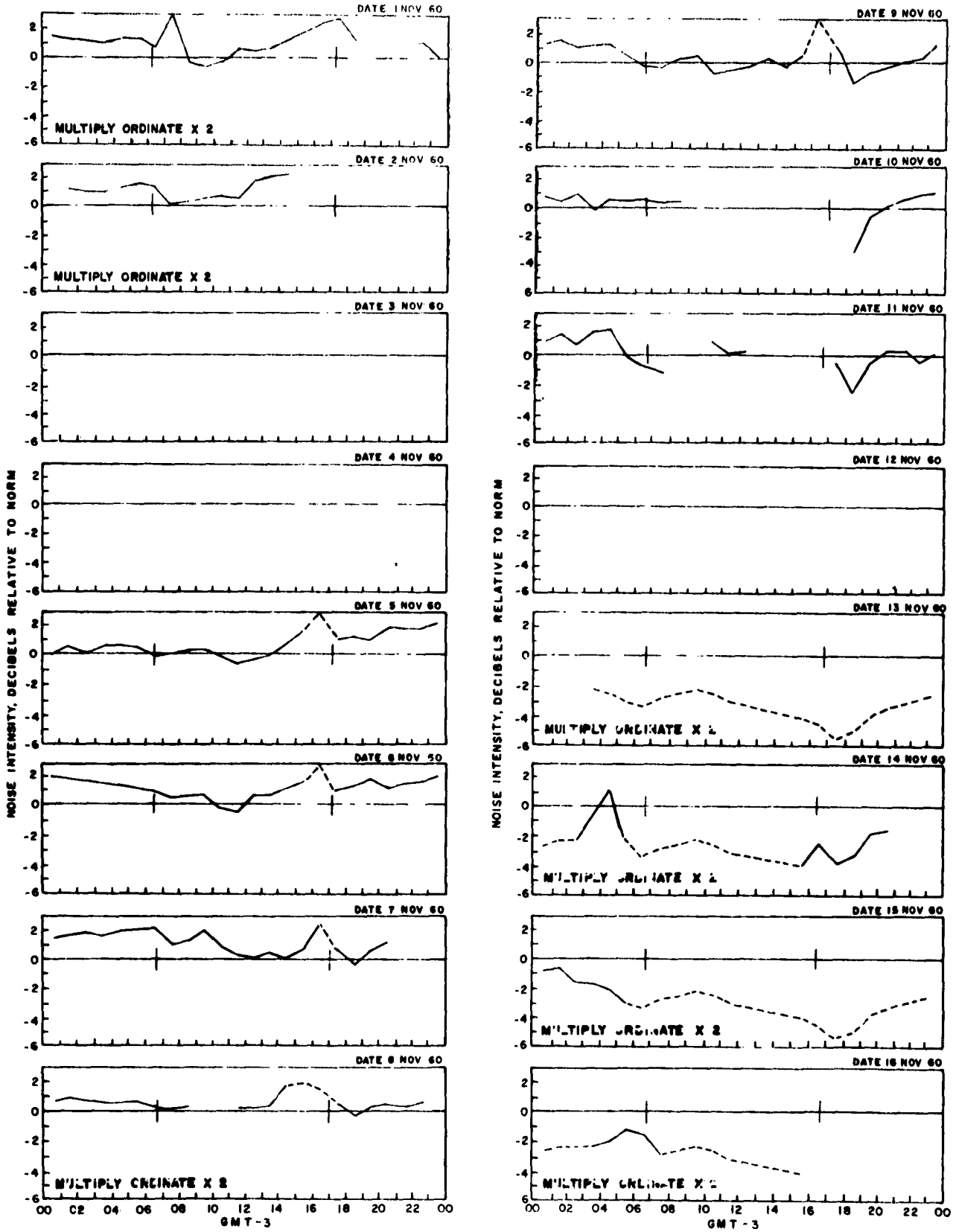

Goose Bay, November 1960

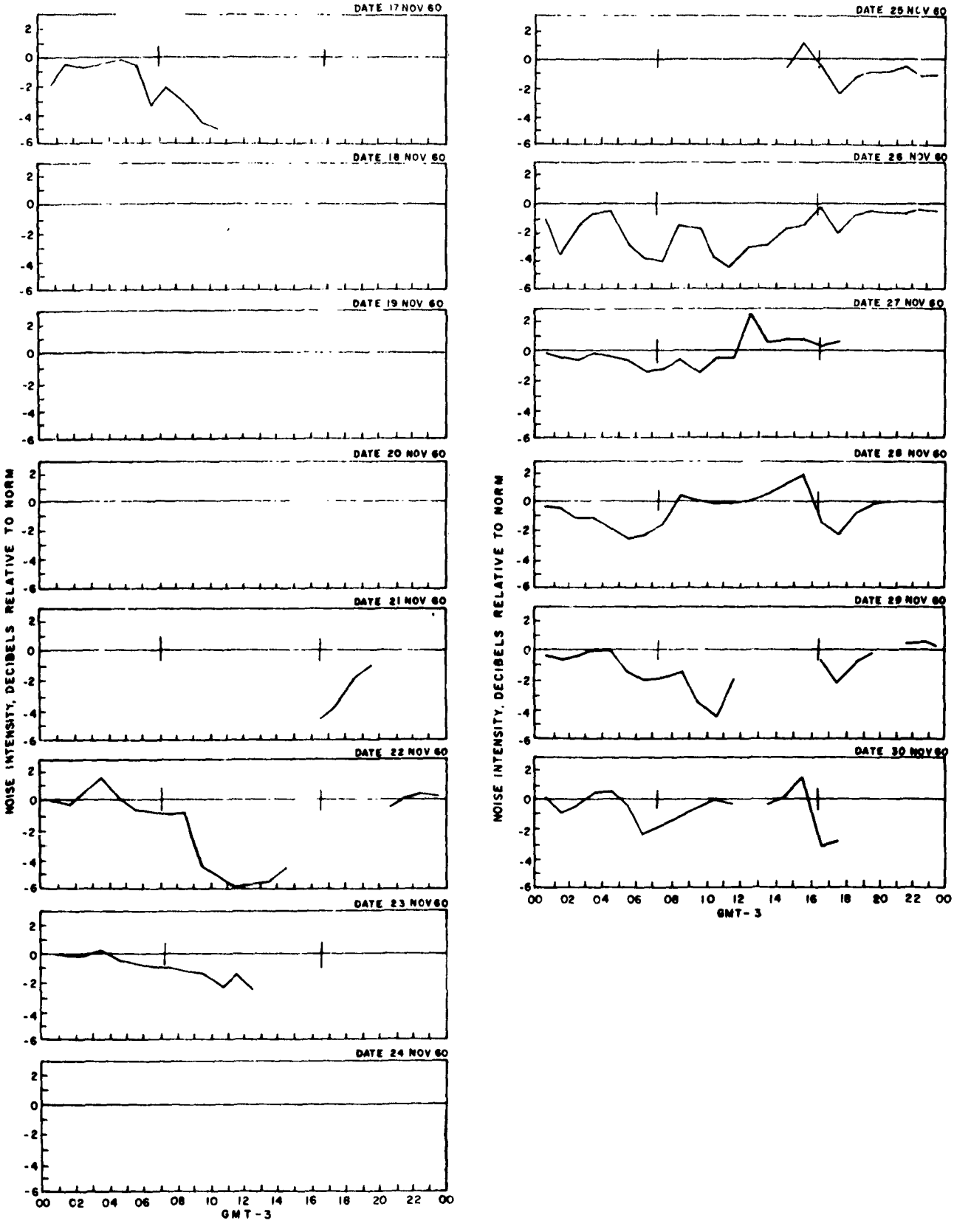

Goose Bay, November 1960

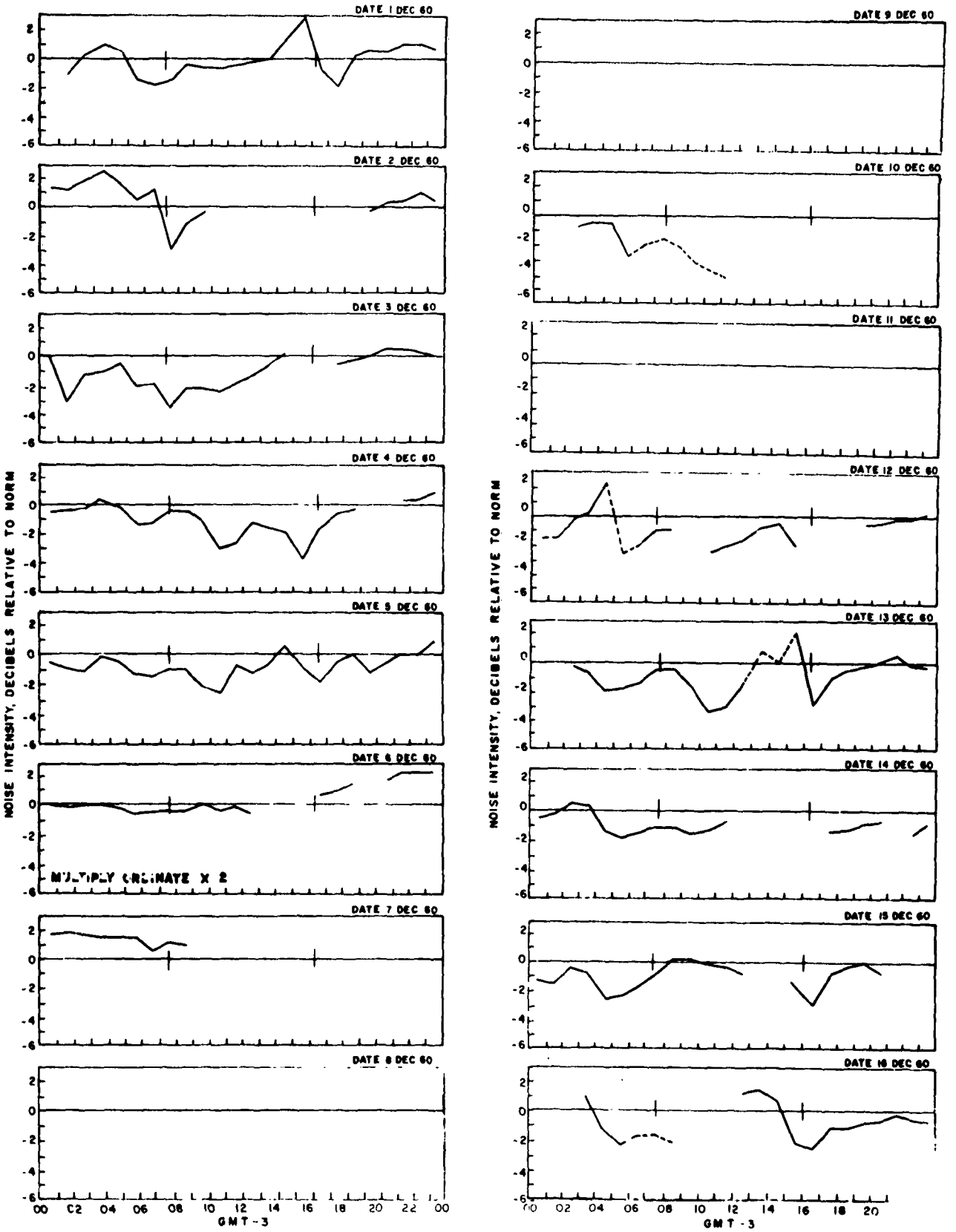

Goose Bay, December 1960

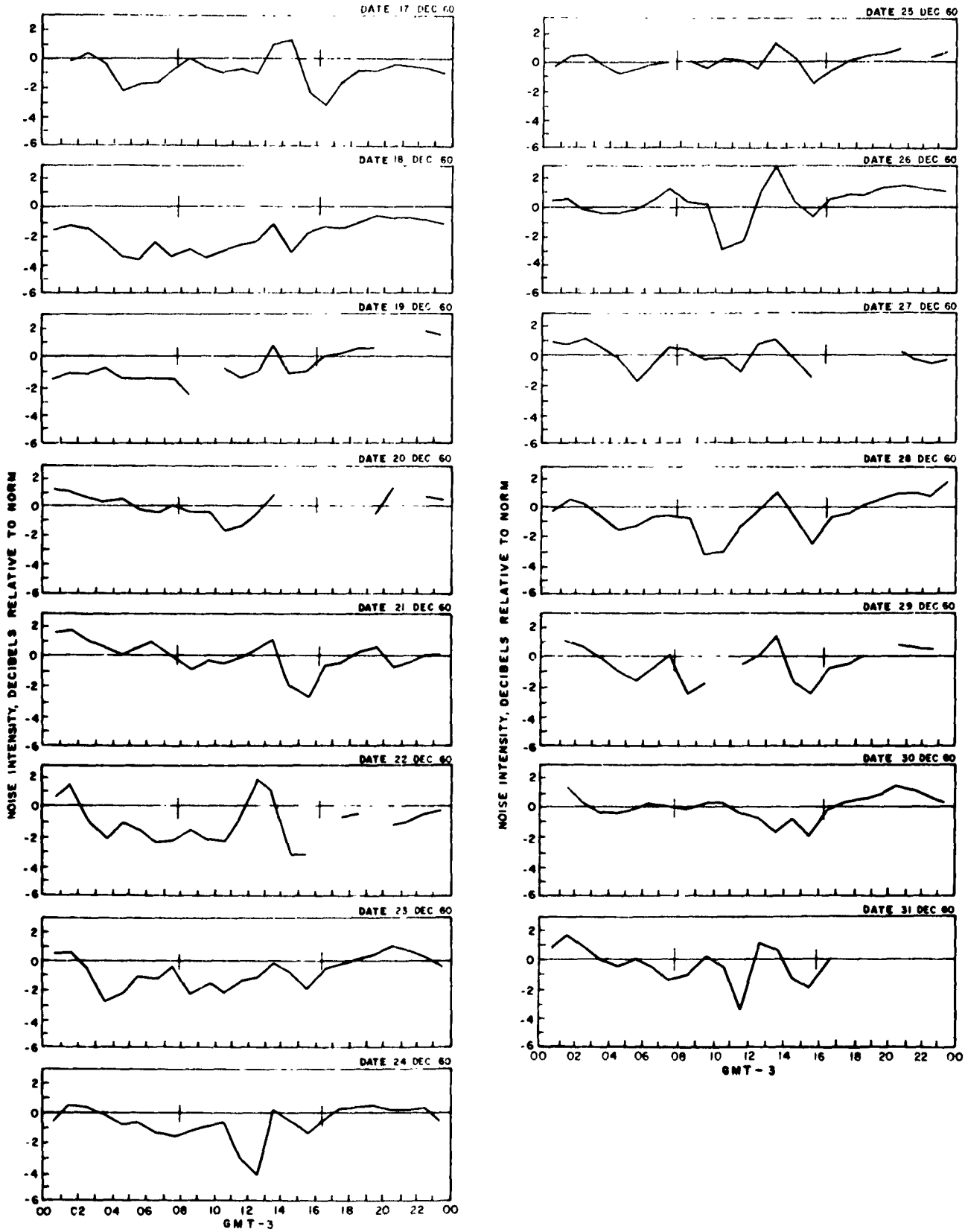

Goose Bay, December 1960

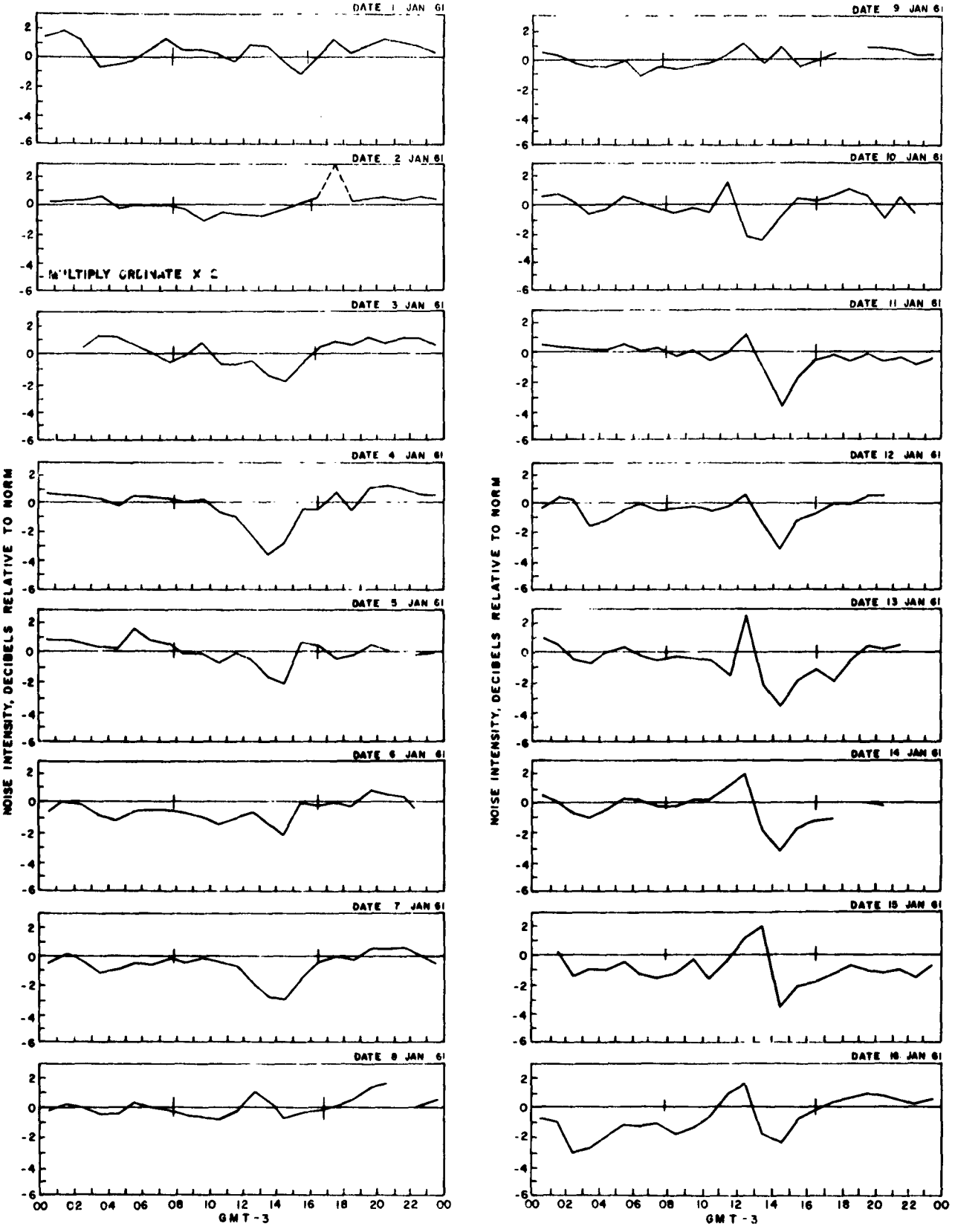

Goose Bay, January 1961

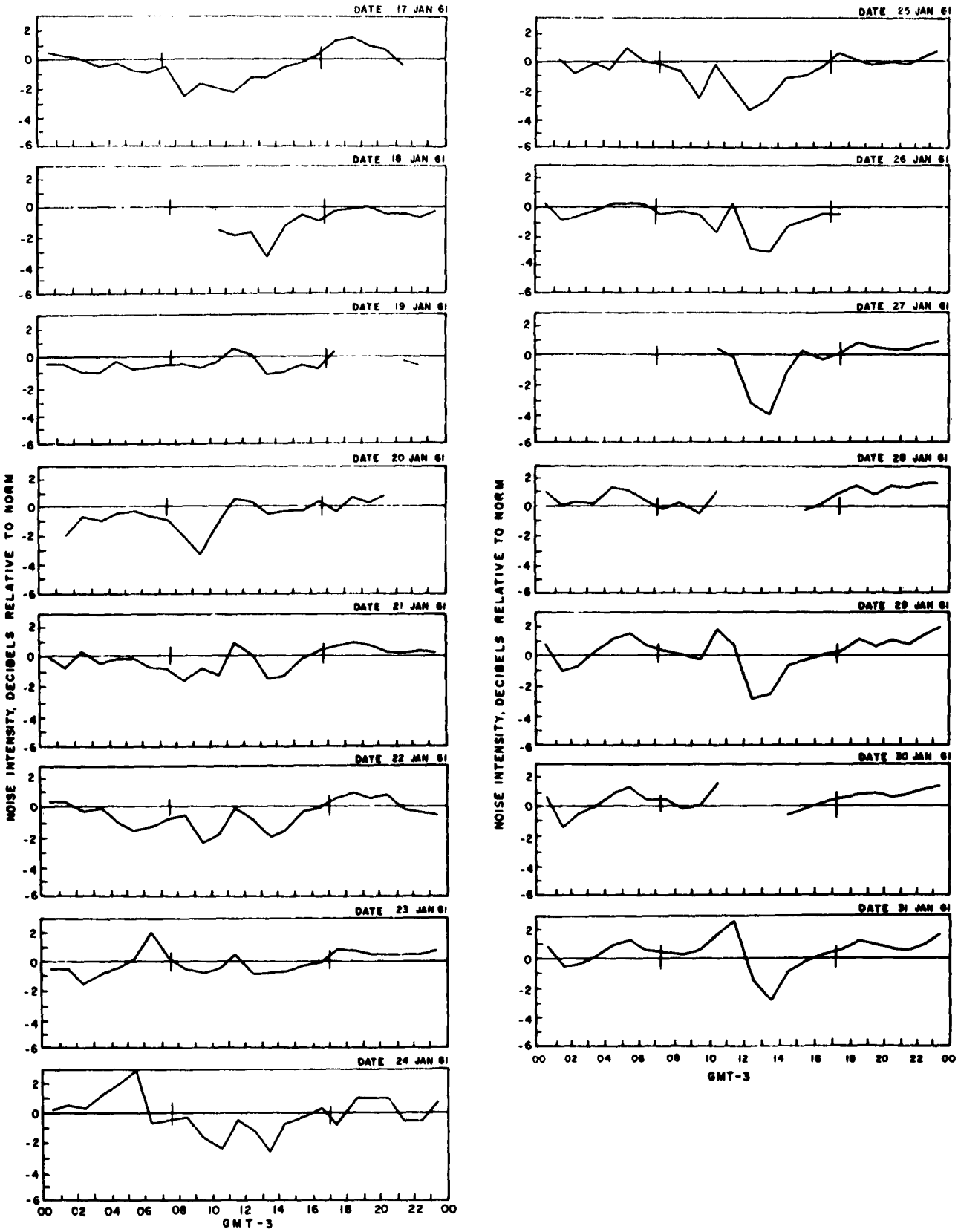

Goose Bay, January 1961

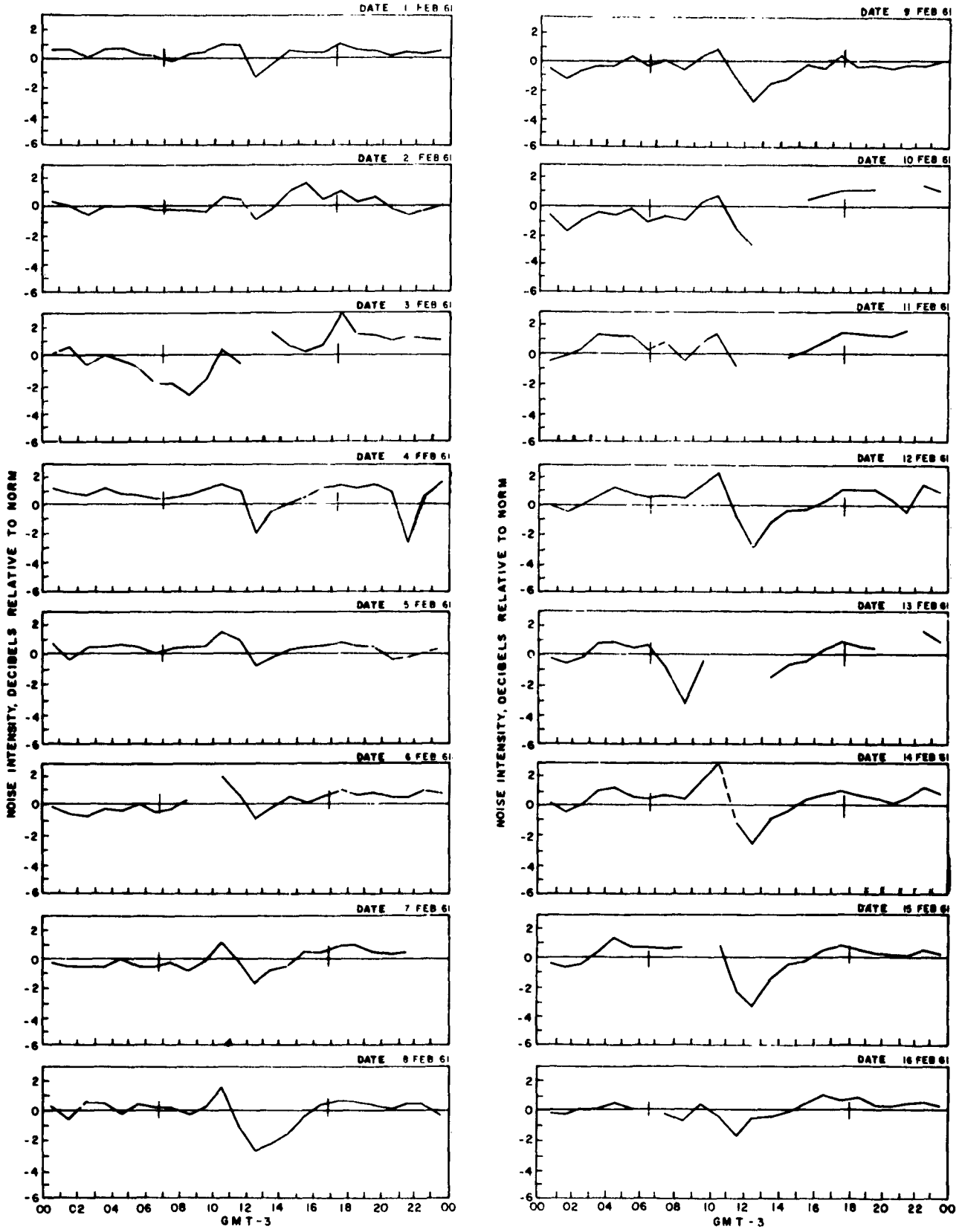

Goose Bay, February 1961

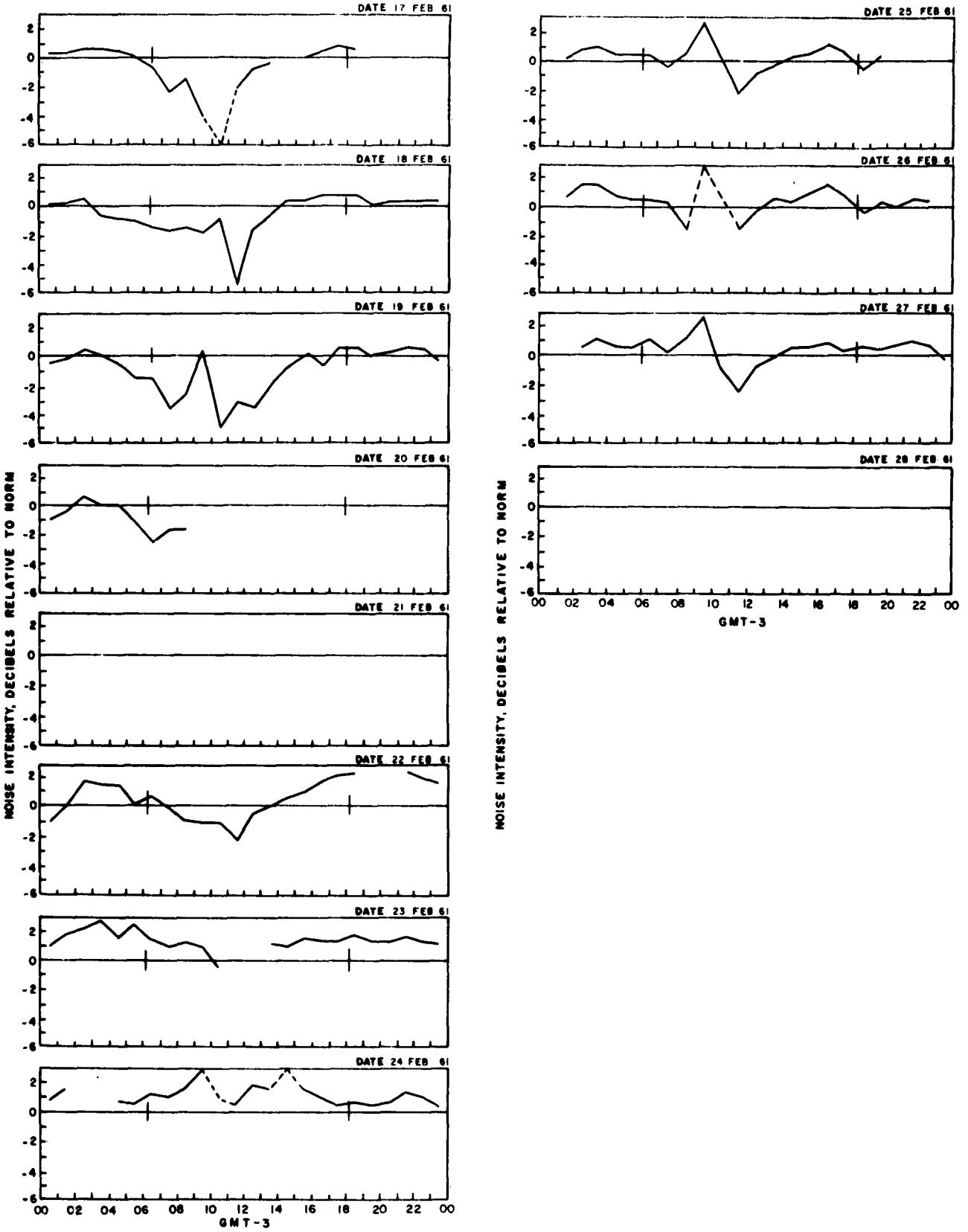

Goose Bay, February 1961

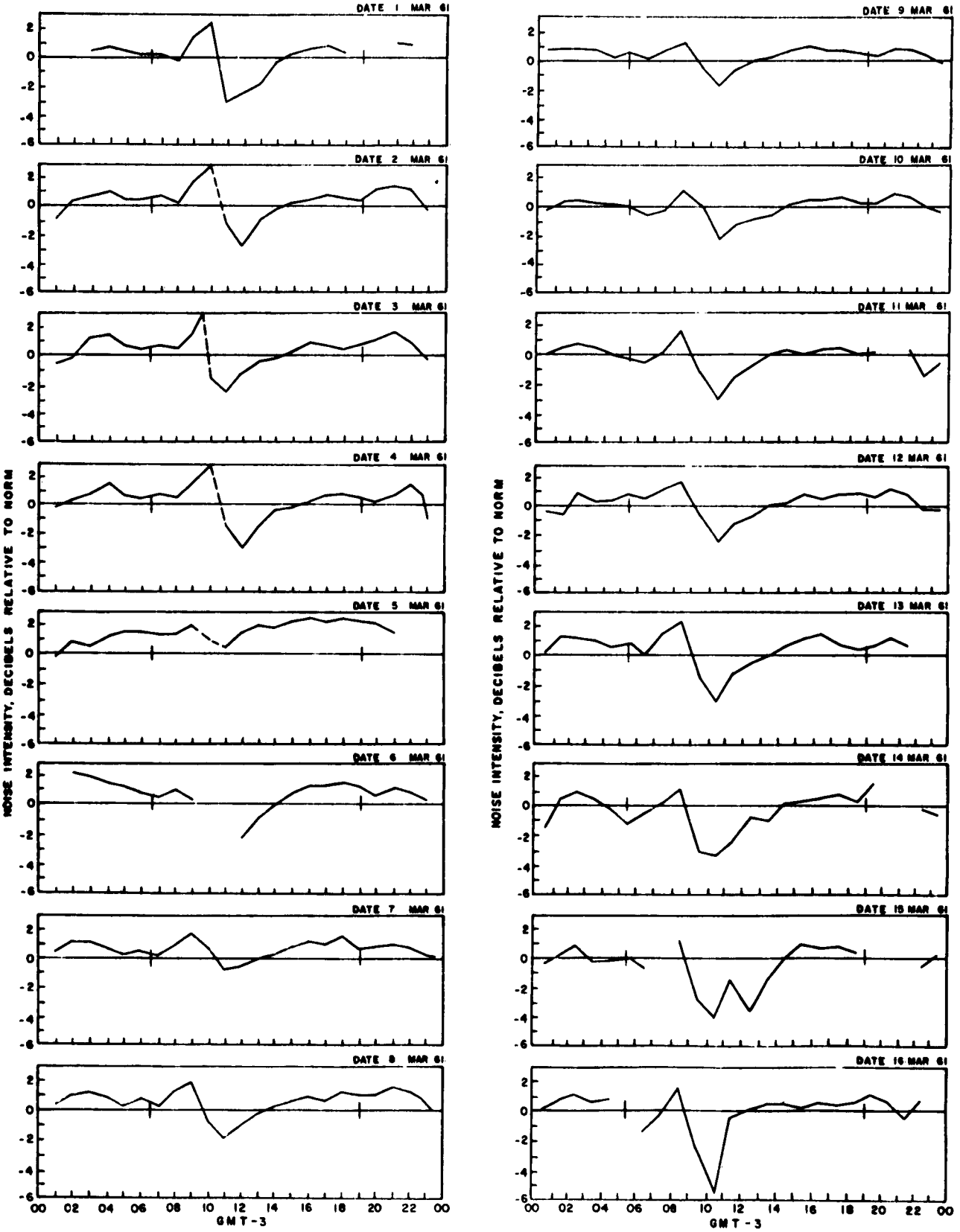

Goose Bay, March 1961

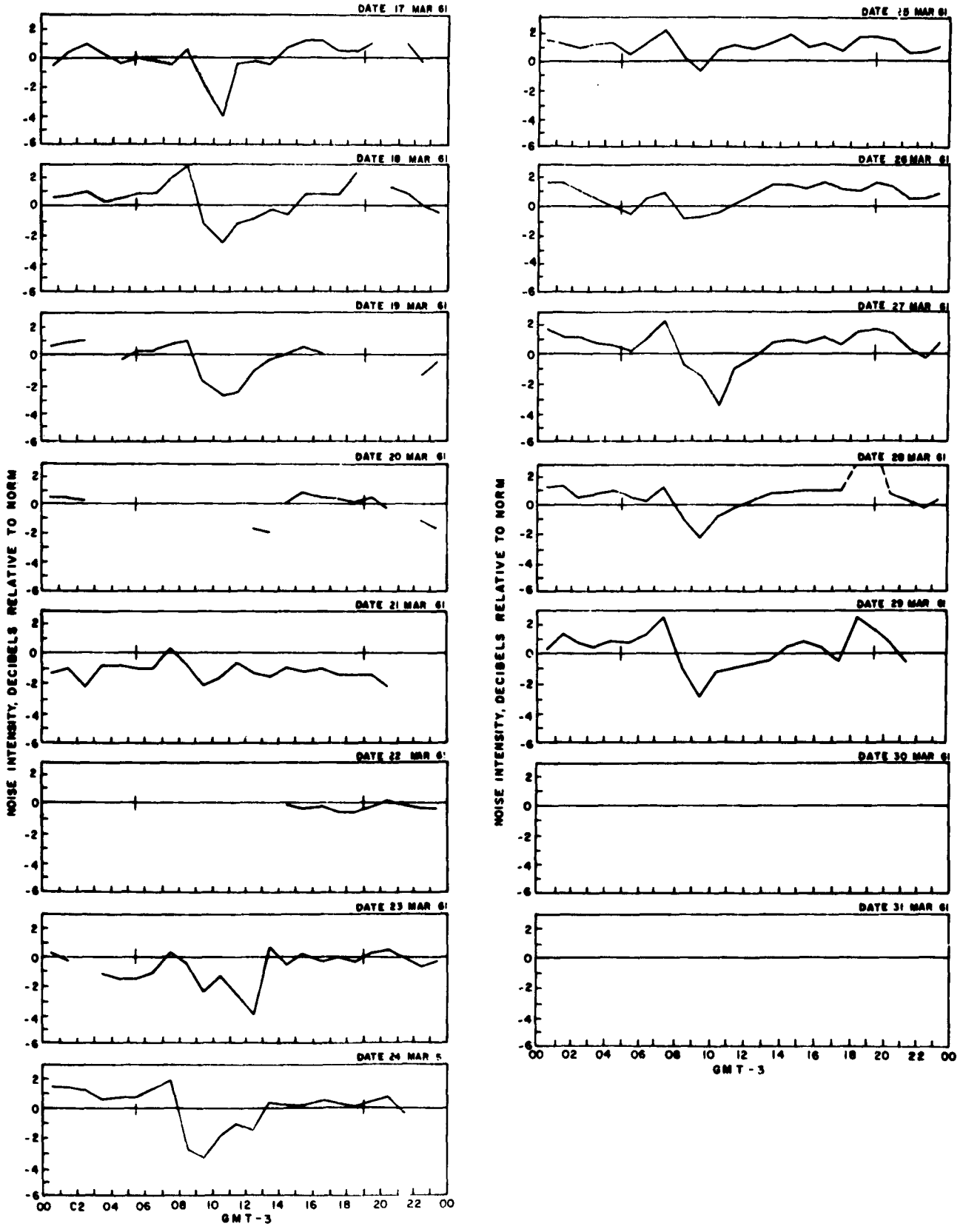

Goose Bay, March 1961

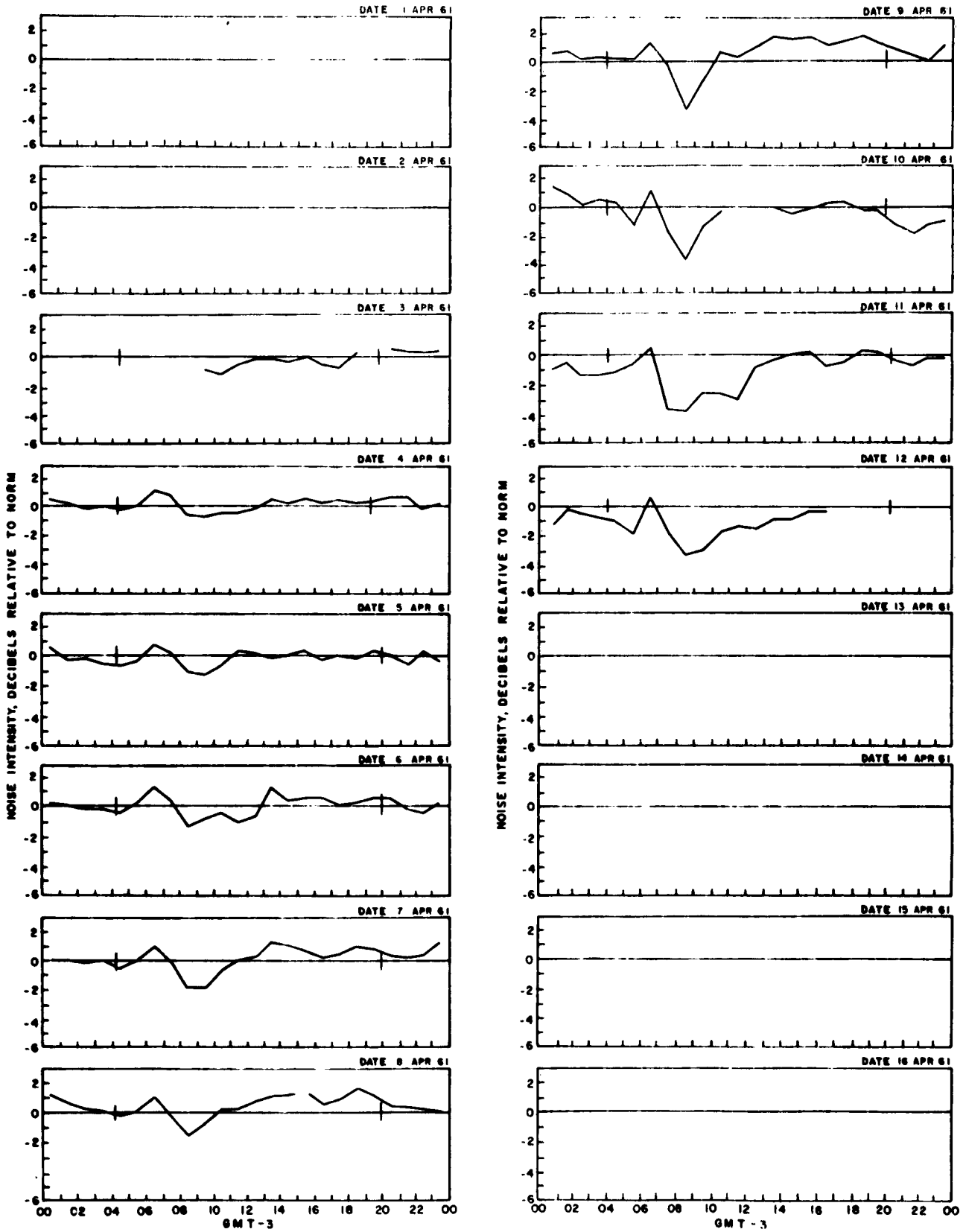

Goose Bay, April 1961

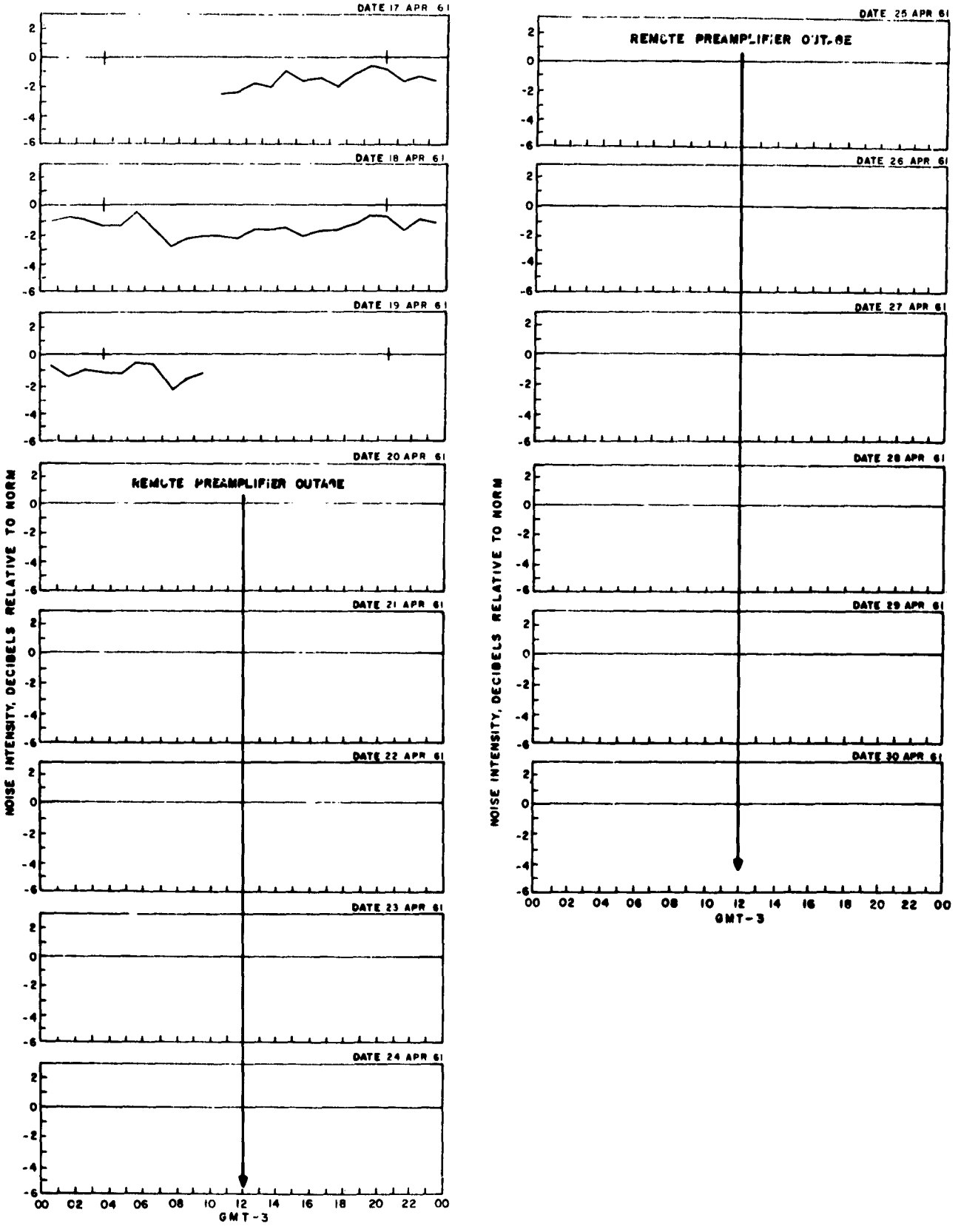

Goose Bay, April 1961

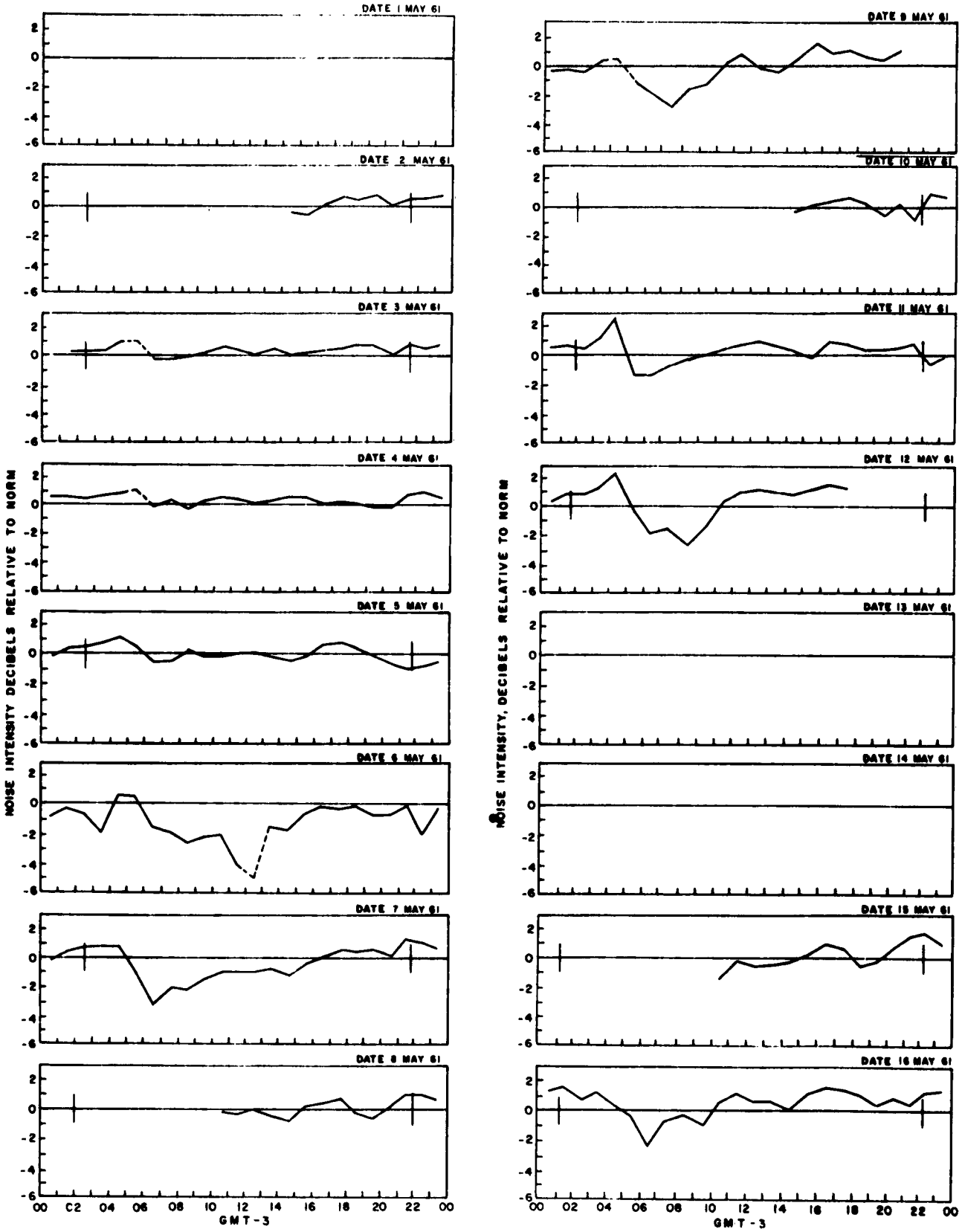

Goose Bay, May 1961

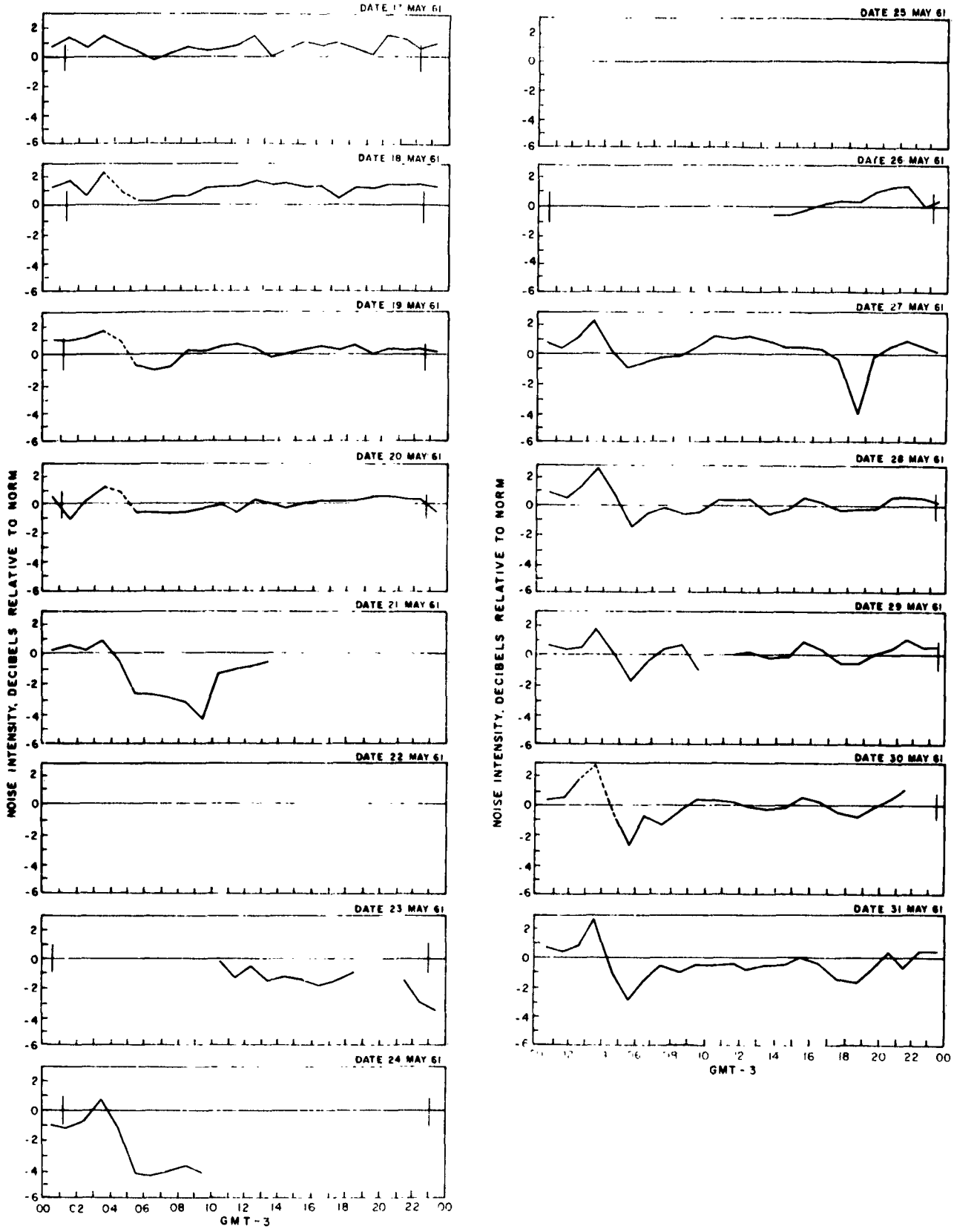

Goose Bay, May 1961

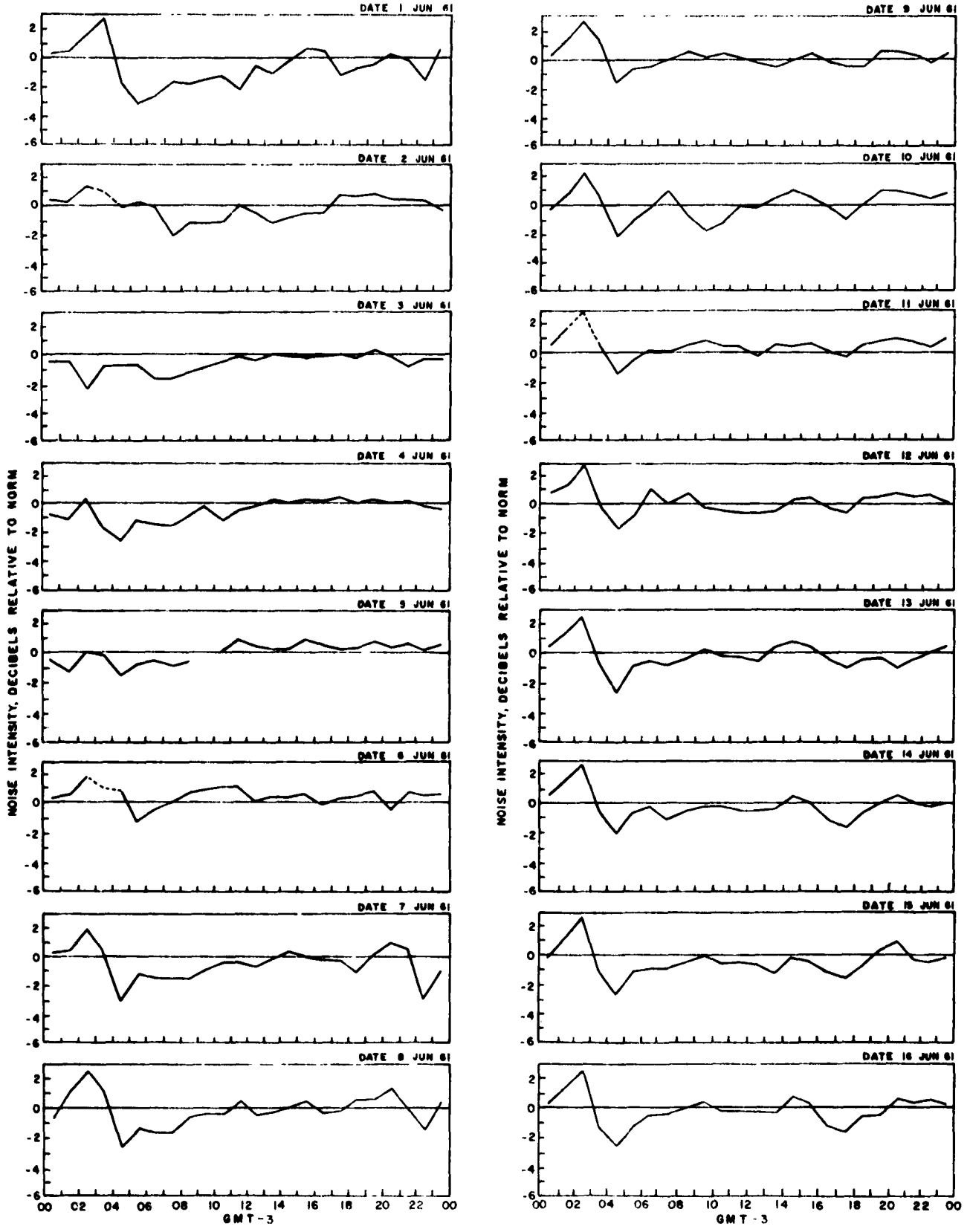

Goose Bay, June 1961

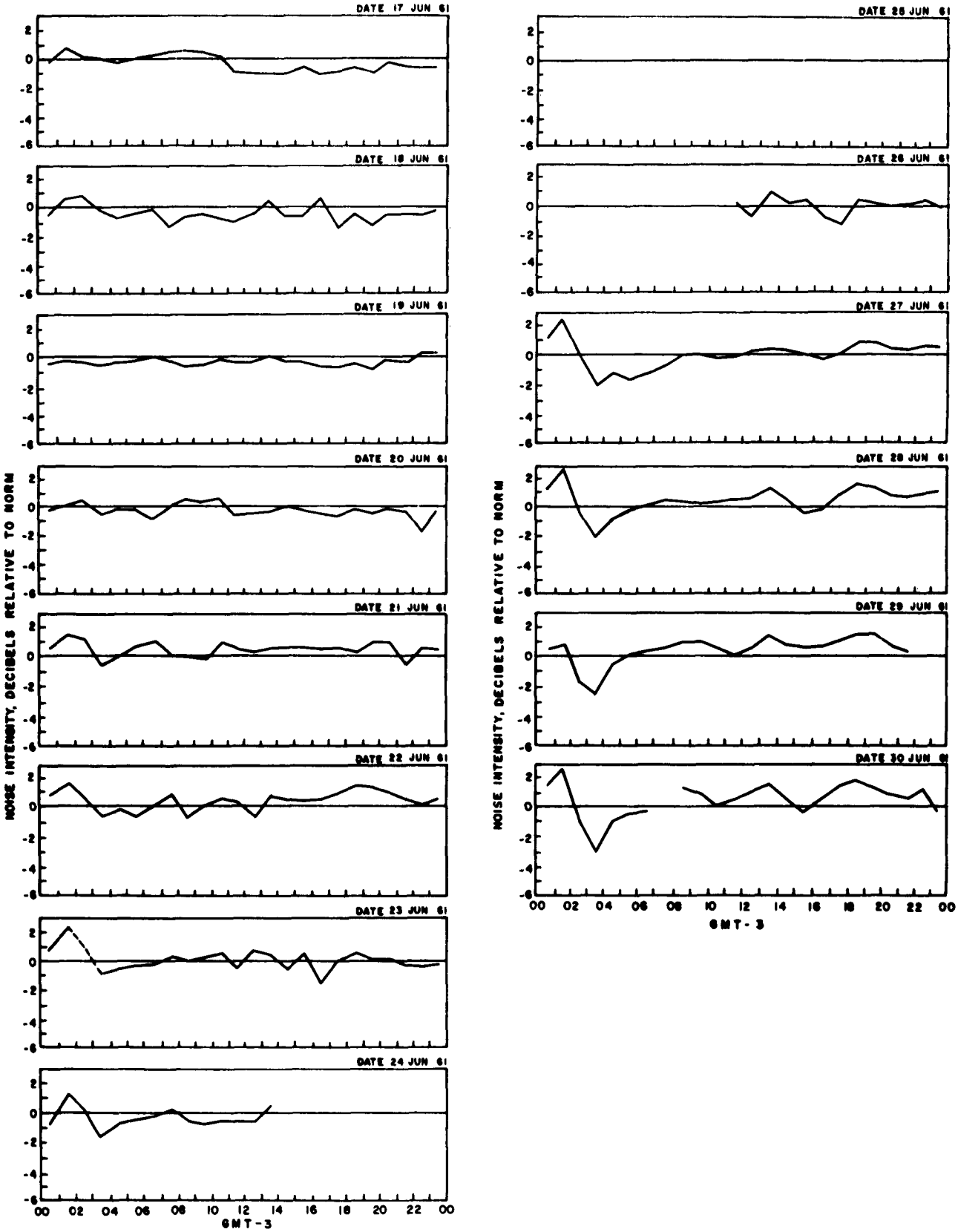

Goose Bay, June 1961

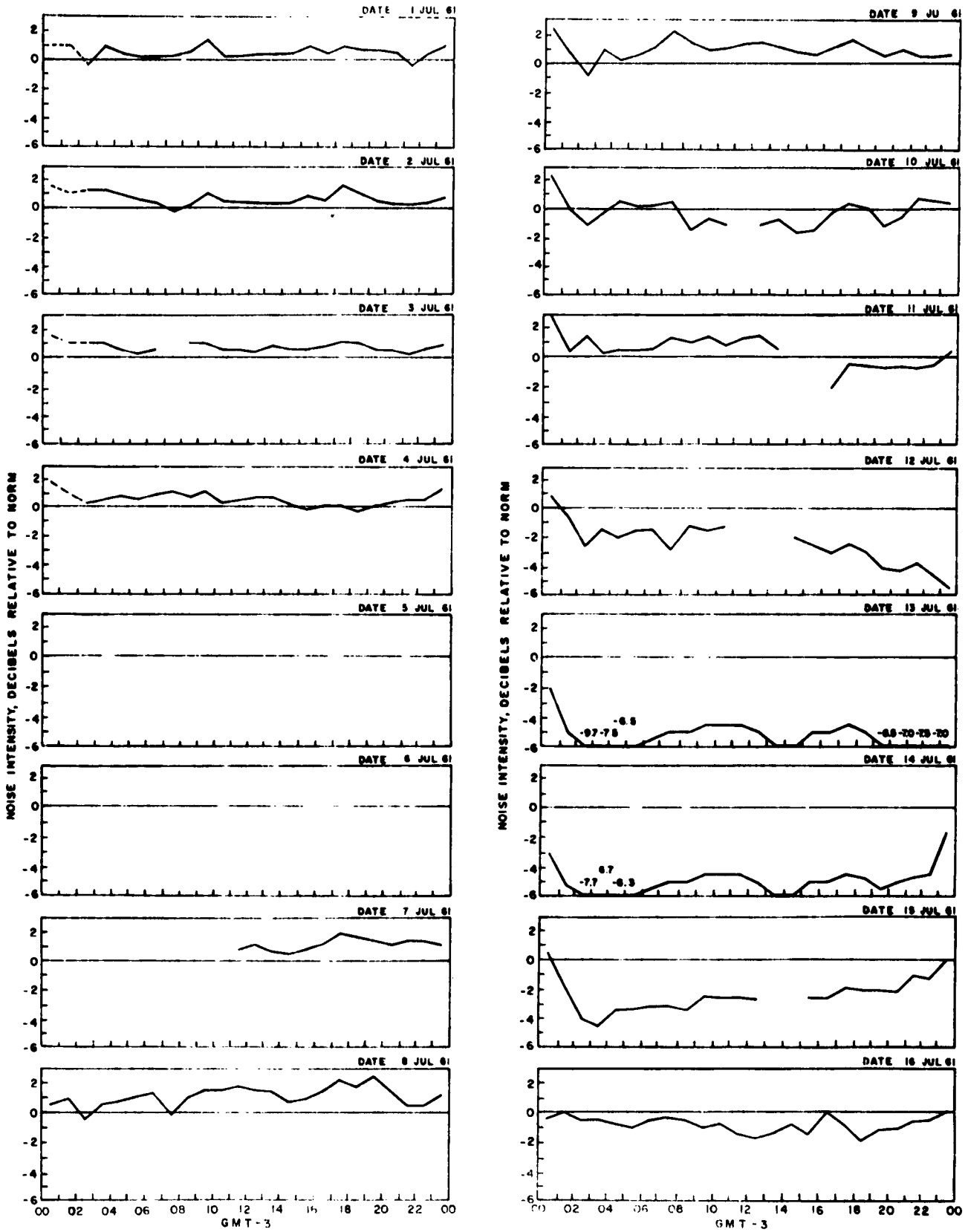

Goose Bay, July 1961

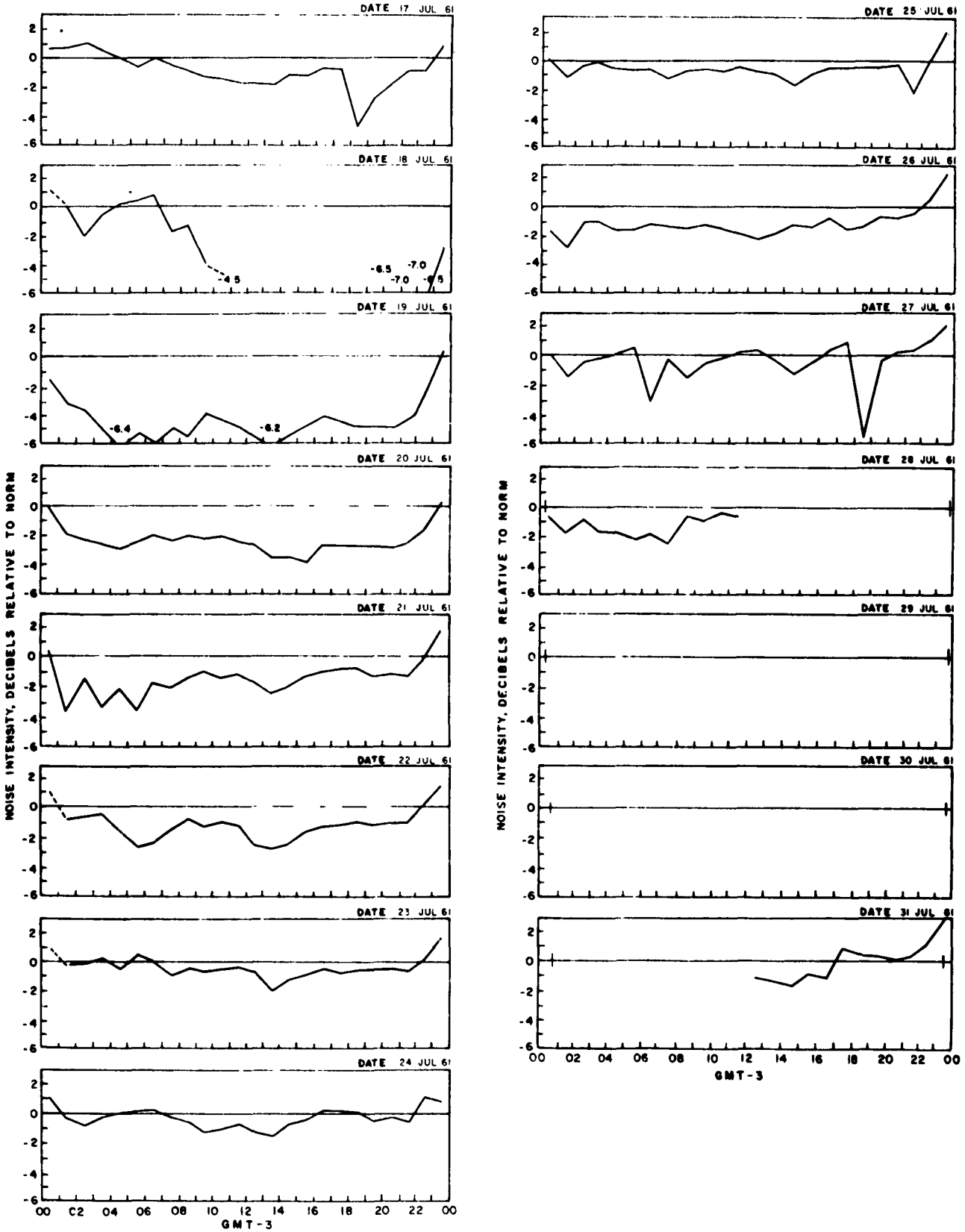

Goose Bay, July 1961

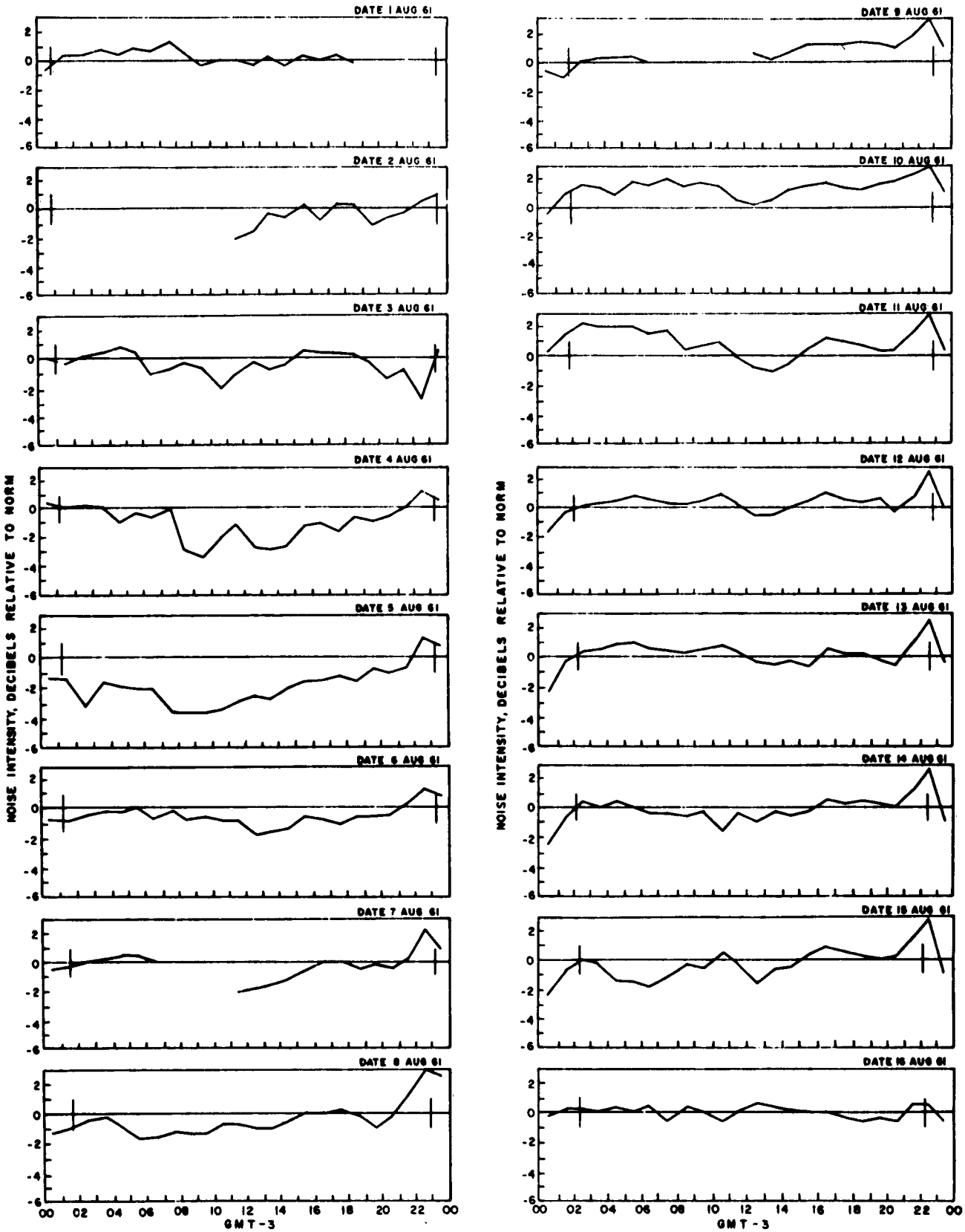

Goose Bay, August 1961

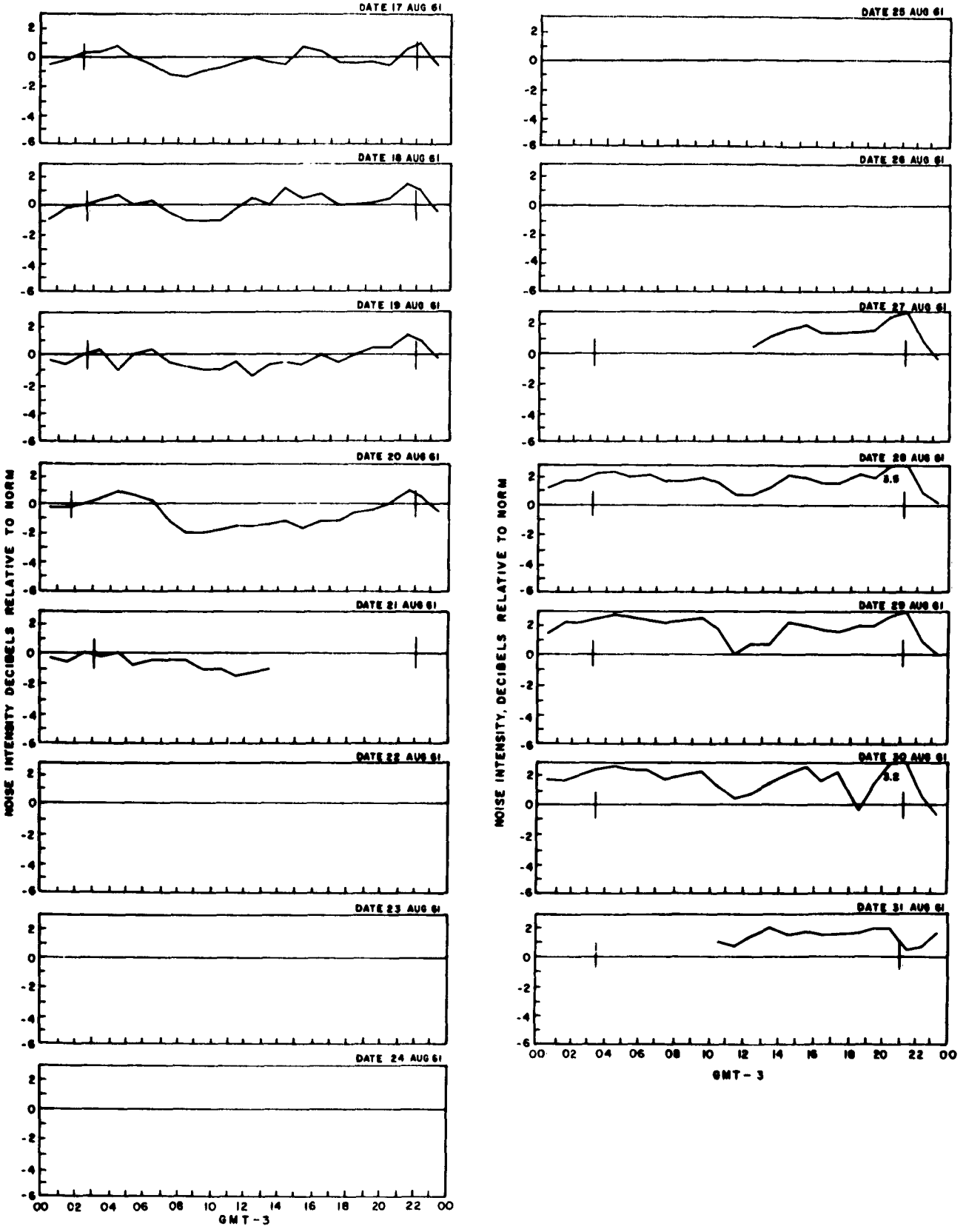

Goose Bay, August 1961

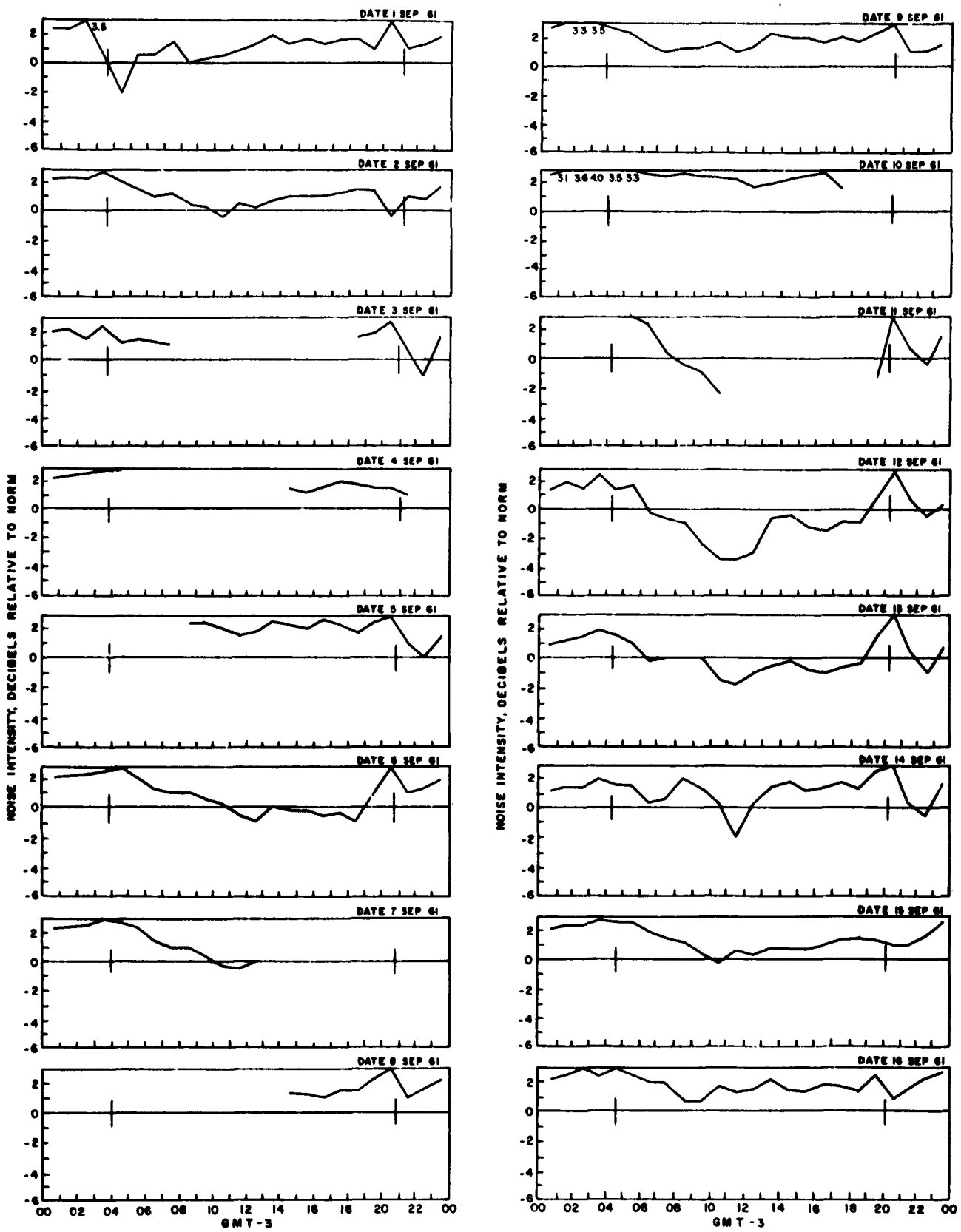

Goose Bay, September 1961

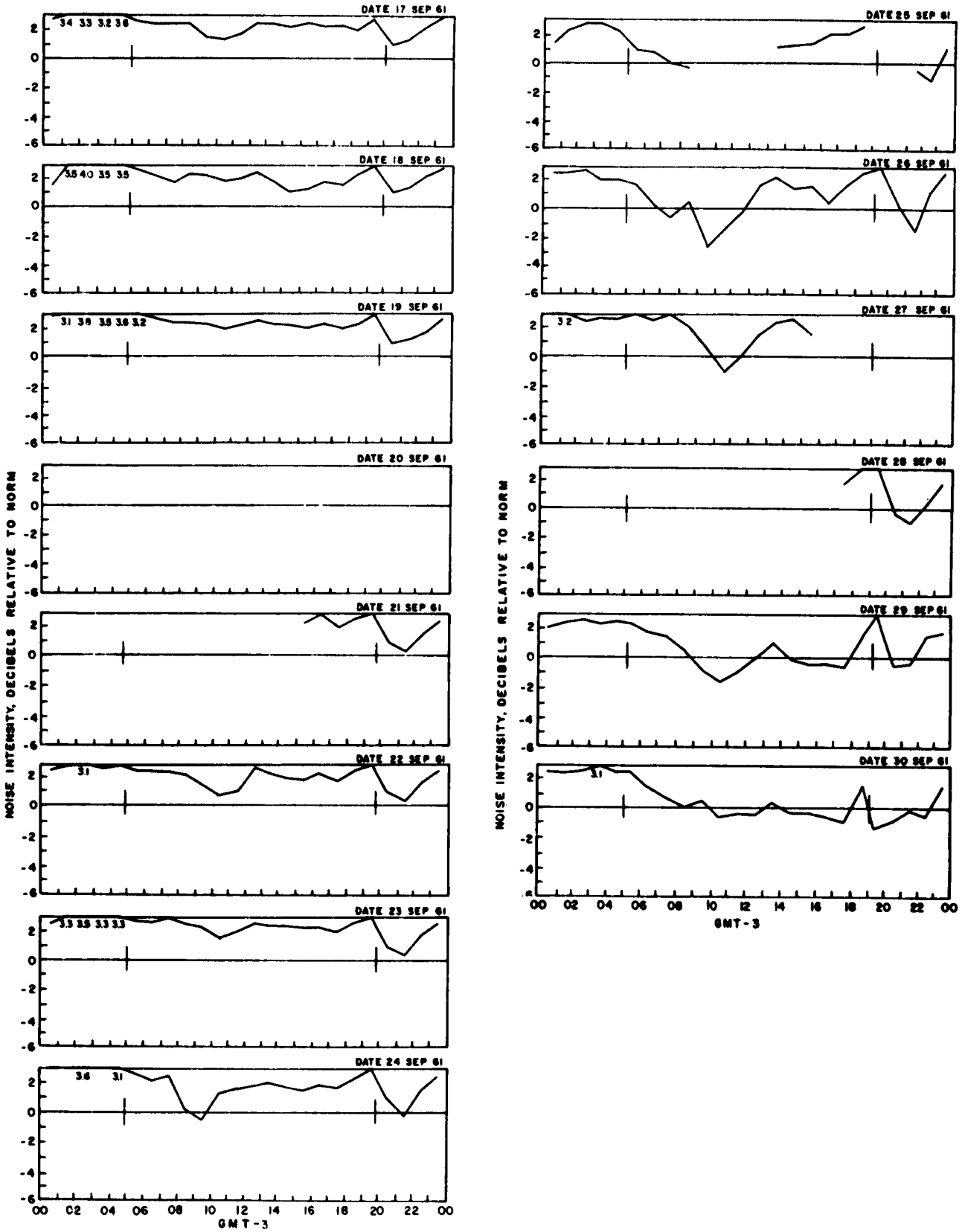

Goose Bay, September 1961

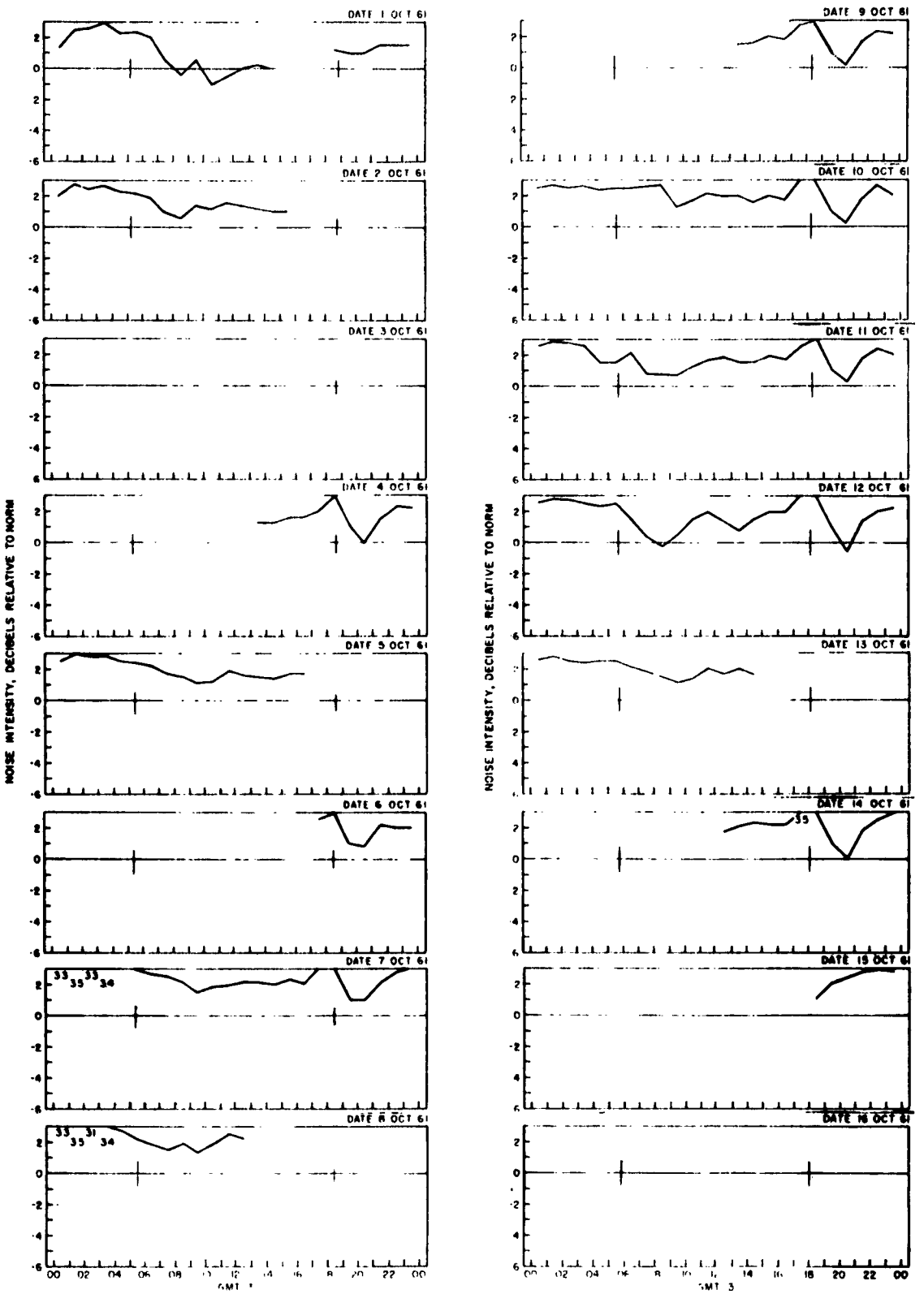

Goose Bay, October 1961

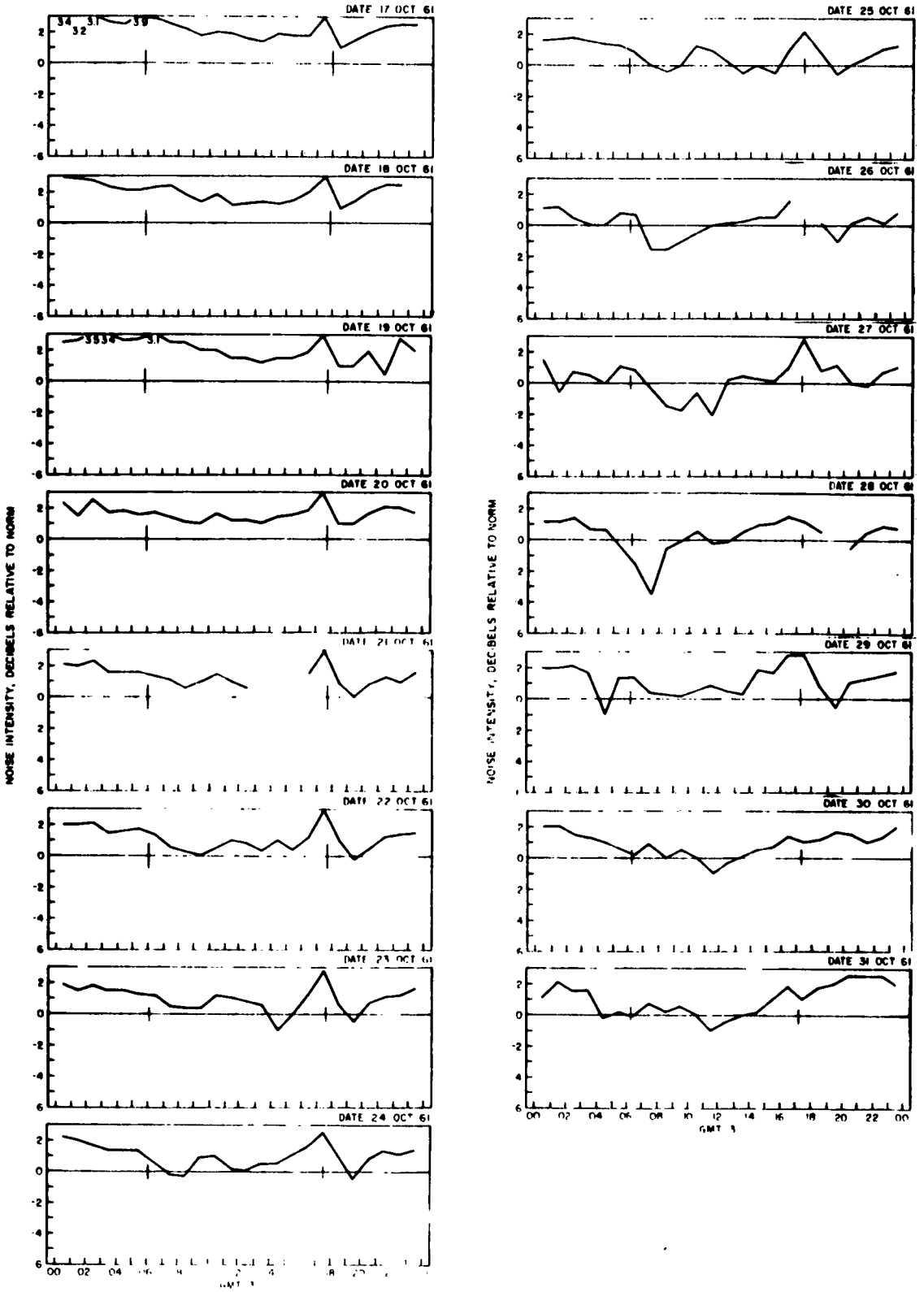

Goose Bay, October 1961

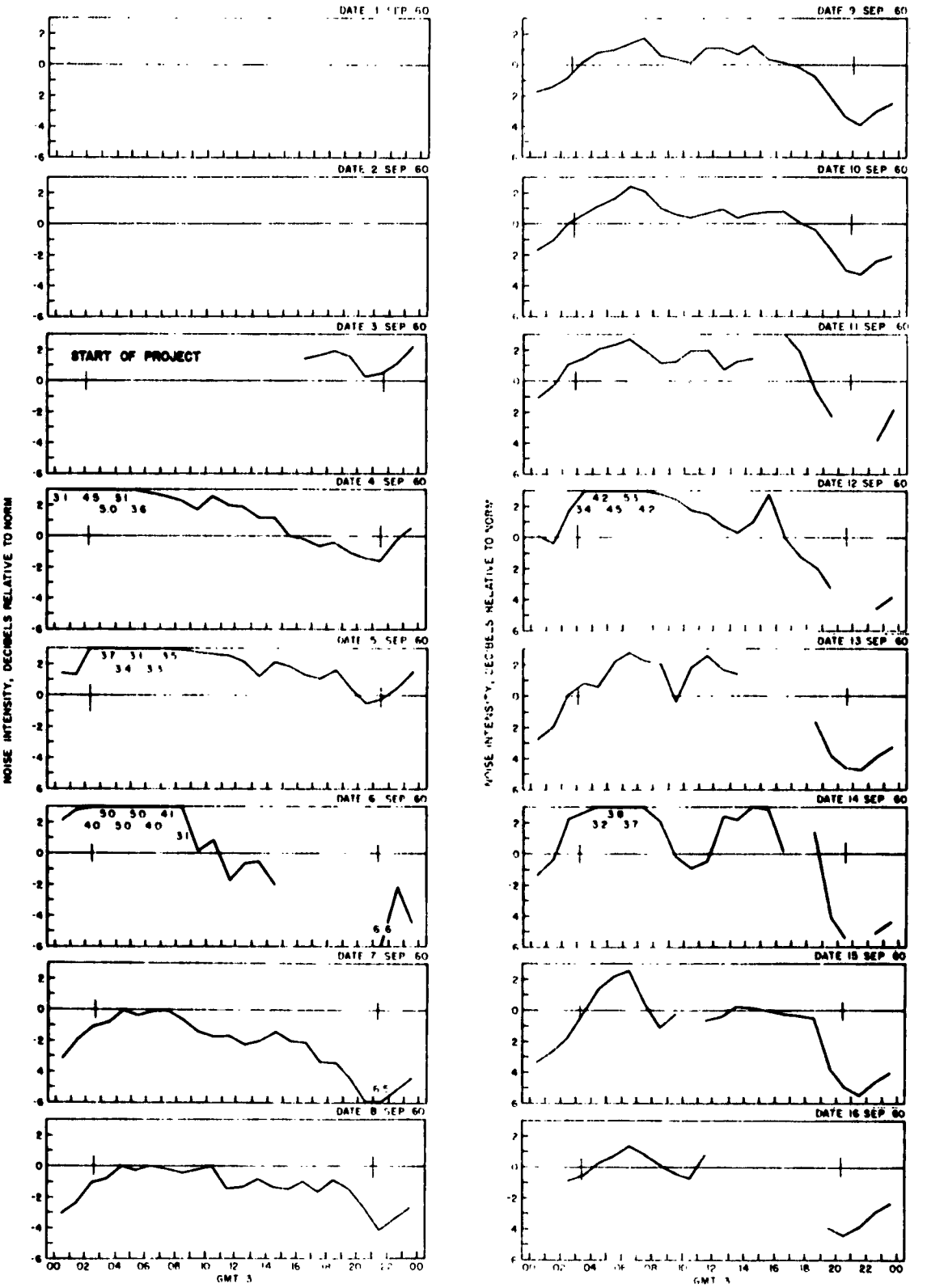

Thule, September 1960

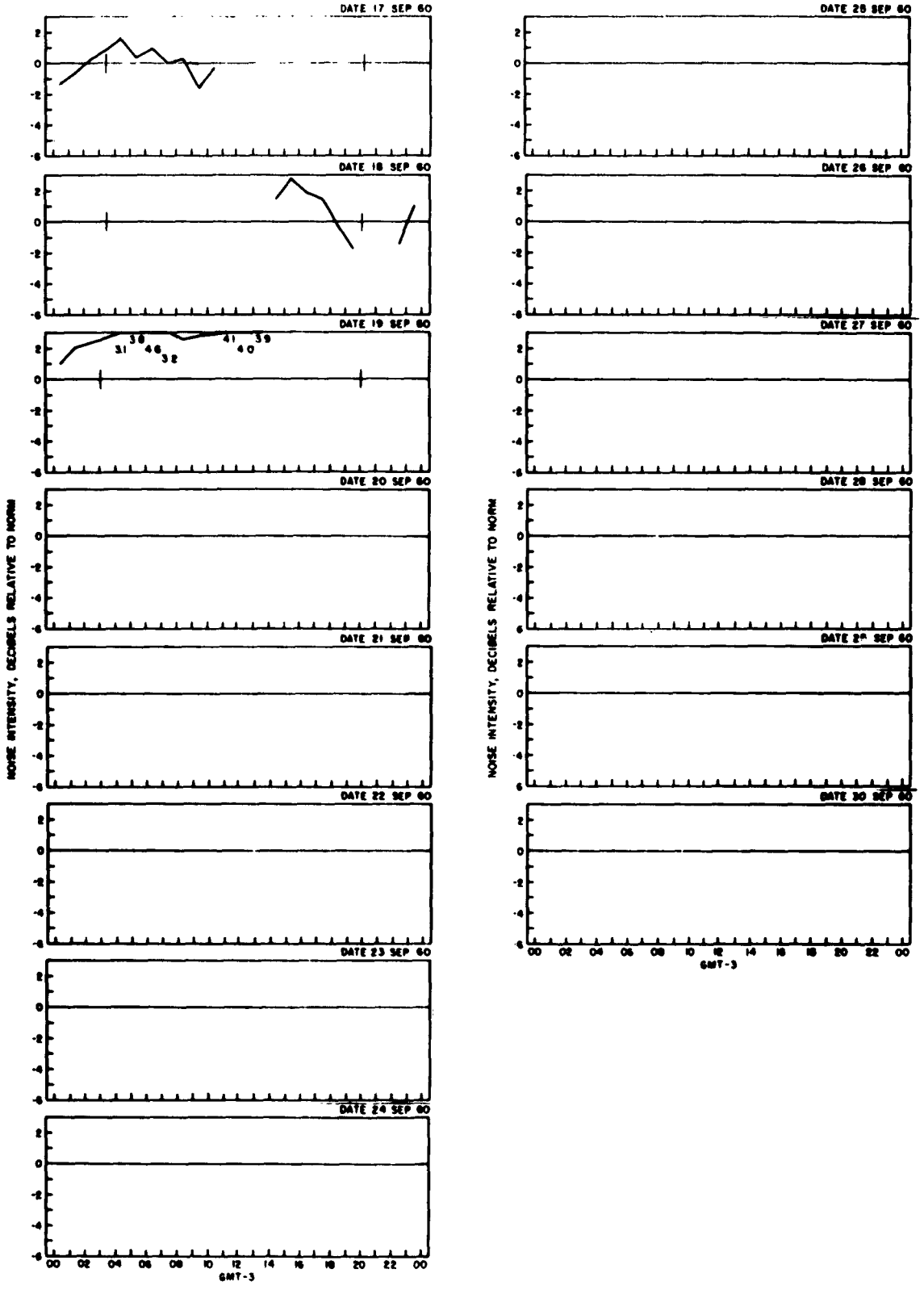

Thule, September 1960

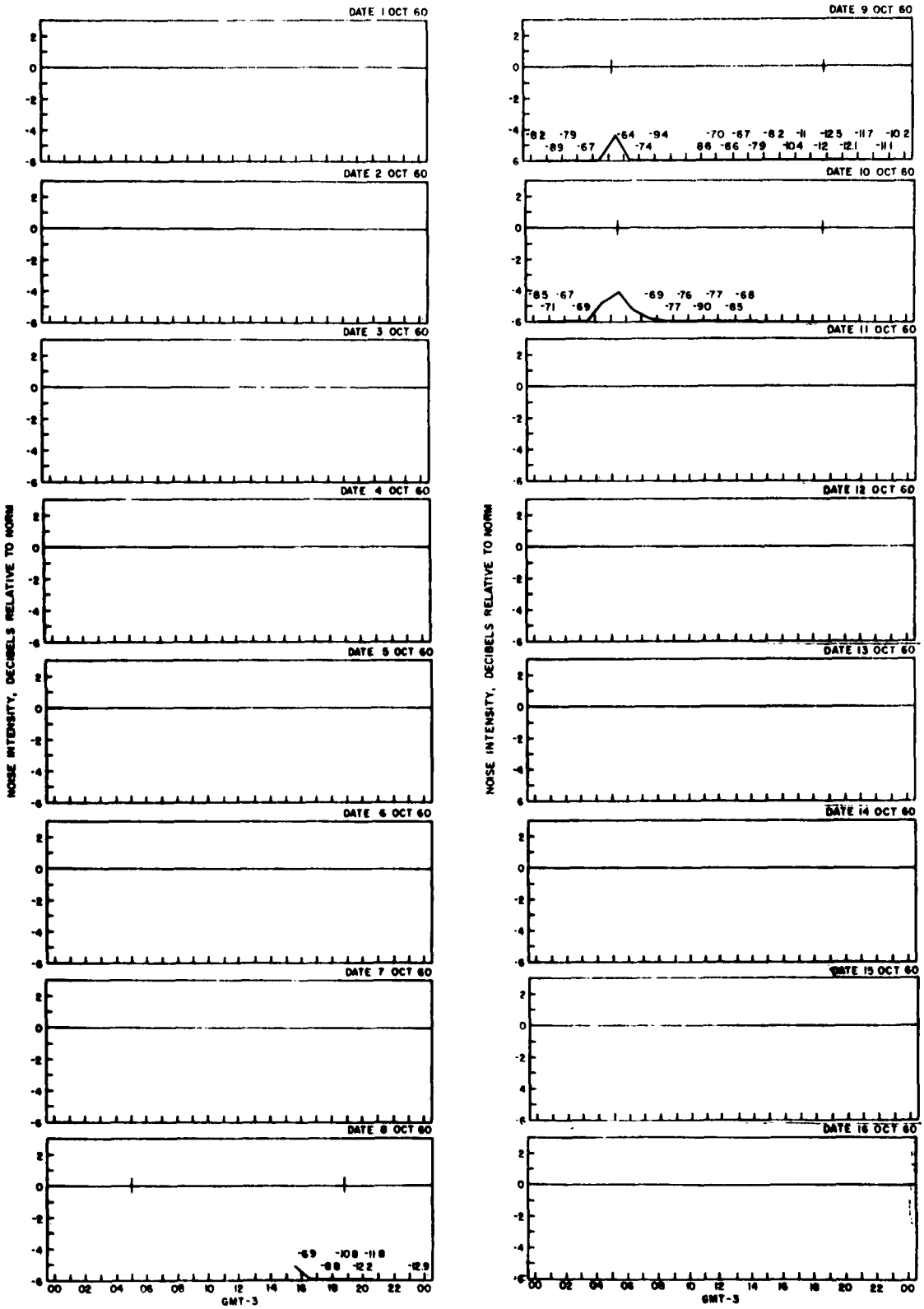

Thule, October 1960

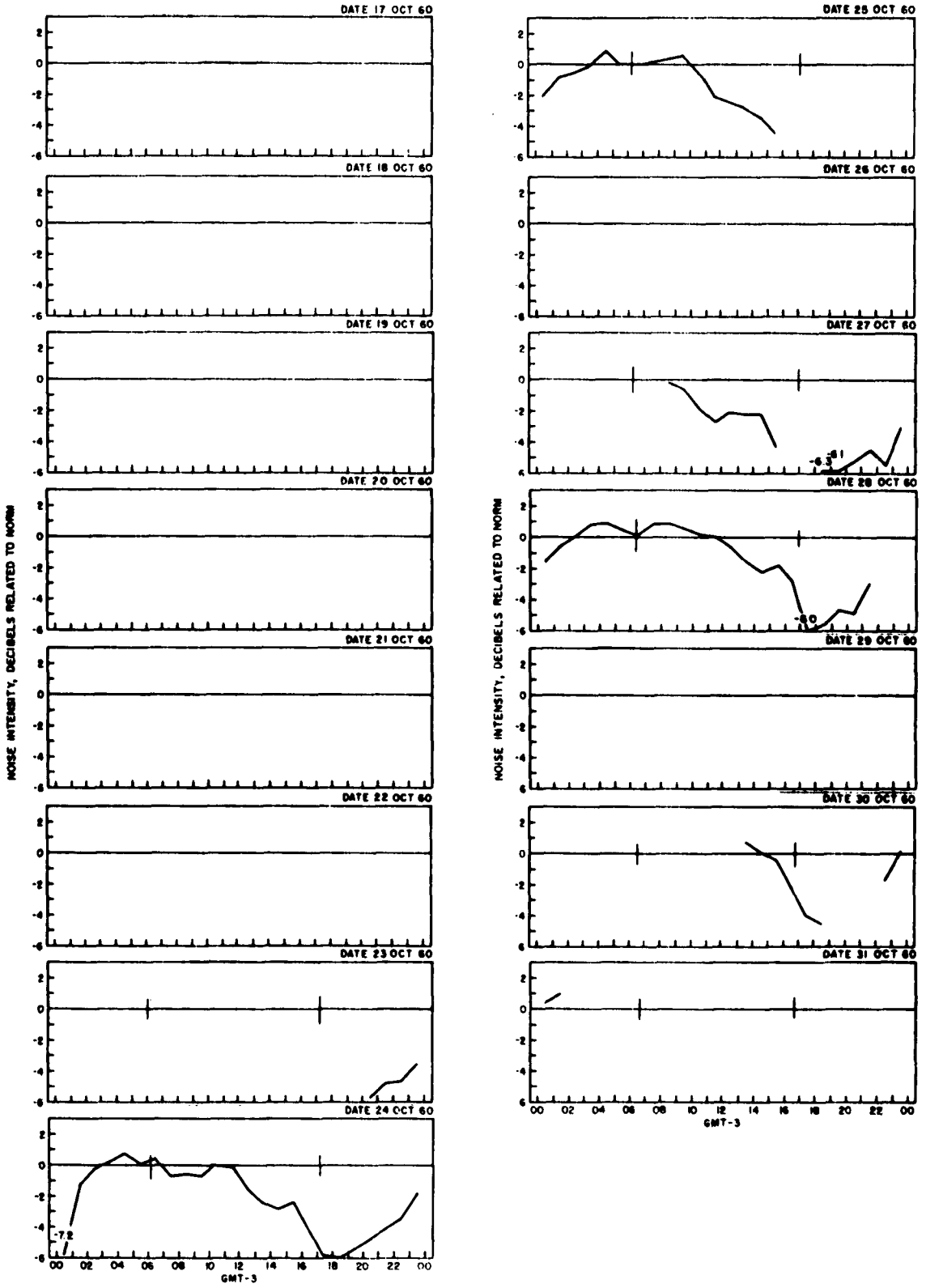

Thule, October 1960

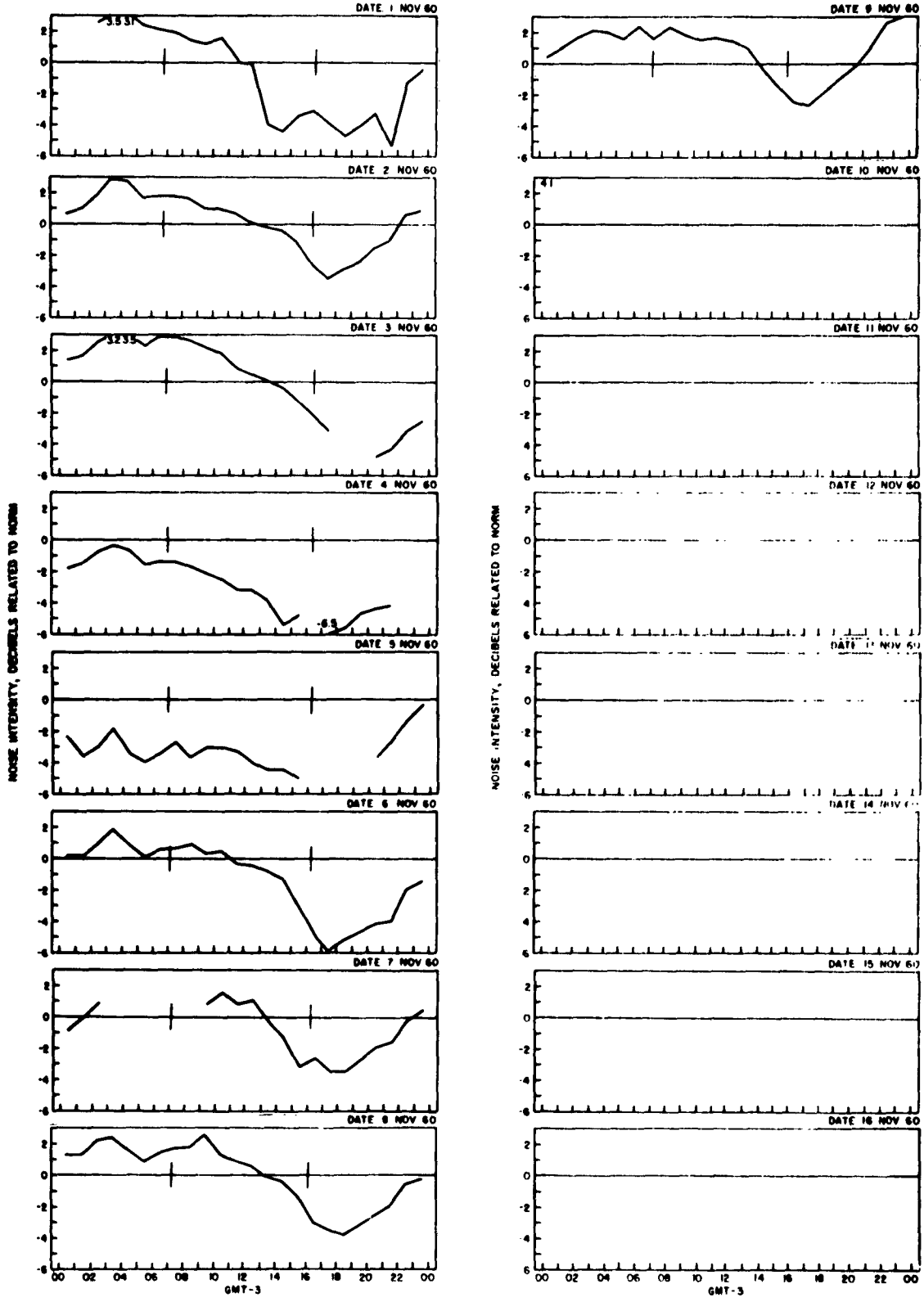

Thule, November 1960

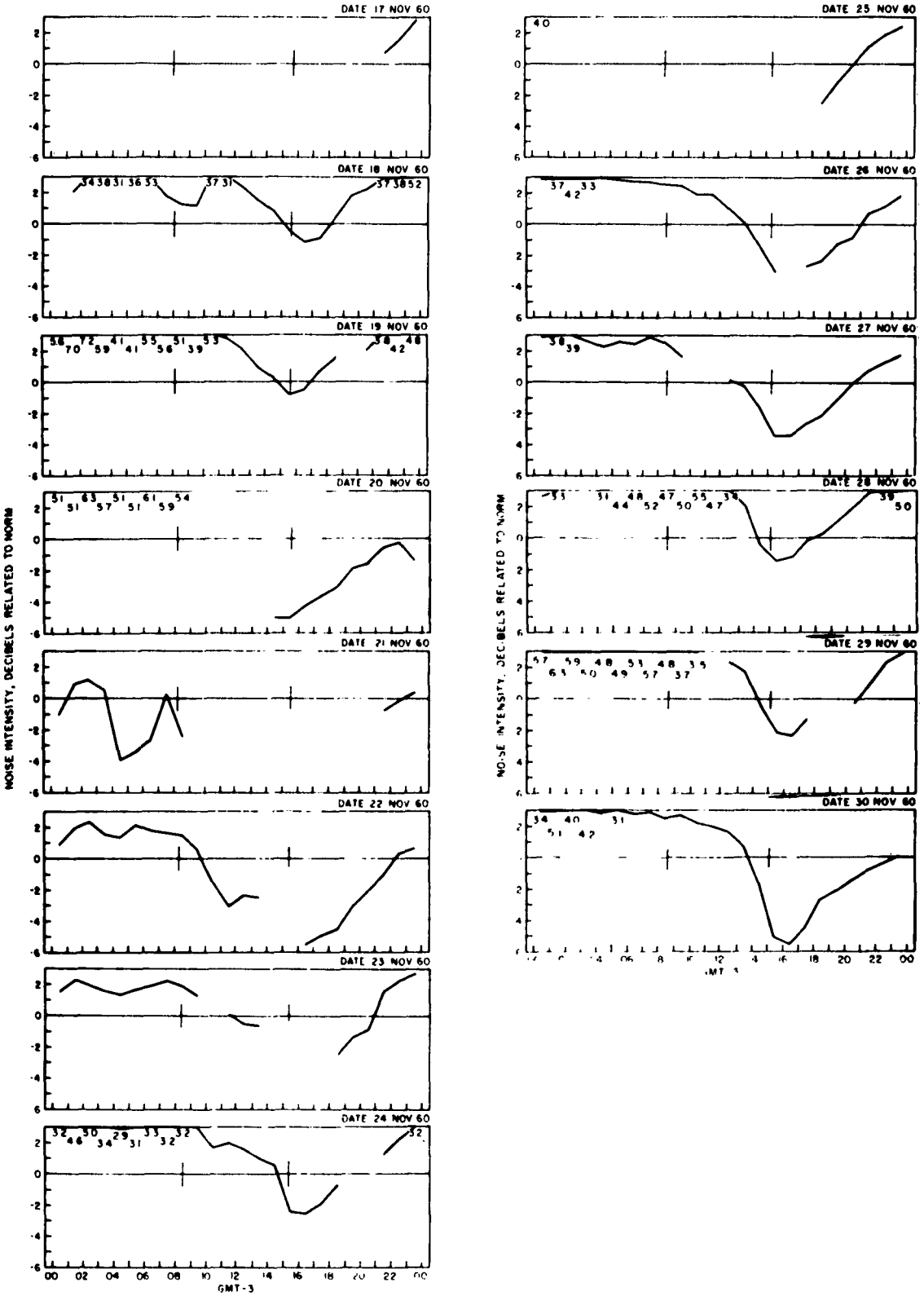

Thule, November 1960

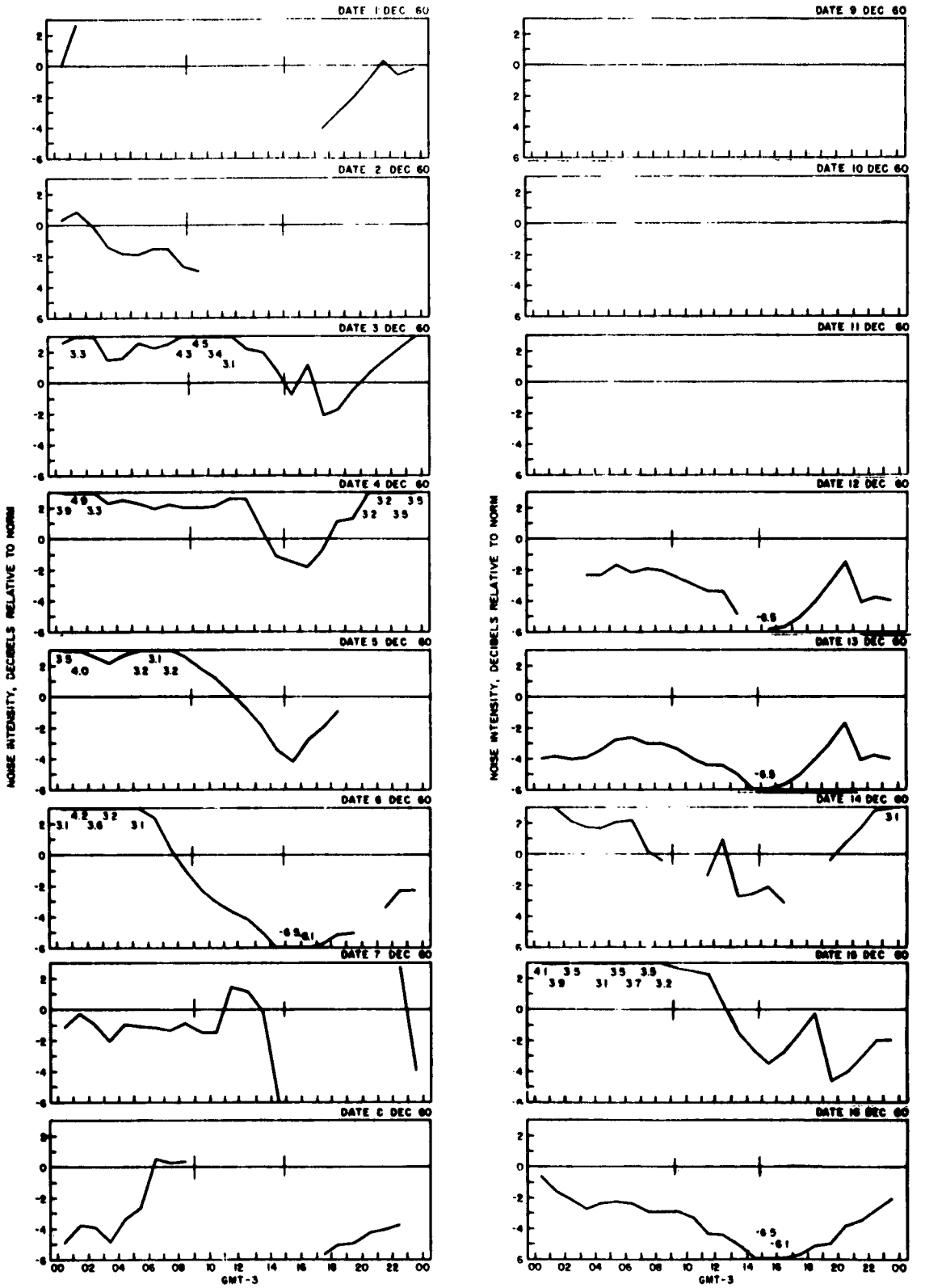

Thule, December 1960

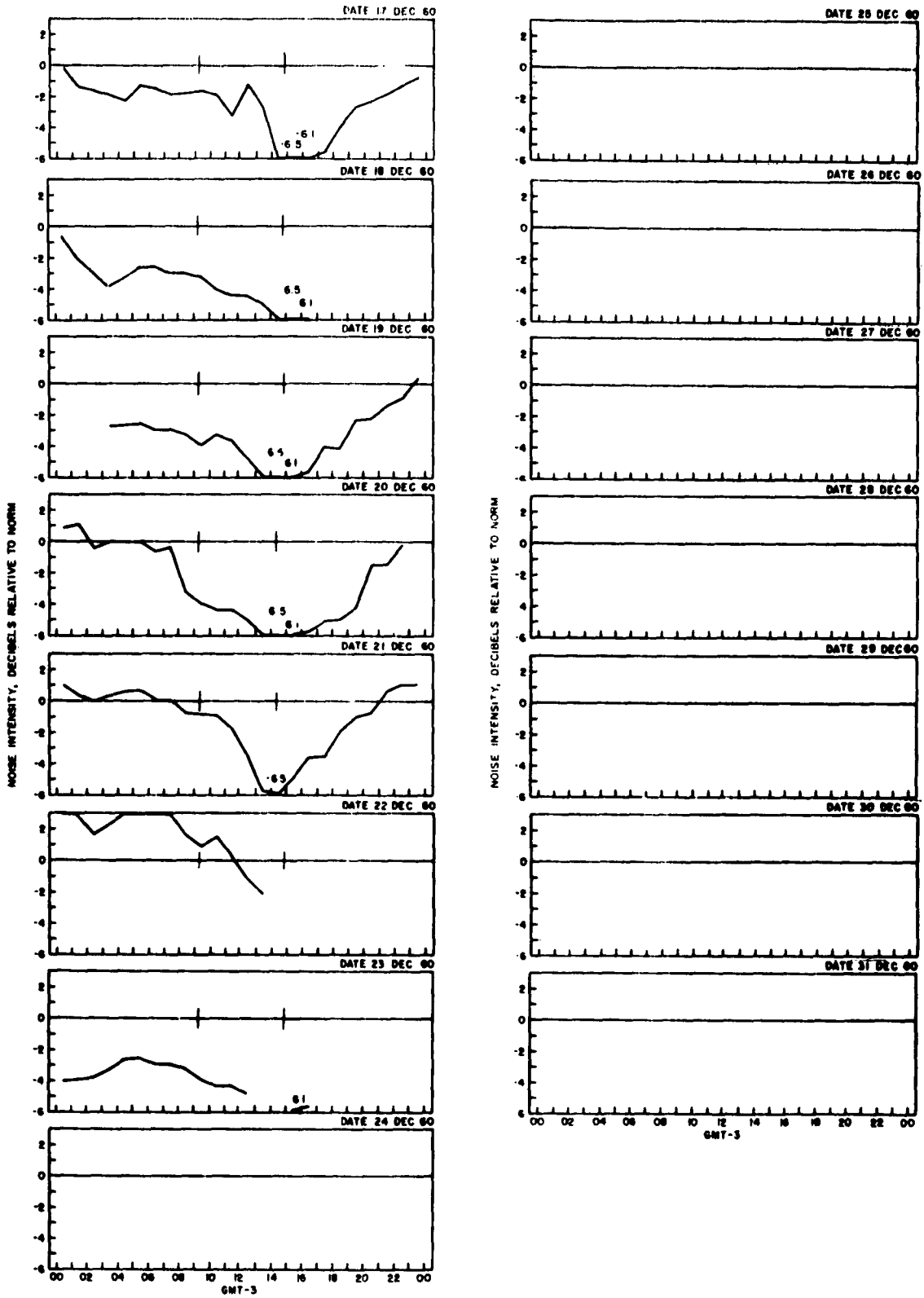

Thule, December 1960

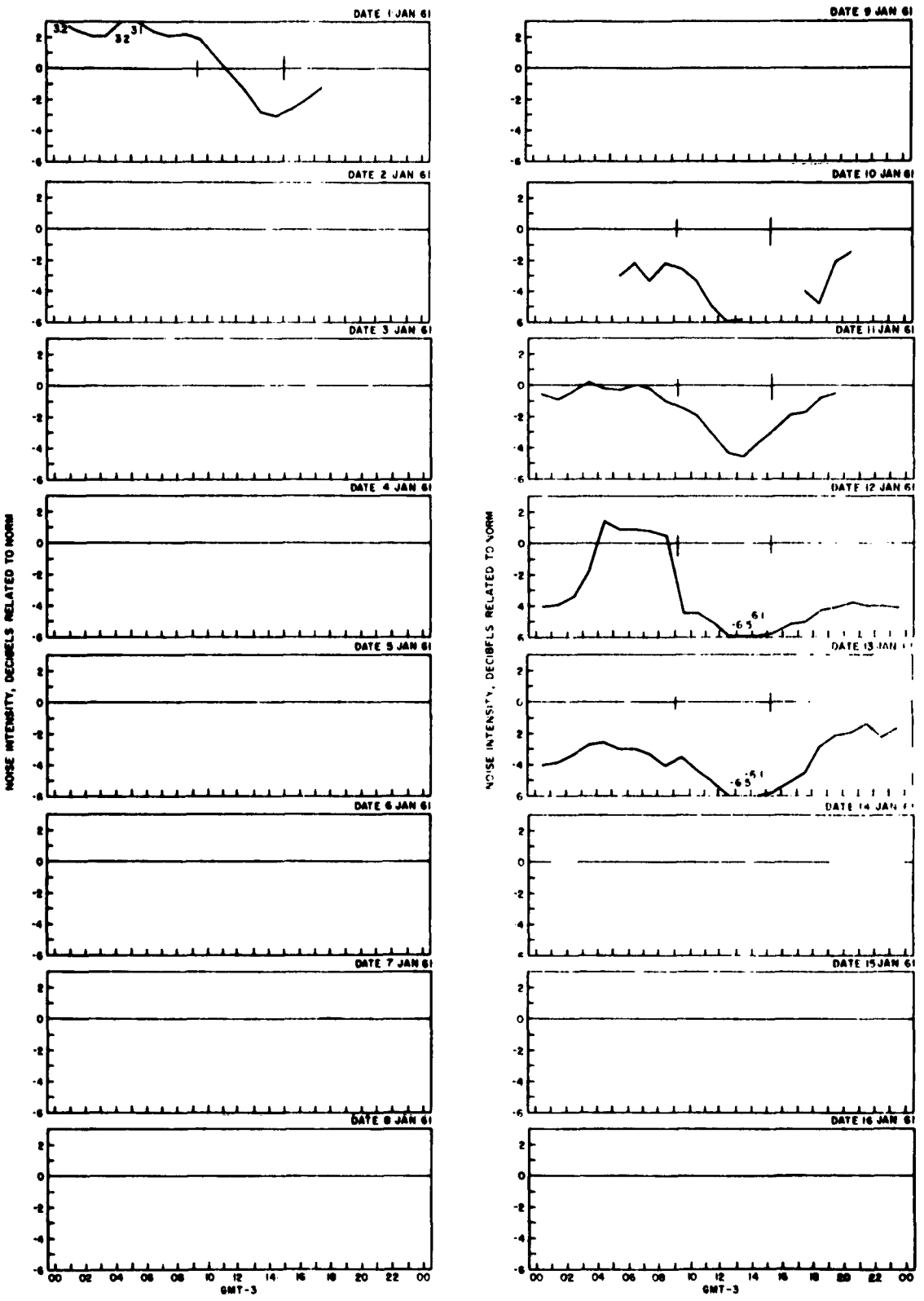

Thule, January 1961